

Nuclear matrix metalloproteinase-2 and investigation of its potential targets in myocardial ischemia-reperfusion injury

by

Sabina Baghirova

A thesis submitted in partial fulfillment of the requirements for the degree of
Master of Science

Department of Pharmacology
University of Alberta

© Sabina Baghirova, 2016

Abstract

Matrix metalloproteinases (MMPs) are zinc-dependent proteases involved in intra- and extra-cellular matrix remodeling. MMP-2 was the first to be localized to the nucleus; however the biological functions and substrates of nuclear MMP-2 are mostly unknown. We hypothesized that MMP-2 is present in the nucleus under normal physiological conditions but increases during myocardial ischemia-reperfusion (I/R) injury induced oxidative stress, proteolyzing nuclear structural proteins (lamins). Lamin A/C, a putative nuclear MMP-2 target, is an intermediate filament protein that provides structural support to the nucleus. Immunofluorescent confocal microscopy and subcellular fractionation showed the presence of MMP-2 in cytoplasm and nuclei of neonatal rat ventricular myocytes. The distribution of MMP-2 in cytoplasm and nuclei was verified by immunofluorescent confocal microscopy in the human fibrosarcoma HT 1080 cells. Further analysis by flow cytometry determined that 88.6% of a sample of ~10,000 HT 1080 cells had MMP-2 concentrated to the nucleus. Rat hearts were isolated and perfused by the Langendorff method aerobically, or subjected to global, no-flow ischemia followed by aerobic reperfusion in the presence or absence of an MMP inhibitor (100 μ M o-phenanthroline). Nuclear fractions extracted from the rat hearts showed increased MMP-2 activity, but not protein level in hearts subjected to I/R injury. To identify possible targets, an in vitro proteolysis assay was performed with lamin A or B incubated with MMP-2. Lamin A, but not lamin B, was proteolysed by MMP-2 in to a putative 50 kDa fragment, which was also predicted by in silico cleavage site analysis. Protein levels of troponin I, a known sarcomeric target of MMP-2 showed a trend for decrease in I/R hearts and was normalized by o-phenanthroline, demonstrating efficacy of the MMP inhibitor.

However, lamin A and lamin C protein levels remained unchanged in I/R hearts. PARP-1, a nuclear DNA repair protein, previously shown to be proteolysed by MMP-2 in vitro was measured in I/R hearts. It was observed that PARP-1 protein levels were decreased in I/R hearts treated with o-phenanthroline compared to I/R hearts without o-phenanthroline. Nuclear MMP-2 is present in cardiomyocytes under normal physiological conditions, and is increased as a result of I/R injury. This increase of MMP-2 activity in extracts from I/R hearts leads to proteolysis of troponin I, but not, PARP-1, lamin A or C. The activation of genes in myocardial I/R injury suggests that other nuclear functions of MMP-2 are likely.

Preface

This thesis is an original work by Sabina Baghirova. The research project, of which this thesis is a part, received research ethics approval from the University of Alberta Animal Care and Use Committee, "Nitric oxide and cardiovascular function and breeding colony", AUP 00000329, Dr. Richard Schulz, Principal Investigator.

Chapter 2, section 2.4 of this thesis has been published as: Baghirova, S., B.G. Hughes, M.J. Hendzel and R. Schulz. 2015. Sequential fractionation and isolation of subcellular proteins from tissue or cultured cells. *MethodsX* **2**: 440-445. doi:10.1016/j.mex.2015.11.001. I was responsible for the data collection and analysis as well as the manuscript composition. B.H., M.H. and R.S. contributed to manuscript edits. R.S. was the supervisory author and was involved with concept formation, data analysis, interpretation and manuscript composition.

The isolated rat heart perfusions for this thesis were performed by Mathieu Poirier, technician in the Schulz lab.

The experiment for Figure 3.13 was done by Marcia Y. Kondo, post-doctoral fellow in the Schulz lab.

Dedication

*To my hard-working parents for moving across the world to seek out a new
life with greater opportunities for our family*

Acknowledgments

I would like to take this opportunity to express my gratitude to everyone who supported me throughout the course of this project:

To my supervisor, Dr. Richard Schulz for the guidance, encouragement and advice he has provided throughout my time as his student. I appreciate his vast knowledge and skill in many areas, his assistance in editing reports and providing all the feedback throughout the process of writing this thesis.

To my supervisory committee members, Dr. Frances Plane and Dr. Michael Hendzel, for the support and for responding to my questions and queries so promptly. Your ideas and feedback have been absolutely invaluable throughout this process.

To the members of Dr. Schulz' lab past and present, Bryan Hughes, Mathieu Poirier, Brandon Chan, Carolina Morais and Vivian Figueiredo, for teaching me many of the techniques used in this thesis when I first embarked on this journey. Special thank you to Mathieu Poirier for performing the rat heart perfusions. I wish you all bright and successful futures in your experiments and journey through science.

To everyone who helped and taught me the techniques I used in this thesis, Darin McDonald for showing me how to prepare and stain cells for immunofluorescence confocal microscopy, and helping me obtain my very first immunofluorescence images. To Stephen Ogg for providing guidance in taking confocal images with the Leica SP5. I would also like to thank Aja Rieger of the Flow Cytometry Core facility for her invaluable help with all of the setting up, and analysis of the flow cytometry experiments.

To the support staff in the department and Cardiovascular Research Centre, Joy Pedersen and Marie-José Boeglin for the administrative support, and sometimes the moral support.

To my friends in the department Stephanie Lunn, Ran Wei and Xenia Cravetchi for making the last two years memorable.

To my parents for encouraging, supporting and standing by my side with every one of my decisions, without their support I could not have achieved and come as far as I have today.

To my second family Colin and Luna Beaver, who kept me sane throughout this process. Colin, for continued support and encouragement, always listening to me, and standing by my side when things got difficult. Luna, for purring away all the troubles, and keeping me company while I wrote this thesis.

Table of contents

CHAPTER 1 - INTRODUCTION

| | | |
|------------|---|-----------|
| 1.1 | General introduction to MMPs | 1 |
| 1.1.1 | Matrix metalloproteinase-2..... | 1 |
| 1.1.2 | Activation pathways of MMP-2..... | 2 |
| 1.1.3 | Regulation of MMP-2 activity..... | 3 |
| 1.1.4 | Subcellular localization of MMP-2..... | 4 |
| 1.1.5 | MMP inhibitors..... | 5 |
| 1.2 | Myocardial ischemia-reperfusion injury and MMP-2 | 6 |
| 1.2.1 | Role of MMP-2 in I/R injury..... | 7 |
| 1.2.2 | MMP-2 intracellular targets in heart..... | 8 |
| 1.3 | Biology of the nucleus | 9 |
| 1.3.1 | Nuclear structure..... | 9 |
| 1.3.2 | Nuclear matrix | 11 |
| 1.3.3 | Nuclear lamins | 11 |
| 1.4 | Possible roles of MMPs in the nucleus | 13 |
| 1.4.1 | MMP-1 | 14 |
| 1.4.2 | MMP-2 | 14 |
| 1.4.3 | MMP-3 | 17 |
| 1.4.4 | MMP-9 | 17 |
| 1.4.5 | MMP-13..... | 18 |
| 1.4.6 | MMP-12 | 19 |
| 1.4.7 | MMP-14..... | 19 |
| 1.5 | Hypothesis | 20 |
| 1.6 | Study Objectives | 20 |

CHAPTER 2 - MATERIALS AND METHODS

| | | |
|------------|--|-----------|
| 2.1 | Materials | 29 |
| 2.1.1 | Reagents..... | 29 |
| 2.1.2 | Antibodies | 29 |
| 2.1.3 | Markers and standards | 31 |
| 2.2 | Animal Protocol | 32 |
| 2.3 | Isolated rat heart perfusions | 32 |

| | |
|--|-----------|
| 2.4 Preparation of subcellular fractions from tissue and cells | 34 |
| 2.4.1 From perfused rat hearts | 34 |
| 2.4.2 From cultured cells | 35 |
| 2.5 Preparation of frozen tissue homogenates | 37 |
| 2.6 Protein quantification assay | 37 |
| 2.7 Western blotting | 38 |
| 2.8 Gelatin zymography | 40 |
| 2.9 Immunofluorescence confocal microscopy | 40 |
| 2.10 Isolation and culture of neonatal rat ventricular myocytes | 42 |
| 2.11 Cell Culture | 43 |
| 2.11.1 HT1080 cells | 43 |
| 2.12 In silico cleavage site analysis for lamin A or B | 44 |
| 2.13 In vitro proteolysis assay | 44 |
| 2.13.1 4-aminophenylmercuric acetate activation of MMP-2 | 44 |
| 2.13.2 Lamin A proteolysis | 45 |
| 2.13.3 Lamin B proteolysis | 46 |
| 2.14 SDS PAGE gel electrophoresis | 46 |
| 2.15 Flow cytometry | 47 |
| 2.16 Correlational analysis of protein levels versus recovery of heart contractile function | 49 |
| 2.17 Statistical analysis | 49 |
| CHAPTER 3 - RESULTS | |
| 3.1 Subcellular distribution of MMP-2 | 54 |
| 3.1.1 NRVM | 54 |
| 3.1.2 HT 1080 cells | 55 |
| 3.1.3 Wild type and MMP-2 knock out neonatal fibroblasts from mice | 56 |
| 3.2 Functional performance of rat hearts subjected to I/R injury | 58 |
| 3.3 Subcellular fractions isolated from rat hearts | 59 |
| 3.3.1 Subcellular fraction purity | 59 |
| 3.3.2 Changes in MMP-2 protein levels and activity with myocardial I/R injury | 59 |
| 3.4 Identifying nuclear targets of MMP-2 | 60 |
| 3.4.1 In silico analysis of lamin A or B proteolysis by MMP-2 | 60 |
| 3.4.2 In vitro proteolysis assay of lamin A or B by MMP-2 | 60 |

| | |
|---|------------|
| 3.5 Effect of myocardial I/R injury on putative nuclear MMP-2 targets..... | 61 |
| 3.5.1 Troponin I | 61 |
| 3.5.2 PARP-1 | 62 |
| 3.5.3 Lamin A and C..... | 63 |
| | |
| CHAPTER 4 - DISCUSSION | |
| 4.1 Nuclear MMPs..... | 104 |
| 4.2 Nuclear localization of MMP-2 | 105 |
| 4.3 Nuclear MMP-2 in I/R hearts..... | 108 |
| 4.4 Proteolysis targets of MMP-2 in cytoplasm and nucleus | 110 |
| 4.5 Limitations | 113 |
| 4.6 Future directions..... | 115 |
| | |
| References | 118 |
| | |
| Appendix A - Buffers and Gel Protocols..... | 126 |

LIST OF TABLES

| | | |
|-------------------|--|----|
| Table 1.1: | Potential and confirmed nuclear MMP-2 substrates identified by degradomics screen, in vitro proteolysis and other means..... | 22 |
| Table 1.2: | Summary of all known nuclear MMPs and their possible functions..... | 26 |
| Table 3.1: | In silico analysis of proteolytic cleavage sites by MMP-2 of lamin A/C and B performed by PROSPER..... | 65 |

LIST OF FIGURES

| | | |
|--------------------|---|----|
| Figure 1.1: | Domain structures of 72 and 64 kDa MMP-2..... | 27 |
| Figure 2.1: | The schematic diagram of the three groups of isolated rat hearts perfused aerobically or subjected to ischemia-reperfusion (I/R) injury..... | 50 |
| Figure 2.2: | Schematic summary diagram of the protocol of subcellular fractionation from either isolated perfused rat hearts or from cultured cells..... | 52 |
| Figure 3.1: | Nuclear localization of MMP-2 in neonatal rat ventricular myocytes by confocal immunofluorescence microscopy..... | 66 |
| Figure 3.2: | Distribution of intracellular MMP-2 protein levels in subcellular fractions of neonatal rat ventricular myocytes..... | 68 |
| Figure 3.3: | Distribution of intracellular MMP-2 activity in subcellular fractions prepared from neonatal rat ventricular myocytes..... | 70 |
| Figure 3.4: | Nuclear localization of MMP-2 in HT1080 cells by confocal immunofluorescence microscopy..... | 72 |
| Figure 3.5: | Nuclear localization of MMP-2 in HT1080 cells analyzed by imaging flow cytometry..... | 74 |
| Figure 3.6: | MMP-2 staining by Ab19015 MMP-2 antibody in wild type and MMP-2 knock out mouse neonatal fibroblasts visualized by confocal immunofluorescence microscopy..... | 76 |
| Figure 3.7: | MMP-2 staining by MMP-2 S1' loop antibody in wild type and MMP-2 knock out mouse neonatal fibroblasts visualized by confocal immunofluorescence microscopy..... | 78 |

| | | |
|---------------------|--|-----|
| Figure 3.8: | Functional performance of isolated rat hearts subjected to ischemia-reperfusion (I/R) injury and the effect of the MMP inhibitor o-phenanthroline (O)..... | 80 |
| Figure 3.9: | Purity of subcellular fractions prepared from normal rat heart ventricular tissue..... | 82 |
| Figure 3.10: | MMP-2 protein levels in subcellular fractions prepared from isolated rat hearts subjected to I/R injury..... | 84 |
| Figure 3.11: | MMP-2 activity in subcellular fractions prepared from isolated rat hearts subjected to I/R injury..... | 86 |
| Figure 3.12: | Nuclear protein lamin B is not proteolysed by MMP-2 in vitro..... | 88 |
| Figure 3.13: | Nuclear protein lamin A is proteolysed by MMP-2 in vitro in a concentration dependent manner..... | 90 |
| Figure 3.14: | Troponin I protein levels in homogenates prepared from rat hearts subjected to ischemia-reperfusion injury..... | 92 |
| Figure 3.15: | Correlational analysis between TnI protein levels and recovery of heart contractile function in isolated rat hearts subjected to ischemia-reperfusion (I/R) injury..... | 94 |
| Figure 3.16: | 116 kDa PARP-1 protein levels in homogenates prepared from rat hearts subjected to ischemia-reperfusion injury..... | 96 |
| Figure 3.17: | Correlational analysis between PARP-1 protein levels and recovery of heart contractile function in isolated rat hearts subjected to ischemia-reperfusion (I/R) injury..... | 98 |
| Figure 3.18: | Lamin A and lamin C protein levels in the insoluble cellular fraction prepared from rat hearts subjected to ischemia-reperfusion injury..... | 100 |

Figure 3.19: Lamin A and lamin C protein levels in homogenates prepared from rat hearts subjected to ischemia-reperfusion injury.....102

LIST OF ABBREVIATIONS

| | |
|-----------------|--|
| AP-1 | activated protein-1 |
| APMA | 4-aminophenyl mercuric acetate |
| DAPI | 4',6-diamidino-2-phenylindole |
| DMSO | dimethyl sulfoxide |
| FBS | fetal bovine serum |
| GAPDH | glyceraldehyde-3-Phosphate Dehydrogenase |
| I/R | ischemia-reperfusion |
| IgG | immunoglobulin G |
| kDa | kilodalton |
| MMP | matrix metalloproteinase |
| NFKB | nuclear factor kappa-light-chain-enhancer of activated B cells |
| NRVM | neonatal rat ventricular myocytes |
| PARP-1 | poly-ADP-ribose polymerase -1 |
| PBS | phosphate buffered saline |
| PROSPER | protease specificity prediction server |
| RIPA | radioimmunoprecipitation assay |
| RONS | reactive oxygen and nitrogen species |
| SDS | sodium dodecyl sulfate |
| SDS-PAGE | sodium dodecyl sulfate polyacrylamide gel electrophoresis |
| SEM | standard error of the mean |
| SERCA2 | sarco(endo)plasmic reticulum Ca ²⁺ ATPase 2 |
| TIMP | tissue inhibitor of metalloproteinases |
| TnI | tropinin I |
| TTBS | Tris-Tween buffered saline |
| VDAC | voltage-dependent anion channels |
| XRCC1 | x-ray cross-complementary factor 1 |

CHAPTER 1 - INTRODUCTION

1.1 General introduction to MMPs

Matrix metalloproteinases (MMPs) are a family of zinc dependent endopeptidases. The first matrix metalloproteinase activity was reported in 1962 when collagenolytic activity was discovered in the tail of a tadpole undergoing metamorphosis (Gross and Lapiere, 1962). Since then 23 different human MMPs have been identified (Cauwe and Opdenakker, 2010). Initially MMPs were classified as secreted proteins and sub-divided according to their extracellular matrix substrates: collagenases (MMP-1, MMP-8, MMP-13, and MMP-18), gelatinases (MMP-2 and MMP-9), stromelysins (MMP-3, MMP-10, and MMP-11), matrilysins (MMP-7 and MMP-26), and membrane-type MMPs (MMP-14, MMP-15, MMP-16, MMP-17, MMP-24 and MMP-25) (DeCoux *et al.*, 2014). It is now known that MMPs are involved in a variety of physiological and pathological processes both outside and inside the cell. MMPs play a role in angiogenesis, embryogenesis, inflammation, metastasis, arthritis and cardiovascular disease (Verma & Hansch, 2007). The general MMP structure consists of an autoinhibitory propeptide domain, a zinc-binding catalytic domain, and a linker or hinge region (Ali *et al.*, 2011).

1.1.1 Matrix metalloproteinase-2

MMP-2 is a ubiquitous enzyme which is best known for proteolysis of extracellular matrix proteins. MMP-2 (and the closely related MMP-9) differ from other MMPs with a unique structure in the catalytic domain with three fibronectin type II

repeats that are crucial for binding gelatin, shown in Figure 1.1 (Morgunova *et al.*, 1999). MMP-2 is now known not only for extracellular matrix remodelling, but intracellular proteolysis as well (Wang *et al.*, 2002). Biological activity of MMP-2 has been detected in many cellular compartments such as: caveolae (Chow *et al.*, 2007), nucleus (Kwan *et al.*, 2004), mitochondria (Wang *et al.*, 2002) and the mitochondria-associated membrane (Hughes *et al.*, 2014).

MMP-2 is one of the most studied of all identified MMPs, since it is expressed in all cardiac cells including cardiomyocytes, endothelium, vascular smooth muscle cells and fibroblasts (DeCoux *et al.*, 2014). MMP-2 plays various roles in cardiac physiology and pathology. It is important for extracellular matrix remodelling during embryonic heart development, especially during heart tube formation (Linask *et al.*, 2005). On the other hand, increased activity of MMP-2 has been detected in cardiovascular diseases including: hypertension, heart failure, and ischemic heart diseases (Youssef & Schulz, 2011). The intracellular targets as well as intracellular localization and functions of MMP-2 in ischemia-reperfusion (I/R) injury are discussed in section 1.2.

1.1.2 Activation pathways of MMP-2

MMP-2 is transcribed as an inactive zymogen of 72 kDa. The N-terminus hydrophobic autoinhibitory propeptide blocks the catalytic site that contains a zinc ion (Youssef and Schulz, 2011). The "cysteine switch", a mechanism of MMP activation described in 1990, refers to the highly conserved cysteine sulfhydryl residue at position 102 that coordinates the active site (Van Wart and Birkedal-Hansen, 1990). The coordination hydrogen bond between the cysteinyl sulfhydryl and the zinc ion

prevents the enzymatic activity of MMP-2. The disruption of this bond or absolute removal of this residue by proteolytic removal of the propeptide results in an active enzyme (Kandasamy *et al.*, 2010). The propeptide domain is removed extracellularly by combined action of membrane bound MMP-14 and tissue inhibitor of metalloproteinases-2 (TIMP-2) resulting in a 64 kDa enzymatically active MMP-2, shown in Figure 1.1 (Strongin *et al.*, 1995).

Reactive oxygen-nitrogen species (RONS) activate MMP-2 by the "cysteine switch" mechanism as well, while leaving the prodomain of MMP-2 intact (Gu *et al.*, 2002). Peroxynitrite (ONOO^-) is an oxidizing agent formed from nitric oxide and superoxide anion radicals. A low concentration of peroxynitrite (0.3-1 μM) activates 72 kDa MMP-2 (Viappiani *et al.*, 2009). Peroxynitrite in combination with glutathione leads to the S-glutathiolation of the cysteine¹⁰² residue, resulting in the formation of a disulfide S-oxide in the prodomain, which allows substrate access to the catalytic site. Other MMPs that can also be directly activated by peroxynitrite include MMP-1, 8 and 9 (Okamoto *et al.*, 2001).

Non-physiological chemicals can activate MMP-2 by disrupting the same cysteine responsible for the "cysteine switch". For example, 4-aminophenyl mercuric acetate (APMA) is commonly used experimentally to activate MMP-2 (Cauwe and Opendakker, 2010), and denaturing agents such as sodium dodecyl sulfate (SDS) activate the enzyme through conformational changes (Sung *et al.*, 2007).

1.1.3 Regulation of MMP-2 activity

The activity of MMP-2 is regulated at gene transcriptional and translational levels, as well as by posttranslational modifications such as phosphorylation and S-

glutathiolation, or binding to tissue inhibitors of metalloproteinases (TIMPs) (Youssef and Schulz, 2011). MMP-2 gene transcription was shown to be upregulated in neonatal rat cardiomyocytes and fibroblasts under hypoxic conditions, as well as by angiotensin II, endothelin I and interleukin 1 β . This was mediated by the functional activating protein-1 JunB–FosB heterodimers (Bergman *et al.*, 2003).

Human MMP-2 was confirmed to have at least five phosphorylation sites (S32, S160, S365, T250, and Y271) accessible at the surface of the protein. It was discovered that dephosphorylation of MMP-2 with alkaline phosphatase lead to an increase in activity in vitro (Sariahmetoglu *et al.*, 2007). The kinase involved in phosphorylation in vivo is still being investigated. There is evidence that both protein kinase C (Sariahmetoglu *et al.*, 2007) and protein kinase CK2 (Filipiak *et al.*, 2014) down-regulate MMP-2 activity in vitro. The changes in activity as a result of dephosphorylation of MMP-2 may be due to a conformational change that results in increased number of α -helices and decreased number of β -strands in comparison to phosphorylated form of MMP-2 (Jacob-Ferreira *et al.*, 2013).

TIMPs (TIMP-1 through TIMP-4) are small 21 kDa proteins that modulate MMP activity by binding to them at a 1:1 stoichiometric ratio. These endogenous inhibitors of MMPs do not have specificity towards a particular MMP (Baker *et al.*, 2002). All four TIMPs were found in heart cells, with TIMP-4 being the most abundant of them all and also shown to be localized inside cardiomyocytes (Schulze *et al.*, 2003).

1.1.4 Subcellular localization of MMP-2

The intracellular localization of MMP-2 is now a well-recognized phenomenon. Its intracellular localization is due to the fact that canonical MMP-2 has a N-terminal

signal sequence that only inefficiently targets it to the endoplasmic reticulum for secretion. Furthermore, cardiomyocytes have been shown to express a splice variant of MMP-2 that is entirely lacking the signal sequence for secretion (Ali *et al.*, 2012). We now know that in cardiomyocytes MMP-2 is localized to the sarcomere (Wang *et al.*, 2002), cytoskeleton (Sung *et al.*, 2007), nucleus (Kwan *et al.*, 2004), caveolae (Chow *et al.*, 2007), mitochondria (Wang *et al.*, 2002), and the mitochondria-associated membrane (Hughes *et al.*, 2014).

Caveolae are plasma membrane invaginations that regulate activity of signaling proteins. MMP-2 was found to colocalize with caveolin-1 (Cho *et al.*, 2007), which reduced MMP-2 activity *in vitro*, furthermore caveolin-1 knockout mice had higher MMP-2 activity in whole heart homogenates than the wild type mice (Chow *et al.*, 2007). It was concluded that MMP-2 activity is inhibited by cellular compartmentalization in caveolae (Chow *et al.*, 2007). Another intracellular locale of MMP-2 is the mitochondria-associated membrane which is a subdomain of the endoplasmic reticulum. The 72 kDa MMP-2 localized mainly to the mitochondria associated membrane and to a lesser degree to the mitochondria (Hughes *et al.*, 2014). The first ever MMP to be localized to the nucleus, MMP-2, will be discussed in more detail in section 1.4.2.

1.1.5 MMP inhibitors

MMPs are involved in various diseases such as arthritis, periodontal disease, atherosclerosis, heart disease and cancer (Yamada *et al.*, 2000). Many pharmaceutical companies were motivated to develop MMP inhibitors; however at the time they did not know which MMP to specifically target. Zn^{2+} chelating agents are a

common type of MMP inhibitor which act by binding to the zinc ion in the catalytic site (eg. batimastat, marimastat, GM-6001 , o-phenanthroline). These are not specific inhibitors as they act on wide range of MMPs (Peterson, 2004). Some tetracycline antibiotics also inhibit MMPs, doxycycline being the most potent among them followed by minocycline (Golub *et al.*, 1998). Doxycycline is able to inhibit MMP activity at sub-antimicrobial plasma concentrations (Golub *et al.*, 1998). It preferentially inhibits MMP-2, -9, and -8, and does not inhibit MMP-3 or -7 (Smith *et al.*, 1999). Doxycycline is the first MMP inhibitor that was approved for clinical use by the US Food and Drug Administration and by Health Canada to be used at 20 mg, two times daily, for periodontal inflammation and rosacea (Novak *et al.*, 2002).

1.2 Myocardial ischemia-reperfusion injury and MMP-2

Ischemia-reperfusion injury is defined as a deficient blood supply to tissue which results in the continued loss of oxygen, followed by reperfusion, which both trigger oxidative stress (Sawicki *et al.*, 2005). Most of the oxidative stress injury to tissue happens in the first few minutes of reperfusion following ischemia. Depending on the duration of ischemia the extent of the damage will vary, irreversible damage will result from longer periods of ischemia inducing cell death (Kalogeris *et al.*, 2012). A shorter period of ischemia will result in myocardial stunning injury that is reversible, where a short lived loss of contractile function, without necrotic cell death, will occur (Chow *et al.*, 2007). Reperfusion re-establishes the delivery of oxygenated blood and rapidly restarts the electron transport chain in mitochondria, consequently producing RONS. Shear stress in the coronary circulation as well as

elevated intracellular Ca^{2+} resulting from ischemia stimulate nitric oxide production (Yasmin *et al.*, 1997).

This leads to the biosynthesis of peroxynitrite from nitric oxide and superoxide anion (DeCoux *et al.*, 2014). The amount of peroxynitrite peaks within the first 30 seconds of reperfusion (Yasmin *et al.*, 1997), and as already discussed, in combination with glutathione the S-glutathiolation of Cys¹⁰² occurs and MMP-2 is activated (Wang *et al.*, 2002). The increase in MMP-2 activity negatively correlates with recovery of contractile function (Cheung *et al.*, 2000), this will be discussed in more detail in section 1.2.1 and 1.2.2. An imbalance between TIMPs and MMPs contributes to myocardial I/R injury (Schulze *et al.*, 2003). The myocardial levels of TIMP-1 (Lalu *et al.*, 2005) and TIMP-4 (Schulze *et al.*, 2003) were decreased in hearts that underwent I/R injury.

1.2.1 Role of MMP-2 in I/R injury

Coronary effluent analysis from rat hearts subjected to I/R injury showed an increase in MMP-2 in the first to fifth minutes of reperfusion. This increase in MMP-2 negatively correlated with the recovery of contractile function (Cheung *et al.*, 2000). The use of MMP inhibitors (o-phenanthroline or doxycycline) resulted in better recovery of hearts that underwent I/R injury, suggesting that MMPs are contributing to myocardial I/R injury (Cheung *et al.*, 2000). Later it was discovered that MMP-2 is activated by peroxynitrite and glutathione, suggesting an intracellular proteolytic role of this protease. Indeed it was determined that intracellular MMP-2 co-localizes with and proteolyzes sarcomeric proteins including troponin I (Wang *et al.*, 2002), myosin light chain 1 (Sawicki *et al.*, 2005), α -actinin (Sung *et al.*, 2007) and

titin (Ali *et al.*, 2010), which contributes to the acute contractile dysfunction of myocardial I/R injury.

1.2.2 MMP-2 intracellular targets in heart

MMP-2 degrades intracellular proteins during ischemia-reperfusion injury (DeCoux *et al.*, 2014). Troponin I (TnI), a biomarker of cardiac injury and regulator of cardiac contractile function, was found to be proteolyzed by MMP-2 *in vitro*. Further experiments showed that troponin I decreased in I/R hearts and this was attenuated by MMP inhibitors, leading to better contractile performance of the hearts (Wang *et al.*, 2002).

Titin is the biggest protein in the human body at 3 megadaltons. This sarcomeric protein is a MMP-2 target. Titin and MMP-2 were found to co-localize near the Z-disk of cardiac sarcomere. Proteolysis of titin in I/R hearts was prevented by the MMP inhibitors o-phenanthroline or ONO-4817 (Ali *et al.*, 2010). Another sarcomeric protein, myosin light chain-1, was proteolyzed by MMP-2, resulting in a loss of the C-terminal helix. The proteolysis of myosin light chain-1 in I/R hearts was attenuated by MMP inhibitors (Sawicki *et al.*, 2005). α -Actinin, a protein that plays role in maintaining sarcomere structure, was found to be proteolysed in hearts infused with peroxynitrite. The MMP inhibitor PD-166793 prevented the reduction in mechanical function and the proteolysis of α -actinin (Sung *et al.*, 2007).

1.3 Biology of the nucleus

The nucleus is one of the identifying features of eukaryotes (Osorio and Gomes, 2013). The first observation of the nucleus dates back to 1700s when Dutch microscopy pioneer Leeuwenhoek observed them in fish erythrocytes (van Leeuwenhoek, 1700). To this day the nucleus, its functions, components and structures remains a highly examined area in science.

The nucleus is the largest organelle in the cell that contains most of the genetic material of a cell (Dahl *et al.*, 2008). DNA is packed tightly by wrapping around histones (H2A, H2B, H3 and H4). Two copies of each histone protein come together to form a histone octamer structure that is defined as a nucleosome. These nucleosomes are further packaged and coiled into a higher-order structure to form the chromosomes (Linnemann and Krawetz, 2009). Chromosomes are organized within the nuclear space, occupying distinct territories. Within these territories there are transcriptionally active chromatin neighborhoods and transcriptionally silent heterochromatin regions (Cremer and Cremer, 2001). The chromatin has to de-condense from the tightly coiled structure in order to be accessed and transcribed (Linnemann and Krawetz, 2009). The nuclei are highly organized but yet dynamic organelles, with an intricate nuclear architecture.

1.3.1 Nuclear structure

The structure of the nucleus is contained within a double phospholipid bilayer that consists of an outer membrane layer connecting with the endoplasmic reticulum, and an inner membrane (Dahl *et al.*, 2008) The nuclear lamina lines the inner

nuclear membrane and acts as structural support; this is discussed in more detail in section 1.3.3 (Liu and Zhou, 2008). The nuclear membrane is perforated by pores which control all nucleocytoplasmic transport (McLane and Corbett, 2009). Transport signals such as the nuclear localization signal (NLS) and nuclear export signal (NES) are amino acid sequences that act as import and export signals of proteins through the nuclear pore, respectively (Ferrai *et al.*, 2010). When the protein signal is recognized by the transport receptors the translocation of macromolecules is mediated accordingly. As already mentioned, the genetic material is packed and organized into territories within the nucleus, and the remaining nuclear space is taken up by proteinaceous nuclear bodies. The entire nuclear interior is subdivided into compartments with specific functions. These sub-compartments include the nucleolus, splicing speckles, cajal bodies, promyelocytic leukemia bodies and polycomb group bodies (Dahl *et al.*, 2008).

The nucleolus is the largest sub-compartment in the nucleus with 700 identified human proteins that reside in this space. The nucleolus contains transcription and processing machineries of ribosome-subunit production and is responsible for ribosome biogenesis (Boisvert *et al.*, 2007). Splicing speckles contain the splicing machinery required for pre-mRNA processing (Ferrai *et al.*, 2010). Cajal bodies are the sites of modification and production of the spliceosomal small nuclear ribonucleoprotein particles (Gall, 2003). Polycomb group complexes contain regulatory proteins that control gene expression through repression and chromatin modification (Ferrai *et al.*, 2010). Despite being tightly packed and containing all the genomic information and proteinaceous bodies, the nucleus still requires structural support to be able to withstand mechanical stress.

1.3.2 Nuclear matrix

The nuclear matrix was first observed in 1949 by two Russian scientists (Zbarsky and Debov, 1949) that introduced a whole new concept of nuclear architecture and has been a topic of huge debate in cell biology ever since. The fibrogranular, non-chromatin structures observed in the mammalian nucleus suggested the existence of a protein skeleton analogous to the cytoskeleton (Nickerson, 2001). It is yet unknown which protein(s) form the primary structure of the nuclear matrix (Albrethsen *et al.*, 2009). Some of the major components of the nuclear matrix include: nuclear mitotic apparatus protein, heterogeneous nuclear ribonucleoprotein, matrins, actin and lamins (Nickerson, 2001; Razin *et al.*, 2014). There is evidence that the nuclear matrix is interconnected with the cytoskeleton and the extra-cellular matrix through complex structures (Albrethsen *et al.*, 2009). Therefore, mechanical feedback can be relayed from the extracellular matrix, through the intracellular cytoskeleton all the way to the nuclear matrix. The cells are able to adjust their internal stiffness with increased mechanical stress (Albrethsen *et al.*, 2009; Dahl *et al.*, 2008). The cytoskeleton link to the nuclear matrix forms through lamins and LINC (linker of nucleoskeleton and cytoskeleton) complex (Carmosino *et al.*, 2014).

1.3.3 Nuclear lamins

Lamins are type V intermediate filament proteins further subdivided into A-type lamins (lamin A & C) and B-type lamins (lamin B1 & B2). Lamin A and C are alternative splice products of the same gene (LMNA) (Schreiber and Kennedy,

2013). Lamin A and C share the first 566 amino acids of their sequence, out of a total of 664 and 572 amino acids for lamin A and C, respectively (Carmosino *et al.*, 2014). Lamin B1 & B2 are products of two genes (LMNB1,2) (Sieprath *et al.*, 2012). B type lamins are essential for cell survival and embryogenesis, while A type lamins are essential for development and differentiation (Pekovic *et al.*, 2011). Lamin A and C knock out mice were reported to have stunted growth, muscle weakness and died by 6 weeks of age, and the isolated fibroblasts had misshapen and weakened nuclei (Fong *et al.*, 2006). Lamin B knock out mice survived embryonic development, however, died at birth. The fibroblasts of lamin B knock out mice had grossly misshapen nuclei, impaired differentiation, increased polyploidy, and premature senescence (Vergnes *et al.*, 2004).

The structure of lamin consists of a globular N-terminal domain, the central α -helical rod domain containing four coiled-coil repeats, and a C-terminal globular domain. The lamins dimerize and polymerize into more complex structures (Stuurman *et al.*, 1998) incorporating lamin-binding proteins and supporting a wide range of functions (Schirmer *et al.*, 2003), including chromatin organization (Liu *et al.*, 2000), gene expression (Spann *et al.*, 2002), cell cycle control (Lopez-Soler *et al.*, 2001), DNA repair mechanisms (Hutchison, 2011) and positioning of the nucleus in the cell (Starr and Fridolfsson, 2010).

In cardiomyocytes, lamin A and C in conjunction with other proteins, forms a link from the nuclear matrix to the cytoskeleton connecting with the sarcomere and plays a role in protecting the nucleus from rupture under mechanical stress. Lamin A and C are able to control the structural stiffness or weakness of the nuclear envelope. It has been suggested that beyond structural control, lamin is also able to al-

ter gene expression when the cell is under mechanical stress. The loss of lamin A or C in heart cells by proteolytic cleavage can cause weak nucleus prone to damage and rupture under physical stress (Carmosino *et al.*, 2014). Oxidative stress during the reperfusion phase of I/R injury in hearts can cause changes in lamin structure without proteolysis. It has been shown that lamin A and C undergo irreversible oxidation of the cysteine residues in their tail domains that result in dysmorphic nucleus, cellular senescence and lead to further susceptibility to RONS-induced damage (Pekovic *et al.*, 2011; Sieprath *et al.*, 2012). Therefore the decrease in lamin A or C in cardiomyocytes due to proteolysis could result in growth arrest and an altered cell cycle.

1.4 Possible roles of MMPs in the nucleus

The discovery of the first nuclear MMP, MMP-2 (Kwan *et al.*, 2004), has opened up a whole new research area. The summary of all known nuclear MMPs with their possible functions are listed in Table 2. Kwan *et al.* (2004) identified that MMP-2 possessed the nuclear localization sequence that suggested that it can be transported to the nucleus. The nuclear localization sequence is found on the C-terminus of the enzyme, which means it can easily be accessed by the receptor so that MMP-2 can be transported through the nuclear pore. Many other MMPs possess a nuclear localization sequence: MMP 1, 3, 8, 10, 13, 14, 16, 17, 19, 20, 23A, and 24 (Si-Tayeb *et al.*, 2006). Thus far, nuclear MMPs have been shown to play a role in processes such as proteolysis of DNA repair proteins (Hill *et al.*, 2012; Kwan *et al.*, 2004; Yang *et al.*, 2010), transcription (Eguchi *et al.*, 2008; Zuo *et al.*, 2014) apoptosis (Pirici *et al.*, 2012) and participate in mitotic events leading up to cellular

proliferation (Zimowska *et al.*, 2013). Our improved understanding of the novel localization and functions of MMPs under conditions of both homeostasis and stress will allow us to develop better, more specific MMP inhibitors, by targeting them to specific cellular compartments.

1.4.1 MMP-1

MMP-1, a collagenase was reported to be localized to the nucleus (Limb *et al.*, 2005). MMP-1 was previously known to be involved in inflammation, wound healing, tumor invasion, and metastasis. It was found that MMP-1 protein levels were highest in fragmented nuclei as well as during metaphase of the cell cycle. Therefore MMP-1 was suggested to be involved in the dissociation of nuclear membrane proteins during the mitotic phase of the cell cycle or the breakdown of the nuclear membrane during apoptosis (Limb *et al.*, 2005). However, no direct evidence, beyond its nuclear localization, was presented for the assessment of MMP-1 function. MMP-1, along with MMP -2 and -10, were later reported to be localized to the nucleus of breast cancer tumor cells by immunostaining (Kohrmann *et al.*, 2009). The function of nuclear MMP-1 still requires further studies.

1.4.2 MMP-2

MMP-2 was the first ever MMP reported to have nuclear localization (Kwan *et al.*, 2004). MMP-2 protein levels and activity were discovered in commercial nuclear extracts from human hearts and rat liver. Immunogold electron microscopy was used to show the localization of MMP-2 to the nucleus of cardiac myocytes. Poly-

ADP-ribose polymerase -1 (PARP-1) detects oxidized DNA and plays an important role in DNA repair and cell survival. MMP-2 proteolyzed PARP-1 in vitro, providing a clue about its possible nuclear function(s) (Kwan *et al.*, 2004).

Nuclear MMP-2 was investigated further in pulmonary artery endothelial cells that were subjected to cigarette smoke. Cytosolic and nuclear fractions were collected from resting cells, which had low gelatinolytic activity, and cells subjected to cigarette smoke (15 min of smoke followed by 45 min recovery, performed 6 times) which showed higher gelatinolytic activity in the nuclear fraction. Immunoprecipitation and western blot analysis confirmed that it was from MMP-2. Increased activity of MMP-2 in the nucleus was suggested to be due to RONS produced from cigarette smoke, leading to activation of MMP-2 by S-glutathiolation (Ruta *et al.*, 2009)

Nuclear MMP-2 function was further explored by Yang *et al.* (2010) in rat brains that were subjected to 90 min of middle cerebral artery occlusion and reperfusion either for 3, 24 or 48 hr. Nuclear MMP-2 and MMP-9 activities were increased 3 hr after reperfusion, and human tissue from stroke patients showed increased gelatinolytic activity. PARP-1 and X-ray cross-complementary factor 1 (XRCC1), which is a DNA base excision repair protein, were both decreased in ischemic rat brains. BB1101, an MMP inhibitor, attenuated PARP-1 and XRCC1 proteolysis, as well as decreased early oxidative DNA damage in ischemic rat brains (Yang *et al.*, 2010), and decreased neuronal apoptosis at 48 hr reperfusion in rat ischemic hemispheres (brain contains a right and left cerebral hemispheres separated by a groove) (Hill *et al.*, 2012).

Oxygen-glucose deprivation, which is an in vitro model of ischemia/reperfusion, was performed with primary cortical rat neurons, subjected to 2 hr

of oxygen-glucose deprivation followed by 24 hr re-oxygenation. Increased nuclear gelatinase activity was measured at the end of reperfusion and it co-localized mainly with MMP-2. Both MMP-2 and -9 were detected in nuclear extracts. PARP-1 and XRCC1 protein levels were decreased, as well as PARP1 activity was decreased. Neurons pre-treated with MMP-2/9 inhibitor II ((2R)-[(4-Biphenylsulfonyl)amino]-N-hydroxy-3-phenylpropionamide) decreased gelatinase activity, normalized PARP-1 and XRCC1 protein levels, decreased oxidative DNA damage and improved neuronal survival after oxygen-glucose deprivation (Hill *et al.*, 2012).

Other studies have focused on finding the tissues where intranuclear MMP-2 is most abundant. Mouse tissues under normal physiological conditions were visualized with a combination of in situ gelatin zymography and immunohistochemistry. Most prominent gelatinolytic activity and MMP-2 staining was in kidney tubular cells (Solli *et al.*, 2013). MMP-2 activity was found in the nucleus of human vascular endothelial cells and primary neonatal rat neurons, but not in glial cells or a Schwannoma cell line. The distribution of MMP-2 was described to be localized with nuclear speckles, and co-localized with TIMP-1 (Sinha *et al.*, 2014).

Cauwe and Opdenakker (2010) have performed a high throughput, non-biased, degradomic screen that identified many possible intracellular protein targets for MMPs. In Table 1 I have summarized the confirmed and possible nuclear targets of MMP-2.

1.4.3 MMP-3

MMP-3, also known as stromelysin-1, proteolyzes various extracellular matrix proteins, and proteolytically activates some MMPs. MMP-3 was reported to be localized to the nucleus in cultured cells but also in human liver tissue and may be associated with the onset of apoptosis. The rate of apoptosis was reduced by transfection of cells with a mutant MMP-3 without catalytic activity, and confirmed once again by use of an MMP inhibitor, GM6001 (Si-Tayeb *et al.*, 2006).

Eguchi *et al.* (2008) pursued a study of nuclear MMP-3 through a chance discovery of transcriptional factor-like activity on the connective tissue growth factor gene. MMP-3 was found in the nucleus of chondrocytes *in vitro* and *in vivo*, and it could bind the enhancer sequence of connective tissue growth factor, promote and trans-activate gene transcription (Eguchi *et al.*, 2008).

Another study found that MMP-3 was translocated into the nucleus upon dengue virus infection of cells. MMP-3 co-localized with nuclear factor kappa-light-chain-enhancer of activated B cells (NFkB) in the nucleus. Interaction between MMP-3 and the NFkB complex was via the C-terminal hemopexin-like domain of MMP-3, which resulted in enhanced transcriptional factor activity of NFkB (Zuo *et al.*, 2014). The nuclear functions of MMP-3 appear to be related in some way to transcription, and this should be explored for other MMPs.

1.4.4 MMP-9

MMP-9, also known as gelatinase B, is a close relative of MMP-2. Kwan *et al.* (2004) also found nuclear MMP-9 activity in human heart and rat liver nuclear ex-

tracts. MMP-9 was reported to be localized to the nucleus of aging human brain cells, or brain tissue after a stroke. 95% of the MMP-9 localization was in neuronal cells, the remaining was in astrocytes. MMP-9 was suggested to be involved in apoptosis of neuronal and glial cells, since cells with nuclear MMP-9 showed presence of activated caspase 3, an important protein for the execution of cell apoptosis (Pirici *et al.*, 2012).

In a different study nuclear MMP-9 was suggested to play a role in skeletal muscle myoblast proliferation and in DNA replication during the cell cycle. MMP-9 was found to localize to the nucleus of myoblasts by immunolocalisation and in situ zymography during S-phase of the cell cycle, when DNA is replicated in preparation for cell division. The inhibition of MMP activity by doxycycline, TIMP-1 or neutralising, MMP-9 antibody reduced the proliferation of myoblasts (Zimowska *et al.*, 2013).

1.4.5 MMP-13

MMP-13 (collagenase 3) was found to be localized to the nucleus and increased in neuronal nuclei after acute cerebral ischemia. Similar results were seen in human post-mortem brain tissue with cerebral ischemia. In vitro experiments with rat cortical neuron cultures that underwent oxygen and glucose deprivation had increased nuclear MMP-13. However, the function of nuclear MMP-13 during ischemia was not identified and further research is required (Cuadrado *et al.*, 2009).

1.4.6 MMP-12

MMP-12, also known as macrophage metalloelastase, plays an important role in inflammatory processes. MMP-12 was shown to have a nuclear localization in mouse cardiac and epithelial cells that normally possess little to no MMP-12. The mice were infected with coxsackievirus type B3, an unenveloped virus which causes systemic infection in mice and humans. MMP-12 was taken up from the extracellular space and transported into the nucleus of the cell during viral infection. MMP-12 was shown to bind the promoter and engage in transcription of the gene of nuclear factor of kappa light polypeptide gene enhancer in B-cells inhibitor. This resulted in secretion of interferon- α . Further analysis revealed the nuclear localization of MMP-12 in human myocardial biopsies with enteroviral myocardial infection. It was therefore confirmed that nuclear MMP-12 plays a transcriptional role in virus infected cells, and is vital for antiviral immunity (Marchant *et al.*, 2014).

1.4.7 MMP-14

MMP-14 is a membrane type 1-matrix metalloproteinase that contains a transmembrane domain and a short cytoplasmic C-terminal tail which anchors it to the cell membrane. MMP-14 plays a role in the proteolytic activation of MMP-2 with TIMP-2 (Mannello and Medda, 2012). MMP-14 along with MMP-2 were localized to the nucleus of the same hepatoma cells by immunohistochemistry. It was suggested that MMP-14 plays a role in MMP-2 activation in the nucleus, which might lead to a proteolytic cascade in the nucleus as a result of active MMP-2. However, this function still requires further studies to fully confirm this phenomenon. In the same

study fibronectin, a nuclear matrix protein, was suggested to be a possible proteolytic target for MMP-2 (Ip *et al.*, 2007). However, further studies are required to look at the relationship between nuclear MMP-14 and MMP-2, and identify if MMP-2 can proteolyze fibronectin.

1.5 Hypothesis

I hypothesize that MMP-2 is present in the nucleus of cardiac myocytes under normal physiological conditions and its activity and protein levels increase during oxidative stress induced by myocardial I/R injury, proteolyzing structural (lamin A, B and C) and DNA repair proteins (PARP-1).

1.6 Study Objectives

The first study objective is to show that MMP-2 is localized to the nucleus of myocytes under normal physiological conditions. I will use immunofluorescence confocal microscopy to visualize MMP-2 in neonatal rat cardiomyocytes, and compare the nuclear activity and protein levels of MMP-2 to the isolated subcellular fractions from these cells. The sub-populations of cells with or without nuclear MMP-2 will be visualized and analyzed by live cell imaging flow cytometry.

The hypothesized MMP-2 substrates will be tested with in vitro degradation assays, in which the purified recombinant proteins are incubated with activated MMP-2. The changes in protein levels and the appearance of lower molecular weight products using Coomassie blue-stained SDS-PAGE gels will be performed.

Myocardial I/R injury increases MMP-2 activity and protein levels. I will use isolated rat hearts perfused by the Langendorff method in one of three ways: aerobically (control), inducing I/R injury by global, no-flow ischemia followed by reperfusion, and inducing I/R injury in the presence of an MMP inhibitor (o-phenanthroline). The subcellular fractions will be isolated from ventricular rat heart tissue to obtain purified cytosolic, membrane and nuclear protein fractions. MMP-2 activity will be determined via gelatin zymography, while Western blotting will be used to detect protein levels of MMP-2 in all fractions. The protein levels of MMP-2 substrates (lamin A/C, PARP-1 and TnI as a positive control) will be measured in homogenates of aerobic and I/R hearts, with or without MMP inhibitor.

Table 1.1: Potential and confirmed nuclear MMP-2 substrates identified by degradomics screen, in vitro proteolysis and other means

| Name of protein | Function | Localization | Reference |
|------------------------|--|---|--|
| PARP-1 | Repair of single-stranded DNA (ssDNA) breaks, involved in Base Excision Repair (BER) during oxidative stress | Nucleus | Kwan <i>et al.</i> , 2004 Yang <i>et al.</i> , 2010 |
| XRCC1 | Efficient repair of DNA single-strand breaks formed by exposure to ionizing radiation and alkylating agents, involved in BER | Nucleus | Yang <i>et al.</i> , 2010 |
| ADAR1 | Responsible for pre-mRNA editing by site-specific deamination of adenosine to inosine in both coding and noncoding regions | Nucleus | In vitro proteolysis Schulz lab unpublished |
| Lamin A/C | Involved in nuclear stability, support of nuclear envelope, chromatin structure, and necessary to direct the proper function of transcription factors | Nucleus | In vitro proteolysis Schulz lab unpublished |
| Nucleophosmin* | Involved in diverse cellular processes such as ribosome biogenesis, centrosome duplication, protein chaperoning, histone assembly, cell proliferation, and regulation of tumor suppressors; associated with nucleolar ribonucleoprotein structures and binds nucleic acids | Nucleus | ND |
| Cyclophilin A,E* | Acceleration of protein folding, catalysis of <i>cis-trans</i> isomerization of peptidyl-prolyl bonds in oligopeptides; binding of RNA with potential role in pre-mRNA splicing | Nucleus | ND |
| Calreticulin * | Molecular calcium binding chaperone promoting folding, oligomeric assembly and quality control in the ER via the calreticulin/calnexin cycle; extracellular modulation of cell motility and promotion of tumor progression and metastasis | Cytoplasm, ER lumen, nucleus, cell surface, secreted, ECM | Hughes <i>et al.</i> , 2014 |

| | | | |
|-------------------------------------|---|--|----|
| Nucleolin * | Regulation of RNA polymerase I transcription; folding and maturation of pre-ribosomal RNA; ribosome assembly; nucleo-cytoplasmic transport; histone chaperone activity; interaction with viruses at the cell membrane | Nucleus, cytoplasm, cell surface | ND |
| Nucleoside diphosphate kinase B* | Major role in the synthesis of nucleoside triphosphates other than ATP; negative regulation of Rho activity; transcriptional activator of the <i>Myc</i> gene | Cytoplasm, cytoskeleton, nucleus | ND |
| Ubiquitin-activating enzyme E1* | Activates ubiquitin by first adenylating its C-terminal glycine residue with ATP, and thereafter linking this residue to the side chain of a cysteine residue in E1, yielding an ubiquitin-E1 thioester | Cytoplasm, nucleus | ND |
| Ubiquitin conjugating enzyme E2 L3* | Catalyzes the covalent attachment of ubiquitin to other proteins, mediating the selective degradation of short-lived proteins | Cytoplasm, nucleus | ND |
| Elongation factor 1-alpha2* | Promotion of the GTP-dependent binding of aminoacyl-tRNA to the A-site of ribosomes during protein biosynthesis | Nucleus | ND |
| Trangelin 2* | Putative actin cross-linking/gelling protein | Nuclear membrane, cell membrane | ND |
| Moesin* | Cross-linking of cortical actin filaments and plasma membranes; roles in ECM interactions, cell-cell communication, apoptosis, carcinogenesis and metastasis | Cytoplasm, cell membrane, cell projections, nucleolus, extracellular | ND |
| Enolase- α * | Glycolytic enzyme; role in growth control, hypoxia tolerance and allergic responses; receptor and activator of plasminogen | Cytoplasm, cell membrane, myofibril, sarcomere, M-band, nucleus, extracellular | ND |

| | | | |
|---|--|--|----|
| Cofilin-1* | Actin filament depolymerization and severing protein. Promotion of apoptosis by translocating to mitochondria and delivering actin | Cytoplasm, cytoskeleton, nuclear matrix, extracellular | ND |
| Actin regulatory protein CAP-G* | Reversible blocking of actin filament barbed ends without filament severing; may have important roles in macrophage function and regulation of cytoplasmic and/or nuclear structures through interactions with actin; potential DNA binding | Cytoplasm, melanosome, nucleus, secreted | ND |
| Filamin A* | Promotion of actin filament branching and connection of the actin cytoskeleton to various transmembrane proteins; scaffold for a wide range of cytoplasmic signaling proteins; tethers cell surface-localized furin, modulates its rate of internalization and directs its intracellular trafficking; defects are the cause of many developmental diseases | Cytoplasm, cytoskeleton, nucleus, cell membrane, | ND |
| Hepatoma-derived growth factor (HDGF)* | Heparin-binding protein with mitogenic activity for fibroblasts; acts as a transcriptional repressor | Cytoplasm, nucleus, extracellular | ND |
| High-mobility group protein B1 (HMGB1)* | Intracellular function: stabilization of nucleosome formation and facilitation of transcription factor binding by bending DNA, role in DNA repair; cytosolic nucleic acid sensor; extracellular function: pro-inflammatory cytokine, alarmin | Nucleus, cytoplasm, extracellular | ND |
| High-mobility group protein B2 (HMGB2)* | Intracellular function: stabilization of nucleosome formation and facilitation of transcription factor binding by bending DNA, role in DNA repair; cytosolic nucleic acid sensor | Nucleus, cytoplasm, extracellular | ND |

| | | | |
|---|--|-----------------------------------|----|
| High-mobility group protein B3 (HMGB3)* | Intracellular function: stabilization of nucleosome formation and facilitation of transcription factor binding by bending DNA, role in DNA repair; cytosolic nucleic acid sensor; regulation of proliferation and differentiation of common lymphoid and myeloid progenitors | Nucleus | ND |
| Histone H1.2* | Histones H1 are necessary for the condensation of nucleosome chains into higher order structures | Nucleus | ND |
| Histone H1.3* | Histones H1 are necessary for the condensation of nucleosome chains into higher order structures | Nucleus | ND |
| Histone H2A* | Core component of nucleosome; central role in transcription regulation, DNA repair, DNA replication and chromosomal stability | Nucleus, extracellular | ND |
| Histone H2B* | Core component of nucleosome; central role in transcription regulation, DNA repair, DNA replication and chromosomal stability | Nucleus, extracellular | ND |
| Histone H4* | Core component of nucleosome; central role in transcription regulation, DNA repair, DNA replication and chromosomal stability | Nucleus, extracellular | ND |
| Lupus La protein* | Plays a role in the transcription of RNA polymerase III, most probably as a transcription termination factor as it binds to the 3' termini of virtually all nascent polymerase III transcripts; major autoantigen in SLE | Nucleus, cell surface | ND |
| 14-3-3 protein $\eta/\zeta/\delta$ * | Adapter protein implicated in the regulation of a large spectrum of signaling pathways by binding and modulating the activity of a large number of partners, usually by recognition of a phospho-Ser or phospho-Thr motif | Cytoplasm, nucleus, extracellular | ND |

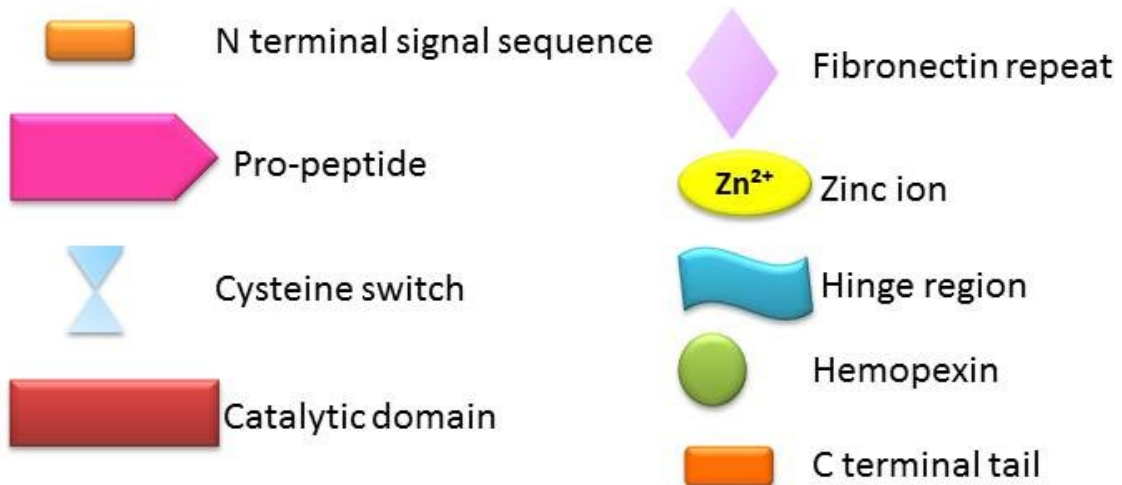
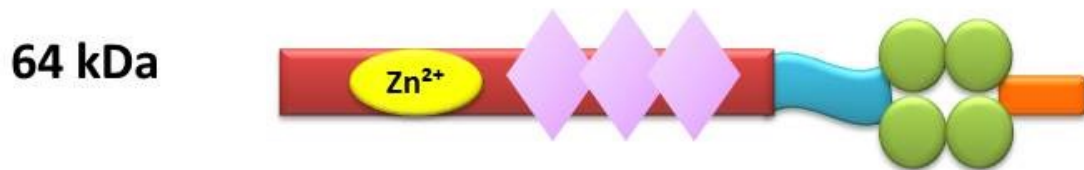
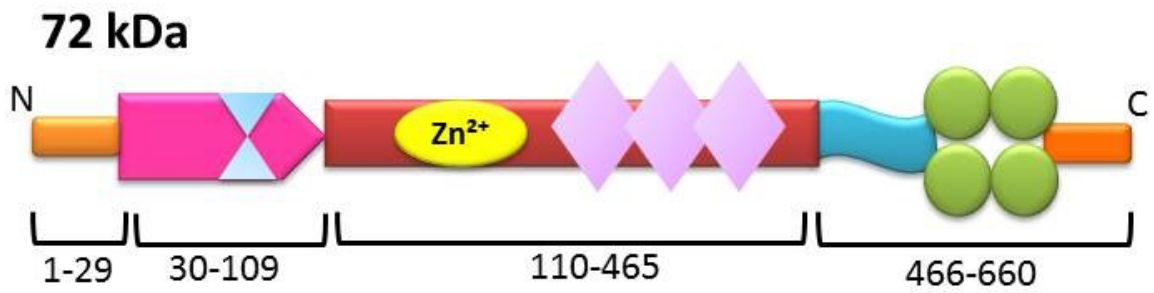
*** denotes proteins that were identified through degradomic screens as summarized by Cauwe and Opdenakker (2010)**
ND: not determined

Table 1.2: Summary of all known nuclear MMPs and their possible functions

| MMP | Function | Biological action Protein / Gene Transcription | References |
|------------|---|---|---|
| MMP-1 | Suggested to be involved in cell cycle/ nuclear membrane breakdown | Unknown | Limb <i>et al.</i> , 2005 Kohrmann <i>et al.</i> , 2009 |
| MMP-2 | Suggested to proteolyse DNA repair proteins and induce apoptosis | PARP-1, XRCC1 | Kwan <i>et al.</i> , 2004 Yang <i>et al.</i> , 2010 Hill <i>et al.</i> , 2012 |
| MMP-3 | Transcription factor | Connective tissue growth factor | Eguchi <i>et al.</i> , 2008 |
| MMP-9 | Suggested to be involved in apoptosis Suggested to be involved in myoblast proliferation | Unknown | Kwan <i>et al.</i> , 2004 Pirici <i>et al.</i> , 2012 Zimowska <i>et al.</i> , 2013 |
| MMP-13 | Not yet identified | Unknown | Cuadrado <i>et al.</i> , 2009 |
| MMP-12 | Transcription factor | Nuclear factor of kappa light polypeptide gene enhancer | Marchant <i>et al.</i> , 2014 |
| MMP-14 | Activation of nuclear MMP-2/ Transcription factor like activity | MMP-2/ phosphoinositide 3-kinase δ | Ip <i>et al.</i> , 2007 (Shimizu-Hirota <i>et al.</i> , 2012) |

Figure 1.1: Domain structures of 72 and 64 kDa MMP-2.

The structure of human MMP-2 consists of an N-terminal domain containing the signal sequence for extracellular export, the propeptide domain containing the cysteine switch, the catalytic domain containing a catalytic Zn²⁺ ion and three fibronectin repeats, the flexible hinge region, the haemopexin domain, and the C-terminal tail. The numbered residues pertaining to the domains of human MMP-2 are shown. The following diagram was adapted from Kandasamy *et al.*, (2010).



CHAPTER 2 – MATERIALS AND METHODS

2.1 Materials

2.1.1 Reagents

The main reagents used in this study were purchased from Sigma-Aldrich (Oakville, ON), unless otherwise specified. UltraPure™ Tris (Tris-HCl) was purchased from Invitrogen (Burlington, ON). NaCl, NaN₃, CaCl₂·2H₂O and HEPES were all purchased from Fisher Scientific (Ottawa, ON). The cell culture reagents were all purchased from Gibco Life Technologies (Grand Island, NY), unless otherwise specified.

Detailed instructions for the preparation of all buffers and gels can be found in Appendix A.

2.1.2 Antibodies

The antibody used to detect MMP-2 in western immunoblotting and immunofluorescence microscopy was a polyclonal antibody against the catalytic domain of recombinant rat 72kDa MMP-2 that was expressed in *Escherichia coli* and raised in rabbit as the host animal (Ab19015, Millipore, Oakville, ON). The MMP-2 antibody used to confirm immunofluorescence results was a kind gift from Dr. David Lovett (UCSF, San Francisco, USA). This polyclonal antibody was produced in a goat from a 16 amino acid peptide of the MMP-2 S1' binding loop within the catalytic domain.

The lamin A/C antibody used was a polyclonal antibody produced in a rabbit injected with a peptide comprised of residues surrounding Asp230 of human lamin

A (2032S, Cell Signaling Technology, Beverly, MA). This antibody can therefore detect full length 70 kDa lamin A (and lamin C), as well as a small 28 kDa fragment of lamin A (and lamin C) resulting from its cleavage by caspase-6 at Asp230-Asn231. The PARP-1 antibody used was a monoclonal antibody produced in a mouse injected with purified PARP from calf thymus (AM-30, Millipore, Oakville, ON). The troponin I antibody, also known as 8I-7, was a monoclonal antibody produced in a mouse from the human cardiac troponin I 100-108 sequence (MA1040, International Point of Care Inc., Toronto, ON).

To assess the purity of the nuclear fractions prepared from rat hearts, a variety of antibodies were used. For cytosolic contamination a GAPDH antibody was used. The monoclonal GAPDH antibody was produced in rabbits with a synthetic peptide near to the carboxy terminus of human GAPDH (14C10, Cell Signaling Technology, Beverly, MA). Antibodies for SERCA 2 and VDAC were used as membrane markers in the test of nuclear fraction purity. The monoclonal SERCA2 ATPase antibody was produced in rabbits with a synthetic peptide corresponding to residues near the carboxy terminus of human SERCA 2 (ab137020, Abcam, Toronto, ON). The polyclonal anti-VDAC1/porin antibody, produced in rabbits with a synthetic peptide derived from residues 150-250 of human VDAC1/ Porin is able to detect all three isoforms of VDAC (ab15895, Abcam, Toronto, ON).

The secondary polyclonal anti-rabbit IgG for immunoblotting was produced in goat. It was conjugated with horseradish peroxidase, followed by treatment to prevent cross reactivity with human immunoglobulins (CLCC42007, Cedarlane, Burlington, ON). The secondary polyclonal anti-mouse IgG was produced in goat, purified by column chromatography and conjugated with horseradish peroxidase, followed

by treatment to prevent cross reactivity with human immunoglobulins (CLCC30007, Cedarlane, Burlington, ON).

The secondary antibodies used for immuno-fluorescence microscopy were a polyclonal goat anti-rabbit IgG conjugated to alexa fluor 488 (A11034, Invitrogen, Burlington, ON) or alexa fluor 594 (A11012, Invitrogen, Burlington, ON). Both were cross-adsorbed against bovine, goat, mouse, rat and human IgGs to prevent cross reactivity. The polyclonal rabbit anti-goat IgG was conjugated with alexa fluor 488 (A11078, Invitrogen, Burlington, ON) and was adsorbed against human and rat serum proteins to prevent cross reactivity.

2.1.3 Markers and standards

Recombinant human lamin A (PRO-690, Prospec Protein Specialists, East Brunswick, NJ) was used in the in vitro proteolysis assay. It was purchased from a company that produced the single non-glycosylated polypeptide in *Escherichia coli*. The recombinant human lamin B (TP301604, Origene, Rockville, MD) was produced with a TrueORF clone with a C-terminal MYC tag (EQKLISEEDL) and was expressed in human embryonic kidney 293 cells and purified with an anti-MYC affinity column.

The molecular weight ladder used in gel electrophoresis experiments was the Blueye prestained protein ladder (GeneDireX, Dubai, UAE) that is a three color set of protein standards with a range from 10 to 245 kDa.

The marker for MMP-2 activity used on gelatin zymography was serum-free conditioned media collected from the human fibrosarcoma (HT1080) cell line (American Type Culture Collection, Manassas, VA) that was produced in the Schulz lab.

2.2 Animal Protocol

This study was done according to the Guide to the Care and Use of Experimental Animals published by the Canadian Council on Animal Care (Olfert *et al.*, 1993), and all animal procedures were approved by the University of Alberta Animal Care and Use Committee.

2.3 Isolated rat heart perfusions

Male Sprague-Dawley rats (250-300 g) were anesthetized by intraperitoneal injection of sodium pentobarbital (240 mg/kg) as previously described (Cheung *et al.*, 2000). The heart was carefully removed from the rat and rinsed in Krebs-Henseleit solution at 4°C. The heart was mounted via the aorta to the cannula of the Langendorff heart perfusion apparatus (LH-04, Experimetria Ltd., Budapest, Hungary) and tied with half of a surgeon's knot using a silk string. The hearts were perfused at constant pressure of 60 mmHg with Krebs-Henseleit solution at 37°C which was continuously gassed with 95% O₂/ 5% CO₂.

The heart was cleaned of any excess epicardial fat tissue, pulmonary veins or arteries. Then deflated latex left ventricular pressure balloon was inserted into the left ventricle of the heart in order to measure the pressure developed during cardiac contraction. The balloon was filled with H₂O with a glass spindle syringe in order to set the left ventricular diastolic pressure to 10 mmHg. The heart was allowed to equilibrate for 15 mins. The experimental time point zero commenced after this equilibration phase. Coronary flow, heart rate and left ventricular pressures were measured during the experiment using SPEL Advanced Haemosys software (Experimetria Ltd.). The difference between left ventricular systolic and diastolic pressures

was defined as left ventricular developed pressure. The rate-pressure product was calculated as the product of heart rate and left ventricular developed pressure.

The three different experimental heart groups were perfused for a total of 75 min (after time zero). The diagram in Figure 2.1 shows the protocols of the different heart perfusions. The aerobic hearts were perfused aerobically for 75 min. The ischemic-reperfused hearts were first perfused aerobically for 20 min, followed by 20 min of global, no-flow ischemia (when the delivery of perfusate was stopped) and then 35 min of aerobic reperfusion (by restoring the flow of perfusate).

The hearts either received the vehicle dimethyl sulfoxide (DMSO, 0.0625% v:v) or MMP inhibitor O-phenanthroline (100 μ M final concentration) through a drug infusion line feeding into the Krebs-Henseleit solution aortic delivery line using a Gilson peristaltic mini-pump (MINIPULS 3, Mandel Scientific, Guelph, ON). The drug or vehicle were infused at flow rate which varied between 50-100 μ L/min. The flow rate of drug infusion was dependent on the coronary flow rate of each heart. The vehicle or drug were infused for a period of 10 min immediately before ischemia, and for the first 10 min after the end of ischemia. It is important to note that aerobic hearts received the vehicle 10 min after the start of perfusion, continuously for a total of 40 min, until the 50 min time point. O-phenanthroline was prepared fresh each day and was dissolved in dimethyl sulfoxide and diluted in 0.9% saline. A similar procedure was followed for the preparation of the vehicle sans drug.

After the perfusion was completed the whole heart was removed from the apparatus, and placed into a 100mm Petri dish filled with ice-cold Krebs-Henseleit solution and left on ice for immediate processing.

2.4 Preparation of subcellular fractions from tissue and cells

The flow chart for isolation of subcellular fractions from tissue and cultured cells is summarized in Figure 2.2.

2.4.1 From perfused rat hearts

Using a scalpel the ventricular heart tissue was minced into small pieces (2-3 mm), collected in a 2 mL Eppendorf tube, and washed with 1 mL of ice cold phosphate buffered saline (PBS) by inverting the tube. Using a new, pre-tared tube 40-60 mg of heart tissue was transferred into it for preparation of heart homogenate. 500 μ L of ice cold cytosolic buffer was added. This was supplemented with 5 μ L of protease inhibitor cocktail (P8340, Sigma-Aldrich, Oakville, ON; inhibits serine, cysteine, and acid proteases, and aminopeptidases).

The heart tissue was then homogenized using a tissue homogenizer (Bio-Gen PRO200, PRO Scientific, Inc., Oxford, CT) for 5 s or until most of the tissue pieces were disrupted. The tissue homogenate was transferred into a QIAshredder (Qiagen, Toronto, ON) microcentrifuge spin-column (1 mL). This device has a unique biopolymer shredding system that homogenizes cell or tissue lysates to reduce viscosity, and to filter any remaining pieces of tissue. In order to form the filtrate the spin-column was centrifuged at 510 g for 5 min at 4°C. The small pellet that formed as a result was re-suspended in the filtrate by pipetting, and 500 μ L of ice cold cytosolic buffer with 5 μ L of protease inhibitor cocktail were added to the tube. This solution was transferred into a clean 1.5 mL Eppendorf tube, and incubated on an end-over-end shaker for 10 min at 4°C. To obtain the cytosolic fraction, the homog-

enate was centrifuged at 4000 g for 10 min at 4°C, and the supernatant containing cytosolic proteins was collected and kept on ice for the duration of the procedure.

The pellet from this was resuspended in 1 mL of ice cold membrane buffer supplemented with 10 µL of the protease inhibitor cocktail, and incubated on an end-over-end shaker for 30 min at 4°C. The suspension was centrifuged at 6000 g for 10 min at 4°C to obtain proteins from membrane bound organelles (contained in the supernatant) and those from nuclei (contained in the pellet), along with cell debris. The digestion of DNA in the nuclear pellet was done by addition of 500 units of benzonase (E1014, Sigma-Aldrich Oakville, ON) in 20 µL of H₂O. By gently flicking the tube with one's finger the pellet was resuspended and incubated for 15 min at room temperature to allow the reaction to proceed. To purify nuclear proteins, 500 µL of ice cold nuclear buffer was added, and the mixture was incubated on an end-over-end shaker for 10 min at 4°C, followed by centrifugation at 6800 g for 10 min at 4°C. The supernatant containing nuclear proteins was collected and kept on ice for the duration of the procedure. The pellet containing insoluble nuclear proteins was resuspended in nuclear buffer supplemented with 8M urea.

Once all subcellular fractions were collected, they were frozen in liquid nitrogen, and kept at -80°C for further analysis. These fractions were later thawed for gelatin zymography and western blotting.

2.4.2 From cultured cells

A 100 mm diameter Petri-dish of confluent HT1080 or neonatal rat ventricular myocytes (NRVM) were used in this protocol (refer to isolation protocol in section 2.9). The cells were washed with PBS and detached using 0.25% trypsin- 0.53

mM EDTA. The cells were collected and centrifuged at 500 g for 10 min at 4°C to pellet the cells, as previously described (Holden and Horton, 2009). The supernatant was discarded, and the pellet was resuspended and washed with 500 µL of ice cold PBS, and pelleted at 500 g for 10 min at 4°C. The supernatant was discarded and the pellet was resuspended by pipetting in 800 µL of ice cold cytosolic buffer containing 8 µL of protease inhibitor cocktail that was added fresh on the day of the fractionation. The suspension was incubated on an end-over-end shaker at 4°C for 10 min to allow the cells to lyse, and the lysate was centrifuged at 2000 g for 10 min at 4°C. The supernatant containing the cytosol enriched fraction was collected and kept on ice, and the pellet was resuspended in 800 µL of ice cold membrane buffer with 8 µL of protease inhibitor cocktail and then incubated for 30 min on ice. To collect the proteins from membrane bound organelles and to pellet nuclei, the suspension was centrifuged at 7000 g for 10 min at 4°C. The supernatant was collected and kept on ice, while the pellet was washed and pelleted once with 500 µL of ice cold PBS to obtain clean nuclear samples. The supernatant was discarded and the pellet was resuspended in 400 µL of ice cold nuclear buffer, containing 500 units of benzonase to digest DNA in the nuclear pellet. It was incubated for 1 h on an end-over-end shaker at 4°C. The cell debris was pelleted at 7800 g for 10 min at 4°C and the supernatant containing nuclear proteins was collected.

Once all subcellular fractions were collected, they were frozen in liquid nitrogen, and kept at -80°C for further analysis. These fractions were later thawed for gelatin zymography and western blotting.

2.5 Preparation of frozen tissue homogenates

The unused minced ventricular tissue (after 2.4.1 preparation) of the perfused rat hearts was collected with tweezers (without being blotted dry) in a 2 mL Eppendorf tube, and frozen in liquid nitrogen and kept at -80°C for further use. The entire procedure of crushing the frozen heart tissue was done with liquid nitrogen cooled equipment. The ventricular tissue segments were removed from the tubes with tweezers and placed into a mortar and crushed into powder with a pestle. To the crushed heart powder ~ 5 mL of liquid nitrogen was added and boiled off, which caused the heart powder to congregate into a pile. The powder was immediately disturbed by tapping the mortar on the bench, and transferred by scooping into a 1.5 mL cryovial through a funnel. The collected cryovial with the heart powder was kept in liquid nitrogen until the homogenization step.

In a pre-tared tube the heart powder was weighed out and radioimmunoprecipitation assay (RIPA) buffer supplemented with 8M urea was added (the volume of RIPA+8M urea added was four times the heart powder weight). The suspension was homogenized using a tissue homogenizer (Bio-Gen PRO200) and centrifuged at 10,000 g for 10 min at 4°C . The supernatant was collected, aliquoted, frozen in liquid nitrogen and kept at -80°C .

2.6 Protein quantification assay

The tissue homogenate and cell lysate protein concentrations were measured using the bicinchoninic acid assay. Bovine serum albumin (Pierce Life Technologies, Rockford, IL) was used as the reference protein to prepare a standard curve with a concentration range of 31.25-1000 $\mu\text{g}/\text{mL}$. 10 μL of the reference protein standard

was loaded into a 96 well plate in triplicate. Unknown samples diluted 1:10 with H₂O and 10 µL of this was loaded in duplicate. Bicinchoninic acid solution (Sigma-Aldrich, Oakville, ON) and copper (II) sulfate solution 4% (w/v) (prepared from copper (II) sulfate pentahydrate) were mixed at a 50:1 ratio. 200 µL of this mixture was added to each well. The plate was incubated for 30 min at 37°C, and the colorimetric change due to the reduction of copper (Cu II → Cu I) was measured at 560 nm with a UVmax Kinetic microplate reader. The data were analyzed using SoftMax Pro (v 5.2 rev C) software.

2.7 Western blotting

Gels for 8% sodium dodecyl sulfate polyacrylamide gel electrophoresis (SDS-PAGE) gels were prepared according to the protocol given in the Appendix A. 15 µg total protein equivalent of the tissue homogenate, or an equal percent (6%) of the total volume of each subcellular fraction were added to SDS-PAGE loading buffer and heated to 95°C for 5 min to denature the proteins. The samples were loaded into individual wells along with a lane loaded with human recombinant MMP-2 or human recombinant lamin A/C as a standard. 5 µL of Blueeye prestained protein ladder was used in the first lane to estimate molecular weights. The gel was run at 100 V for 120 min at room temperature. Proteins were transferred by the semi-dry method from gels onto presoaked (in 100% methanol) 0.2 µm polyvinylidene difluoride membranes (Bio-Rad, Mississauga, ON) at 100 V for 60 min at 4°C in Towbin buffer. The membranes were blocked for 2 h at room temperature in 5% w/v skim milk powder (Carnation, Markham, ON) prepared in TTBS buffer. Then the membranes were transferred into clean containers with a solution containing the

primary antibody for either MMP-2, lamin A/C, SERCA or GAPDH which were diluted (at 1:10,000) in 5% w/v skim milk powder in TTBS and incubated overnight at 4°C on an end-over-end shaker.

The next morning the membranes were washed 5 times for 7 min each with TTBS buffer at room temperature to remove any excess primary antibody. Immediately thereafter they were incubated for 1 h in 5% w/v skim milk powder in TTBS with the appropriate secondary antibody (goat anti-rabbit, 1:10,000; goat anti-mouse, 1:5,000) on a shaker at room temperature. The membranes were washed 5 times for 7 min each with TTBS and the bands were visualized by chemiluminescent detection reagent (Amersham ECL Prime, GE Healthcare, Buckinghamshire, UK). The membranes were exposed to blue medical X-ray film (Fujifilm, Tokyo, Japan), from 1 s to 20 min, depending on the strength of the signal. The film was developed using an OPTIMAX X-Ray film processor (PROTEC GmbH & Co, Oberstenfeld, Germany) and scanned using a GS-800 calibrated densitometer (Bio-Rad, Mississauga, ON). The band densities were analyzed using QuantityOne (Bio-Rad, v 4.6.6) and ImageJ (NIH, v 1.48) software.

In some cases where checking the overall protein load was important in the experiment, the membranes were stained with Ponceau S (0.1 % w/v in 5% acetic acid, Sigma-Aldrich, Oakville, ON) for 15 min. The membranes were then washed with an aqueous solution of 10% v/v acetic acid for 5 min at room temperature. The membranes were immersed in 100% methanol for 5 min, dried and visualized.

2.8 Gelatin zymography

Equal percent (4%) of the total volume of each subcellular fraction was prepared with zymography loading buffer. The samples were loaded into individual wells on an 8% polyacrylamide gel which incorporated 2 mg/mL of gelatin (Sigma-Aldrich, Oakville, ON). 5 μ L of Blueeye prestained protein ladder, and 1.5 μ L of conditioned media from HT1080 cells (used as an MMP-2 standard) were also loaded onto the gel. Electrophoresis was performed for 120 min at 100 V at room temperature. The gels were washed in separate plastic containers with 2.5% (v/v) Triton X-100 (Fisher Scientific, Fair Lawn, NJ) in H₂O three times for 20 min at room temperature to remove sodium dodecyl sulphate and to allow proteins to renature.

The gels were then placed into zymography incubation buffer and incubated for approximately 42-46 h at 37°C. After incubation, the buffer was removed and the gels were stained with Coomassie zymography staining solution for 3 h at room temperature, and destained with destaining solution (2% methanol, 4% acetic acid v/v in H₂O) to remove excess stain (3 times for 30 min at room temperature).

The gels were scanned using a GS-800 calibrated densitometer. The band densities were analyzed using QuantityOne (Bio-Rad, v 4.6.6) and ImageJ (NIH, v 1.48) software.

2.9 Immunofluorescence confocal microscopy

The circular coverslips (#1.5, Electron Microscopy Sciences, Hatfield, PA) 25 mm in diameter, 0.16-0.19 mm thickness, were washed with 70% v/v ethanol for 5 min, and dried before being placed in a 35 mm diameter Petri dish. The coverslips were covered with 1 mL of Dulbecco's modified eagle medium supplemented with

10% v/v fetal bovine serum and 1% penicillin-streptomycin mixture. HT 1080 cells, mouse neonatal fibroblasts or NRVMs were seeded onto the cover slips (300 μ L or 1.0×10^5 cells for each well). The staining procedure below was done in the same way with NRVM, HT 1080 and mouse neonatal fibroblasts isolated from wild type and MMP-2 knock out mice.

The next day the cells were washed with PBS and fixed for 5 min with 1 mL 4% w/v paraformaldehyde prepared in PBS. The cells were washed once with PBS and permeabilized for 5 min with 0.5% v/v Triton X-100 in PBS to allow intracellular and intranuclear antigens to diffuse inside the cells. The permeabilized cells were washed twice with PBS, and the coverslips were incubated face down on parafilm, cells touching the 25 μ L drop of antibody solution (diluted in PBS to 1:200) in the dark for 30 min. The coverslips were placed back in the 35 mm Petri dish and washed once with 0.1% v/v Triton X-100 in PBS, and twice with PBS for one min each, only to remove any excess primary antibody. The coverslips were incubated in a similar manner face down on parafilm, the cells touching the 25 μ L drop of conjugated fluorescent secondary antibody solution (diluted in PBS to 1:500) in the dark for 30 min. The coverslips were then washed with 0.1% v/v Triton X-100 in PBS, and twice with only PBS for one min each, and then mounted onto slides with 10 μ L of Fluoro-gel II mounting media containing 4',6-diamidino-2-phenylindole (DAPI; Electron Microscopy Sciences, Hatfield, PA) in order to stain DNA of the nucleus. The cells were visualized 30 min after allowing DAPI to equilibrate. Leica SP5 microscope was used to collect the images and they were analyzed using Leica LAS AF software and further analyzed by Image J.

2.10 Isolation and culture of neonatal rat ventricular myocytes

Neonatal rat ventricular myocytes were isolated from 1 day old Sprague-Dawley rats (Karnabi *et al.*, 2009). The heart ventricles were carefully excised with as little of the atria attached as possible and washed with ice cold PBS for several washes until clear. In a Petri dish placed on ice any attached atria was removed, and the ventricles were cut into small pieces with a scalpel. The pieces were transferred into a 25 mL flask with a sterile pipette. The tissue was digested by adding 10 mL of PBS containing 0.5 mL of each of the following enzyme solutions: 0.10% w/v collagenase, 0.05% w/v trypsin and 0.025% w/v deoxyribonuclease I (Worthington Biochemical Corporation, Lakewood, NJ). This was then incubated on a shaker at 37°C for 5 min and then transferred into a 50 mL conical tube. 10 mL of Dulbecco's modified Eagle medium with 20% v/v FBS (Gibco Life Technologies) was added and centrifuged at 500 g for 1 min at 37°C. The supernatant was discarded and the pellet was resuspended in 15.5 mL of PBS with 1.5 mL each of collagenase, trypsin and deoxyribonuclease I at the same concentration as above.

The cell suspension was transferred into a 25 mL flask and incubated on a shaker at 37°C for 20 min. After digestion the solution was transferred into a 50 mL conical tube with 20 mL of Dulbecco's modified Eagle medium 20% v/v FBS, and centrifuged for 1 min at 500 g at 37°C. The supernatant was transferred into a clean tube, while the pellet was digested further by the addition of the enzymes at the same concentration as above and incubated on a shaker at 37°C for 20 min. The collected supernatant from the digestions was centrifuged at 1000 g for 7 min at 4°C. The supernatant was discarded and the pellet was resuspended in 15 mL of Dulbecco's modified Eagle F-12 medium supplemented with 1% v/v penicillin-

streptomycin and 10% v/v FBS. The cells were plated to a 150 mm diameter Petri dish, and placed into cell culture incubator (37°C, 5% CO₂) for 2 h. Since the fibroblasts attach faster to the dish than the cardiomyocytes, the media containing the myocytes was collected and plated onto a clean Petri dish as needed.

The next day after isolation of NRVMs, the culture medium was removed and the cells were washed with PBS to remove any unattached cells. New Dulbecco's modified Eagle F-12 medium supplemented with 1% v/v penicillin streptomycin and 10% v/v FBS was added to the plates. The experiments were performed with primary cultures, a few days after isolation to allow the cells to recover from the stresses and damage that occurs during the enzymatic digestion. The cardiomyocytes were considered to be ready for experiments once they began to spontaneously contract when observed under the microscope.

2.11 Cell Culture

Both HT1080 cells, mouse neonatal fibroblasts and NRVMs were incubated at normal conditions of 37°C, 5% CO₂ in a humidified incubator. The media used was Dulbecco's modified Eagle medium F-10 (or F-12 with NRVMs), supplemented with 100 U/mL penicillin, 100 µg/mL streptomycin and 10% v/v FBS.

2.11.1 HT1080 cells

The HT1080 cell line was obtained from the American Type Culture Collection (Manassas, VA). The cryogenically frozen cells were thawed and plated into a T25 flask. The cells were incubated in Dulbecco's modified Eagle medium F-10, supplemented with 100 U/mL penicillin, 100 µg/mL streptomycin and 10% v/v FBS.

The next day the cells were passaged at a 1:10 ratio. The cells were passaged twice per week or until they reached 70% confluency. A new batch of cells was prepared from frozen stock after 20 passages of the cell line.

HT1080 conditioned medium was used as a standard for MMP-2 and MMP-9 gelatinolytic activity in gelatin zymography experiments. Once cells were ready, they were washed three times with serum-free medium and incubated in serum-free medium with 0.1 μM phorbol ester 12-o-tetradecoyl-phorbol-13-acetate for 24 hours. The next day the medium was collected, centrifuged at 1500 g for 10 min at room temperature, the supernatant was collected, aliquoted and flash frozen in liquid nitrogen, and stored at -80°C .

2.12 In silico cleavage site analysis for lamin A or B

The primary amino acid sequence of human lamin A or B was inputted in FASTA format (single letter amino acid code text-based format) into the Protease specificity prediction server (PROSPER, <https://prosper.erc.monash.edu.au/>). This webserver analyses the sequence submitted and predicts the cleavage sites for twenty four different protease types. Once the analysis was complete an e-mail was sent with the link to the results.

2.13 In vitro proteolysis assay

2.13.1 4-aminophenylmercuric acetate activation of MMP-2

The 72 kDa zymogen form of MMP-2 can be chemically activated by 4-aminophenylmercuric acetate (APMA). APMA disrupts the Cys73 sulfhydryl and Zn^{2+} hydrogen bond through perturbation of the proMMP-2 molecule, and the

conformational change results in disruption of the hydrogen bond (Itoh *et al.*, 1995). Purified human recombinant 72 kDa MMP-2 (prepared in our lab) at a concentration of 200 µg/mL was mixed with 1 mM of APMA in activation buffer with the final volume of 200 µL. The mixture was gently flicked to mix and incubated for 2 h at 37°C. This reaction mixture as well as unreacted MMP-2 were diluted with H₂O to give a final concentration of 1 ng/µL and an aliquot of each was subjected to gelatin zymography. Successfully activated MMP-2 was aliquoted and kept at -20°C for any further experiments.

2.13.2 Lamin A proteolysis

Human recombinant lamin A (0.09 µg/µL) was mixed with APMA-activated MMP-2 in incubation buffer with an increasing enzyme:substrate molar ratio from (1:500 to 1:10) to give a final volume of 22 µL. O-phenanthroline was used to see if the proteolysis of lamin A was due to MMP-2 activity. MMP-2 at 1:10 ratio (0.008 µg/µL) was pre-incubated with O-phenanthroline (100 µM, dissolved in DMSO) for 15 min at 37°C before adding lamin A. The proteolysis of purified human recombinant troponin I (prepared in our lab) by MMP-2 was used as positive control (Wang *et al.*, 2002). 0.05 µg/µL of troponin I was incubated with 0.001 µg/µL of APMA-activated MMP-2 (enzyme:substrate molar ratio 1:125). All samples were incubated for 2 h at 37°C. The resulting samples from the proteolysis assay were immediately prepared and run on a 10% SDS PAGE gel.

2.13.3 Lamin B proteolysis

Human recombinant lamin B (0.05 $\mu\text{g}/\mu\text{L}$) was mixed with APMA-activated MMP-2 in incubation buffer with an increasing enzyme:substrate molar ratio from (1:500 to 1:10) to give a final volume of 22 μL . The proteolysis of purified human recombinant troponin I (prepared in our lab) by MMP-2 was used as positive control (Wang *et al.*, 2002). 0.05 $\mu\text{g}/\mu\text{L}$ of troponin I was incubated with 0.001 $\mu\text{g}/\mu\text{L}$ of APMA-activated MMP-2 (enzyme:substrate molar ratio 1:125). All samples were incubated for 2 h at 37°C. The resulting samples from the proteolysis assay were immediately prepared and run on a 10% SDS PAGE gel.

2.14 SDS PAGE gel electrophoresis

SDS-PAGE electrophoresis was performed to determine the cleavage of lamins by MMP-2. SDS loading buffer (4 μL) was added to MMP-2 proteolysis assay samples for a total volume of 26 μL . These were heated to 95°C for 5 min to denature the proteins. The samples (26 μL each) were loaded into individual lanes along with lamin A or B markers and 5 μL of Blueeye prestained protein ladder. The gels were run at 100 V for 120 min at room temperature. The gels were stained with 0.25% w/v Coomassie solution for 3 h to visualize the bands. They were washed three times for 30 min with destaining solution to remove excess stain. The gels were scanned using a GS-800 calibrated densitometer and band densities were analyzed with QuantityOne (Bio-Rad, v 4.6.6) and ImageJ (NIH, v 1.48) software.

2.15 Flow cytometry

4.0×10^6 HT1080 cells (equivalent to two 100 mm Petri dishes) were grown to 80% confluency for this experiment. The cells were detached from their plates as previously described in section 2.4.2, trypsinized and centrifuged at 500 g for 10 min at 4°C. The pelleted cells were resuspended by pipetting up and down with 1 mL tip in 2 mL of PBS, and divided equally into two 1.5 mL Eppendorf tubes containing approximately 1.0×10^6 cells each. The cells were centrifuged and pelleted at 500 g for 5 min at 4°C. The pellet was resuspended in 100 μ L of 4% w/v paraformaldehyde in PBS, and incubated for 15 min at 4°C to fix the cells. The fixed cells were centrifuged at 700 g for 5 min at 4°C, as fixed cells require greater centrifugal force to sediment. The pellet was washed once with PBS, and the fixed cells were permeabilized for 15 min at 4°C with 0.5% v/v Triton X-100 in PBS and pelleted at 700 g for 5 min at 4°C. Once the cells were permeabilized the pellets were gently resuspended by manually flicking the Eppendorf tubes. This is important as the cell membranes are fragile and the cells have to be kept intact for the experiment. The permeabilized cells were washed once with PBS, pelleted and resuspended in 100 μ L of PBS containing the primary antibody solution diluted at 1:200 in PBS. This was incubated first for 20 min on ice, followed by 20 min at room temperature. The cells were pelleted at 700 g for 5 min at 4°C and resuspended in 0.1% v/v Triton X-100 in PBS for one wash, followed by one wash in PBS. After the last wash the pelleted cells were resuspended in 2% w/v paraformaldehyde in PBS, and left overnight at 4°C.

The next morning the cells were pelleted at 700 g for 5 min at 4°C. 100 μ L of secondary antibody solution diluted 1:500 in PBS was added to the pellet and

resuspended by manual flicking, and incubated for 20 min on ice, followed by 20 min at room temperature. The secondary antibody incubation steps were performed in the dark. The cells were pelleted at 700 g for 5 min at 4°C and were resuspended in 0.1% v/v Triton X-100 in PBS for one wash, followed by one wash in PBS. To stain the nucleus DAPI (Sigma-Aldrich, Oakville, ON) was used, as it binds strongly to AT rich regions of DNA. DAPI (0.1 µg/mL in 100 µL of PBS) was added to the cells and this was incubated for 30 min at room temperature. Compensation control samples are single fluorophore stained samples that are required for the calculation of fluorescence compensation that corrects for any false positive signals resulting from the spectral overlap of two or more fluorochromes. One sample that was stained with secondary antibody (the compensation control sample) did not have DAPI added, and was used in the experiment to calculate the compensation matrix. The cells were sorted using a Mark II Amnis Image Stream flow cytometer (Amnis Corporation, Seattle, WA).

The sample data was acquired with the help of Aja Rieger at the Faculty of Medicine and Dentistry Flow Cytometry Facility. The start up on the Mark II Amnis Image Stream was performed, and samples were loaded into the chamber. Using the ISS IDEAS software the population was gated to collect only single cell events. The software was set up the following way: channel 01 (bright field) and channel 06 (scattering channel), plus fluorescence channels as required. 10,000 events at 40X magnification each were collected for the experiment and the compensation matrix.

2.16 Correlational analysis of protein levels versus recovery of heart contractile function

The percentage recovery of mechanical function was defined as the ratio of ventricular developed pressure at the end (75 min) of perfusion over the same parameter at the start of perfusion (0 min during aerobic perfusion). Spearman's rank-order correlation was used to measure the statistical dependence between the protein levels of PARP-1 or troponin I and the percentage recovery of heart contractile function.

2.17 Statistical analysis

Results are expressed as mean \pm SEM for n individual experiments. One-way or two-way ANOVA followed by Fisher's LSD test were used to analyze differences between groups. Differences were considered significant at $p < 0.05$. Statistical analysis was performed using Prism 5 (v5.01) software.

Figure 2.1: The schematic diagram of the three groups of isolated rat hearts perfused aerobically or subjected to ischemia-reperfusion (I/R) injury.

All three groups of hearts were perfused for a total of 75 min which is shown by blue bars. The vehicle or drug infusion is denoted by the dashed line in orange. The period of global, no-flow ischemia is shown by the red bar in I/R hearts. The aerobic control hearts were perfused for 75 min. The I/R hearts were first perfused aerobically for 20 min followed by 20 min global, no-flow ischemia and a 35 min period of aerobic reperfusion. The ventricular tissue from these hearts were used fresh for subcellular fractionation, and the rest of the ventricular tissue was frozen with liquid nitrogen and stored at -80°C until the frozen tissue was homogenized.

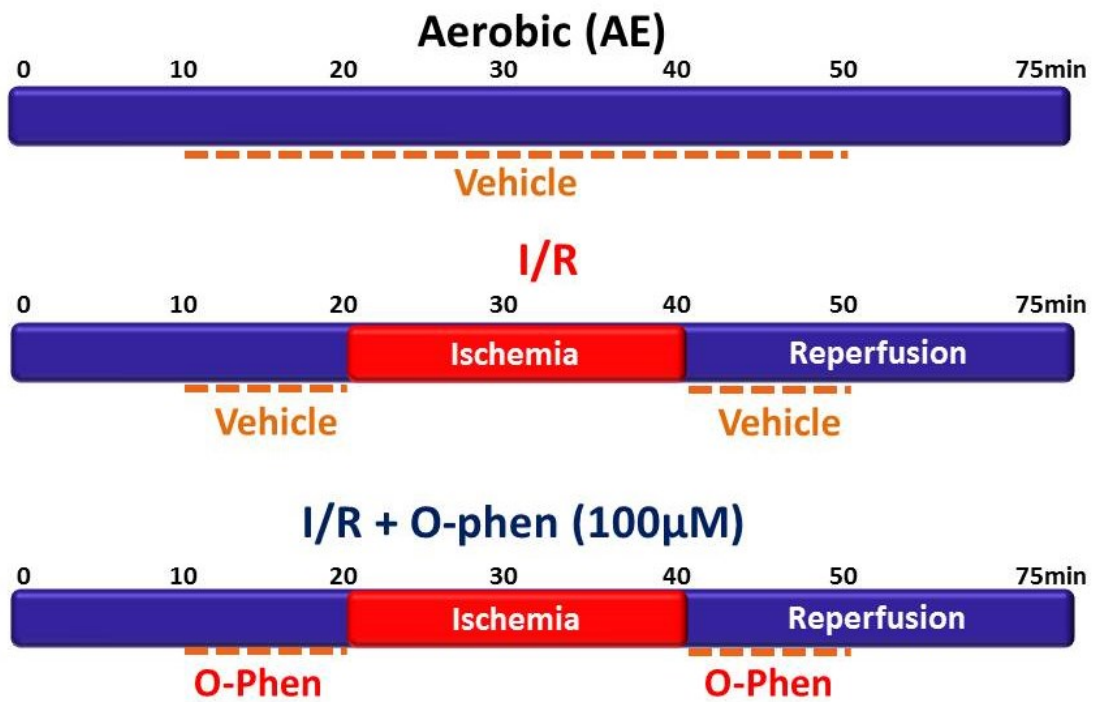
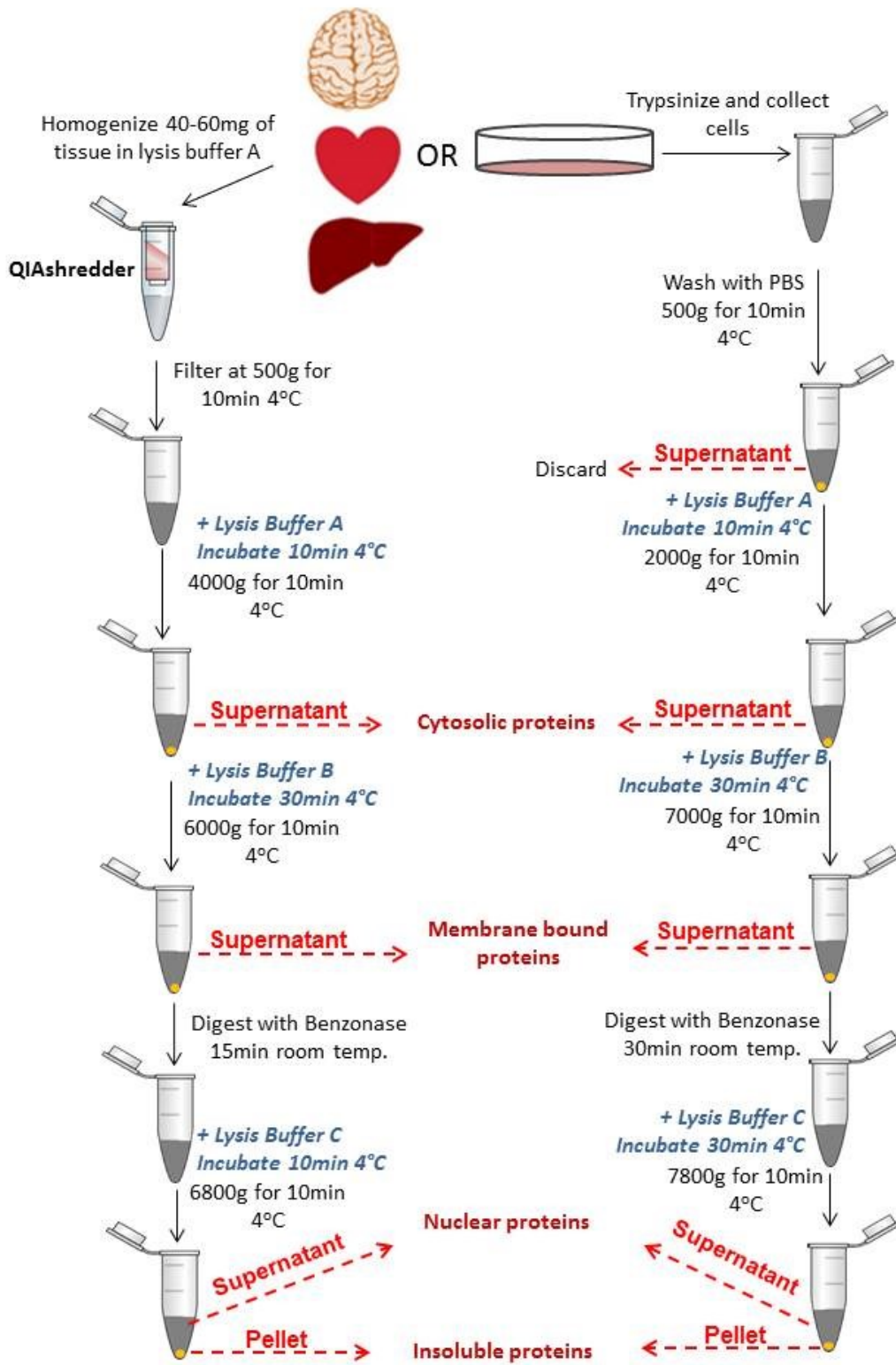


Figure 2.2: Schematic summary diagram of the protocol of subcellular fractionation from either isolated perfused rat hearts or from cultured cells.

The flow chart shows the summary of the protocols for subcellular fractionation from tissue and cultured cells. The differences between the two methods for tissue and cultured cells are easily identified in this visual diagram.



CHAPTER 3 - RESULTS

3.1 Subcellular distribution of MMP-2

3.1.1 NRVM

The first objective of this study was to determine the localization of MMP-2 to the nucleus of myocytes under normal cell culture conditions. The subcellular distribution of MMP-2 in NRVM was assessed by immunofluorescence confocal microscopy (Figure 3.1). MMP-2 was, as expected, dispersed diffusely throughout the cytoplasm and also found in the nucleus of the cells. Colocalization of the DAPI (blue) and MMP-2 (red) signals resulted in purple staining in the merged images. The concentrated nuclear localization of MMP-2 signal was seen in most but not all cells. Staining with the two antibodies against MMP-2, Ab19015 (Figure 3.1, A) and the S1' loop antibody (Figure 3.1, B) yielded a similar distribution. Non-specific fluorescence was not observed in NRVM incubated with either primary or secondary antibody alone (data not shown).

Then we assessed the relative amount of MMP-2 protein level and activity in the nucleus compared to the remainder of the cell. The subcellular fractions from cytosol, membrane and nucleus (C, M and N respectively) were isolated from NRVM. The fraction purity was assessed by western blotting for cellular markers (Figure 3.2, A) specific to certain subcellular locations. Lamin A/C was the nuclear marker and was primarily found in the nuclear fraction as expected, with only a small amount appearing in the membrane fraction. GAPDH was the cytosolic marker and was primarily found in the cytosolic fraction, with markedly less in the membrane fraction and none in the nuclear fraction. Thus, the nuclear fraction was free of any cytosolic contamination.

The nuclear protein levels and activity of MMP-2 were calculated as a percent of the combined total protein level or activity of all three fractions. The protein level of MMP-2 was measured by western blotting (Figure 3.2, B). The percent total protein levels of MMP-2 were highest in the cytosol followed by membrane fraction (45% and 40%, respectively), with 15% of MMP-2 protein levels being in the nucleus (Figure 3.2, C). Gelatin zymography was used to measure the enzymatic activity of MMP-2 in each fraction (Figure 3.3, A). The total percent activity of MMP-2 was highest in the membrane and then cytosol fractions (70% and 20%, respectively), 10% of MMP-2 activity was in the nuclear fraction (Figure 3.3, B).

3.1.2 HT 1080 cells

The subcellular distribution of MMP-2 was also visualized in HT 1080 cells by immunofluorescence confocal microscopy with Ab19015 (Figure 3.4, A) and the S1' loop antibody (Figure 3.4, B). Colocalization of the DAPI (blue) and MMP-2 (red) signal resulted in purple staining in merged images. MMP-2 was dispersed throughout the cytoplasm, as well as being concentrated to the nucleus. Once again concentrated nuclear localization of MMP-2 signal was not seen in all cells. The distribution pattern observed was alike for either of the antibodies. There was no fluorescence observed in HT 1080 cells incubated with either primary or secondary antibody alone (data not shown).

In order to determine what percentage of the HT 1080 cell population had concentrated nuclear MMP-2, imaging flow cytometry was performed on cells stained for MMP-2 (S1' loop antibody) and DAPI (Figure 3.5). In the following experiment 11,889 HT 1080 cells were sorted and imaged; these cells were defined as

the total population. This cell population was further analyzed to see the colocalization of MMP-2 and DAPI signals. The degree of correlation between the nuclear stain and the MMP-2 immunostain from each cell was calculated and defined as a similarity score (Barteneva *et al.*, 2012). The similarity score of >1.5 in this experiment was chosen to define the colocalization of MMP-2 and DAPI spectral signals in the nucleus. The representative images of selected cells that had mainly cytoplasm (Figure 3.5, A) or nuclear (Figure 3.5, B) distribution of MMP-2 in HT1080 cells are shown. The histogram (Figure 3.5, C) showed a normal distribution of the similarity score among the cells analyzed, and the majority of the cells had a similarity score >1.5 . From this, it was determined that 11.4% of the cells had MMP-2 concentrated to the cytoplasm, while 88.6% of the cells had MMP-2 concentrated to the nucleus.

3.1.3 Wild type and MMP-2 knock out neonatal fibroblasts from mice

The distribution of MMP-2 in subcellular fractions of NRVM differs from those seen by immunofluorescence. The western blots of subcellular fractions from NRVM showed that 15% of total MMP-2 protein levels were in the nucleus, while the immunofluorescence showed a much greater amount of MMP-2 localized to the nucleus. The immunofluorescence and western blot experiments were performed using the same antibody (Ab19015); therefore this disparity was not due to a difference in antibodies used between experiments. In order to confirm that this apparent nuclear signal was not due to non-specific binding of the antibody to other nuclear proteins, neonatal fibroblasts isolated from both wild type and MMP-2 knock out mice were examined.

Firstly, antibody Ab19015 (Figure 3.6) was tested on wild type (WT) and MMP-2 knock out (KO) cells. The immunostaining procedure and concentration of primary and secondary antibody used was identical to the procedure performed with NRVM, to validate that the antibody indeed recognized MMP-2 at the concentration used in the original experiment. In wild type cells, stained with Ab19015 for MMP-2 (red) and DAPI (green), MMP-2 was diffusely distributed throughout the cytoplasm and more concentrated in the nucleus. The merged images showed yellow colocalization of the MMP-2 and DAPI signals, indicating that these cells had nuclear MMP-2, consistent with our observations in HT 1080 and NRVM. In contrast, little staining for MMP-2 was observed in MMP-2 knock out cells, indicating that this antibody was not recognizing a non-specific nuclear protein in wild type, NRVM or HT 1080 cells.

Secondly, S1' loop antibody (Figure 3.7) was tested on wild type and MMP-2 knock out cells. The immunostaining procedure and concentration of primary and secondary antibody used was again as used for NRVM. In wild type cells, stained with S1' loop antibody for MMP-2 (red) and DAPI (green), MMP-2 was diffusely distributed throughout the cytoplasm and slightly more concentrated in the nucleus. The merged images showed yellow colocalization of the MMP-2 and DAPI signals, indicating that these cells had nuclear MMP-2, consistent with our observations in HT 1080 and NRVM. In contrast, very little staining for MMP-2 was observed in MMP-2 knock out cells, indicating that this antibody was not recognizing a non-specific nuclear protein in wild type, NRVM or HT 1080 cells.

3.2 Functional performance of rat hearts subjected to I/R injury

The isolated rat hearts were perfused by the Langendorff method in one of three ways: a) aerobically (AE, control), b) inducing I/R injury by global, no-flow ischemia followed by reperfusion (I/R), and c) I/R injury with an MMP inhibitor, o-phenanthroline (I/R+O). The contractile performance of isolated rat hearts subjected to I/R injury was measured and the protective effect of o-phenanthroline was confirmed by measured or derived functional parameters (Figure 3.8). Heart rate (Figure 3.8, A), coronary flow (Figure 3.8, B), left ventricular developed pressure (Figure 3.8, C) and the product of heart rate and developed pressure (Figure 3.8, D) were used to determine the vascular and contractile function of these hearts. The AE hearts received vehicle; the coronary flow and contractile function of these hearts was not impaired by the vehicle treatment. The I/R hearts that only received vehicle had reduced heart rate, coronary flow, developed pressure and rate-pressure product during the reperfusion phase after global, no-flow ischemia. Treatment of I/R hearts with o-phenanthroline conserved coronary flow and left ventricular developed pressure (difference between left ventricular systolic and diastolic pressures) during the reperfusion phase (50 min – 75 min). Heart rate and the rate-pressure product (product of heart rate and left ventricular developed pressure) were improved in I/R+O hearts at 60 and 70 min time points, compared to I/R hearts. Thus, inhibition of MMP activity with o-phenanthroline improved the contractile function of I/R hearts, as previously shown (Wang *et al.*, 2002).

3.3 Subcellular fractions isolated from rat hearts

3.3.1 Subcellular fraction purity

The ventricular tissue from isolated rat hearts (AE, I/R and I/R+O) were used to isolate cytosol, membrane bound organelle and nuclear fractions. The purity of subcellular fractions prepared from normal rat heart ventricular tissue was analyzed by western blot against specific subcellular markers (Figure 3.9). The cytosol marker was GAPDH, membrane bound organelle markers were SERCA2 and VDAC, and the nuclear marker was lamin A/C. The absence of GAPDH, SERCA2 and VDAC bands in the nuclear fraction demonstrated that it was free of cytosol and membrane contamination.

3.3.2 Changes in MMP-2 protein levels and activity with myocardial I/R injury

Myocardial I/R injury activates MMP-2 in heart tissue (Cheung *et al.*, 2000); however it is not known what happens in the subcellular compartments to MMP-2 protein levels and activity. Therefore, the protein level and activity of MMP-2 for each fraction were analyzed and calculated as a percent of total protein levels or activity in all three fractions (cytosol, membrane and nucleus). The changes in MMP-2 protein levels (Figure 3.10) or activity (Figure 3.11) in cytosol, membrane and nuclear fractions in AE, I/R and I/R+O hearts were assessed by western blotting or gelatin zymography, respectively. In I/R+O hearts, nuclear MMP-2 protein level made up a greater proportion of total cellular MMP-2 than in AE hearts (Figure 3.10, B). Likewise, MMP-2 activity in the nuclear fraction of I/R+O hearts made up a greater proportion of total cellular MMP-2 activity than in AE hearts (Figure 3.11,

B). Surprisingly, even though the percent total nuclear protein levels of MMP-2 (Figure 3.10, B) in I/R hearts was not significantly increased relative to AE control hearts, the percent total nuclear activity of MMP-2 (Figure 3.11, B) was significantly increased in I/R hearts. Thus, a factor besides increased protein levels was responsible for the increase in nuclear MMP-2 activity in I/R hearts.

3.4 Identifying nuclear targets of MMP-2

3.4.1 In silico analysis of lamin A or B proteolysis by MMP-2

One of the objectives of this study was to identify potential nuclear substrates of MMP-2. It was hypothesized that lamins, structural nuclear proteins, could be a proteolytic target of MMP-2 in the nucleus under I/R conditions. In order to identify if MMP-2 can proteolyse nuclear lamins, I first performed an in silico analysis which predicts MMP-2 proteolytic sites within the lamin A or lamin B sequence (Table 3.1) using the online protease specificity prediction tool PROSPER (De Bock *et al.*, 2015). This analysis showed that both lamin A and B may be proteolysed by MMP-2 at two sites. MMP-2 could potentially proteolyse lamin A at positions 76 and 308, leading to formation of C-terminal fragments of 70 and 43 kDa, respectively. MMP-2 could also potentially proteolyse lamin B at positions 309 and 562, leading to formation of C-terminal fragments of 33 and 3 kDa, respectively.

3.4.2 In vitro proteolysis assay of lamin A or B by MMP-2

In order to confirm the in silico results, an in vitro degradation assay was performed where human recombinant lamin B (Figure 3.12) or A (Figure 3.13) were individually tested for their susceptibility to proteolytic cleavage by purified human

recombinant MMP-2. The known MMP-2 substrate troponin I (Wang *et al.*, 2002) was used as a positive control for MMP-2 activity (Figure 3.12, A). Incubation of troponin I with MMP-2 yielded several degradation products after 2 hours incubation with MMP-2 at 37°C (1:125 molar ratio of enzyme to substrate). Incubation of increasing concentrations of MMP-2, from 1:500 to 1:10, with lamin B for 2 hours at 37°C did not show evidence for its proteolysis (Figure 3.12). The band densities of lamin B, and a faint 48 kDa band did not change with increasing concentrations of MMP-2 (Figure 3.12, B). In contrast, lamin A incubated with increasing concentrations of MMP-2 for 30 minutes at 37°C yielded a ~50 kDa fragment which became apparent at a molar ratio of MMP-2:lamin A as little as 1:125 (Figure 3.13, A). The band density of lamin A decreased with increasing concentrations of MMP-2, and resulted in increased band density of ~50 kDa proteolysis product (Figure 3.13, B), clearly showing the ability of MMP-2 to proteolyse lamin A.

3.5 Effect of myocardial I/R injury on putative nuclear MMP-2 targets

3.5.1 Troponin I

It was previously described by Wang *et al.* (2002) that troponin I protein levels are decreased in I/R hearts, and attenuated with MMP inhibitor treatment. In order to confirm the proteolytic activity of MMP-2 in I/R hearts, I measured TnI by western blot in heart homogenates (Figure 3.14). There was a trend ($p=0.091$) to reduced protein levels of TnI in I/R hearts compared to AE hearts. I/R+O group had a significantly greater TnI content than I/R hearts (Figure 3.14, B). Similar results were seen with the TnI lower band that is recognized by this antibody (Figure 3.14,

C). Thus, the hearts in this experiment partially replicated this important indicator of the detrimental activity of MMP-2 in I/R injury.

The decrease in myocardial TnI content after ischemia and reperfusion could potentially result in impaired mechanical function of the hearts. Therefore, the relationship between myocardial contractile function and the protein levels of TnI post I/R were explored (Figure 3.15). The percentage recovery of mechanical function was defined as the ratio of left ventricular developed pressure at the end (75 min) of perfusion over the same parameter at the start of perfusion (0 min during aerobic perfusion). There were no significant correlations between TnI protein levels and percentage recovery of heart contractile function in all the different groups of hearts.

3.5.2 PARP-1

Kwan *et al.* (2004) showed that MMP-2 can proteolyse PARP-1 in vitro resulting in the formation of an ~48 kDa fragment. I measured PARP-1 in homogenates prepared from AE, I/R and I/R+O hearts by western blotting (Figure 3.16, A). The densities of 116 kDa (full-length) PARP-1 band (Figure 3.16, B) and 85 kDa PARP-1 fragment band (Figure 3.16, C) were measured. Full-length 116 kDa PARP-1 protein levels were not significantly different in I/R hearts compared to control AE hearts. In contrast the protein level of PARP-1 was significantly lower in I/R+O relative to I/R hearts. No significant change was observed in the 85 kDa PARP-1 fragment band (Figure 3.16, C).

In a similar fashion to the TnI analysis, the relationship between the left ventricular contractile function and protein levels of 116 kDa PARP-1 was explored

(Figure 3.17). The percentage recovery of mechanical function was defined as the ratio of ventricular developed pressure at the end (75 min) of perfusion over the same parameter at the start of perfusion (0 min during aerobic perfusion). There was a significant inverse correlation between full length PARP-1 and the percentage recovery of contractile function among the I/R group hearts and all hearts subjected to I/R (I/R and I/R+O).

3.5.3 Lamin A and C

The protein levels of lamin A and C were measured in the insoluble cellular fraction isolated from AE, I/R and I/R+O hearts (Figure 3.18). The insoluble cellular fraction is collected after the nuclear fraction, and contains insoluble structural proteins including the lamins. There was no significant changes in lamin A or C protein levels, nor in the lamin A to C ratio (Figure 3.18, B). To further solidify these results the protein levels of lamin A or C were measured in total homogenates from isolated perfused rat hearts subjected to I/R injury (Figure 3.19). Neither lamin A, C (Figure 3.19, B) nor the lamin A to C ratio were affected by I/R injury. Thus, the increase of MMP-2 in the nuclear fraction during I/R injury did not result in the proteolysis of lamin A or C, despite its ability to proteolyse lamin A in vitro.

Table 3.1: In silico analysis of proteolytic cleavage sites by MMP-2 of lamin A/C and B performed by PROSPER

| | Amino Acid | Segment | N-fragment | C-fragment | Score |
|----------------|-------------------|----------------|-------------------|-------------------|--------------|
| Lamin A | 76 | EVSG--IKAA | 8.91 kDa | 70.03 kDa | 1.07 |
| | 308 | QLSQ--LQKQ | 36.36 kDa | 42.57 kDa | 7.07 |
| Lamin B | 309 | QLSN--LQKE | 36.36 kDa | 32.76 kDa | 1.18 |
| | 562 | EAAG--VVVE | 66.33 kDa | 2.79 kDa | 1.02 |

Figure 3.1: Nuclear localization of MMP-2 in neonatal rat ventricular myocytes by confocal immunofluorescence microscopy.

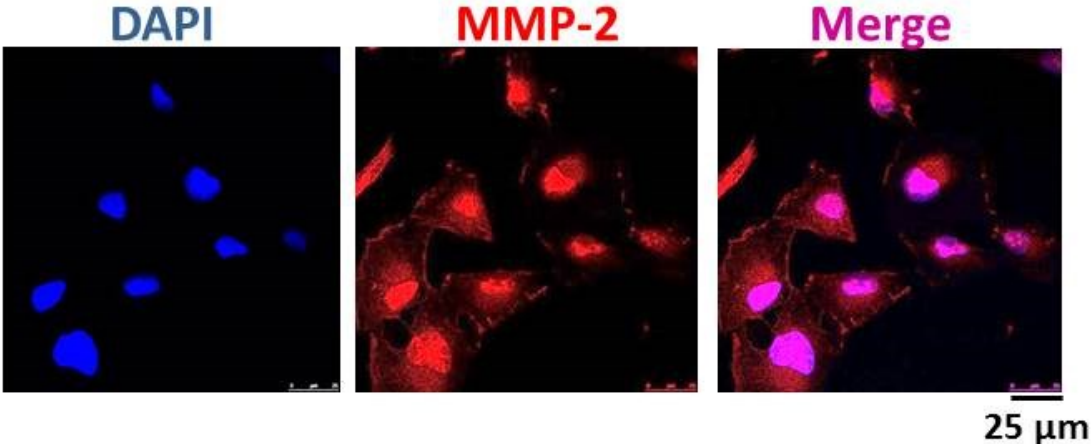
Immunofluorescence confocal microscopy was used to show that MMP-2 localizes to the nucleus in neonatal rat ventricular myocytes. Nucleus was stained with DAPI (blue).

(A) The MMP-2 antibody Ab-19015 or the

(B) MMP-2 antibody against the S1' loop were used to stain for MMP-2 (red).

Fig 3.1

A



B

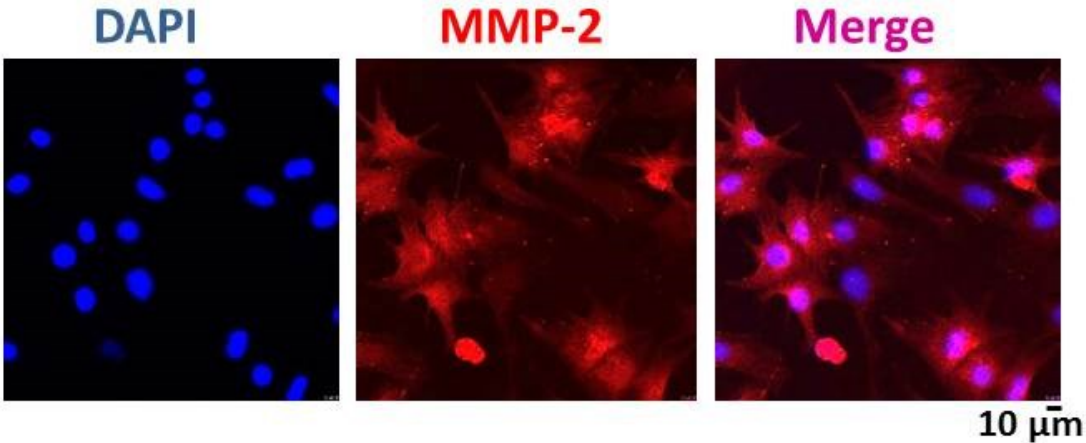


Figure 3.2: Distribution of intracellular MMP-2 protein levels in subcellular fractions of neonatal rat ventricular myocytes.

Western blot showing the distribution of MMP-2 protein levels in cytosolic, membrane and nuclear fractions of neonatal rat ventricular myocytes under normal cell culture conditions. Equal percent volume of each fraction collected was loaded for cytosol (15 μ L), membrane (15 μ L) and nuclear fractions (30 μ L). The cytosol, membrane bound organelle and nuclear fractions are denoted by C, M and N, respectively. The MMP-2 antibody used was Ab19015.

(A) A representative Western blot of fraction purity. Cytosol marker: GAPDH; Nuclear marker: lamin A/C.

(B) A representative Western blot of MMP-2 protein levels in cytosol, membrane and nuclear fraction. Purified human recombinant MMP-2 was used as a standard (Std).

(C) Quantitative analysis of the MMP-2 band by densitometry.

The protein levels were comparable in cytosolic and membrane fractions, with less in the nuclear fraction.

Representative of n=5 individual experiments.

* $p < 0.05$, *** $p < 0.001$, one-way ANOVA followed by Fisher's LSD test

Fig 3.2

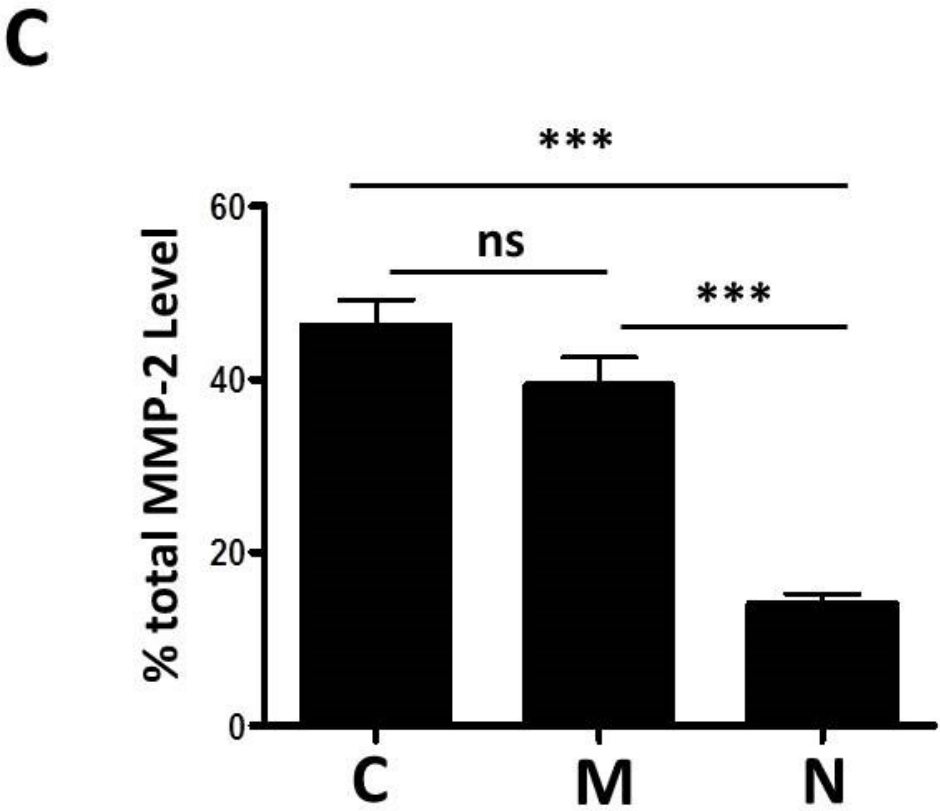
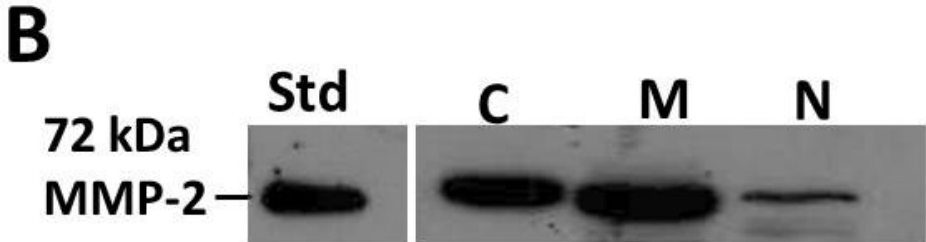
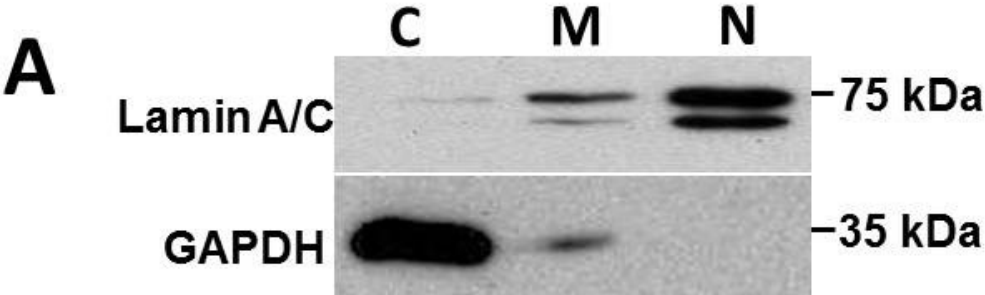


Figure 3.3: Distribution of intracellular MMP-2 activity in subcellular fractions prepared from neonatal rat ventricular myocytes.

Gelatin zymography was used to assess MMP-2 activity in cytosol, membrane and nuclear fractions of neonatal rat ventricular myocytes under normal cell culture conditions. Equal percent volume of each fraction collected was loaded for cytosol (15 μ L), membrane (15 μ L) and nuclear fractions (30 μ L). The cytosol, membrane bound organelle and nuclear fractions are denoted by C, M and N, respectively.

(A) A representative gelatin zymogram examines MMP-2 and MMP-9 activities in cytosol, membrane and nuclear fractions. Conditioned media from HT1080 cells was used as a standard for MMP-2 and MMP-9.

(B) Quantitative analysis of the MMP-2 band by densitometry.

Activity was highest in the membrane fraction, followed by the cytosolic and nuclear fractions; no nuclear MMP-9 activity was detected.

Representative of n=5 individual experiments.

* $p < 0.05$, *** $p < 0.001$, one-way ANOVA followed by Fisher's LSD test

Fig 3.3

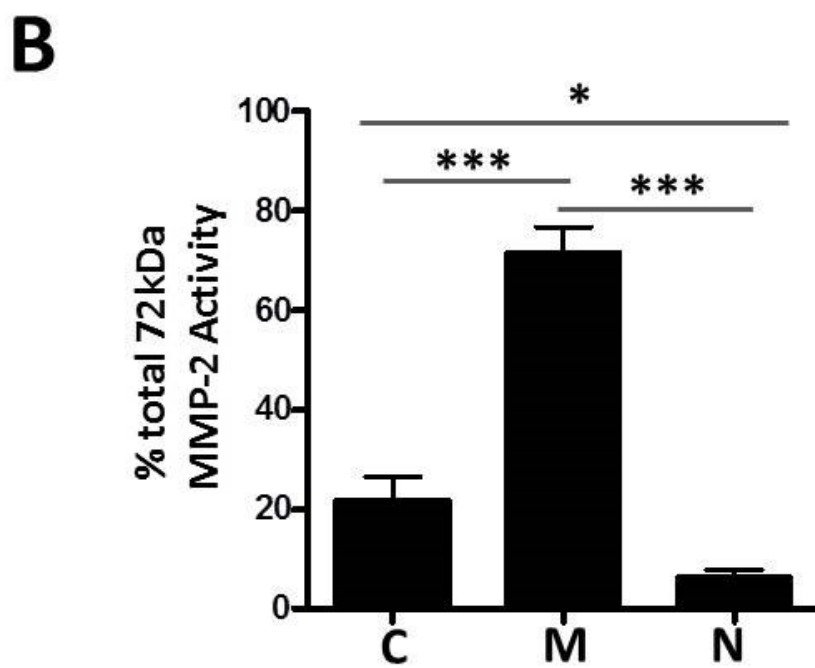
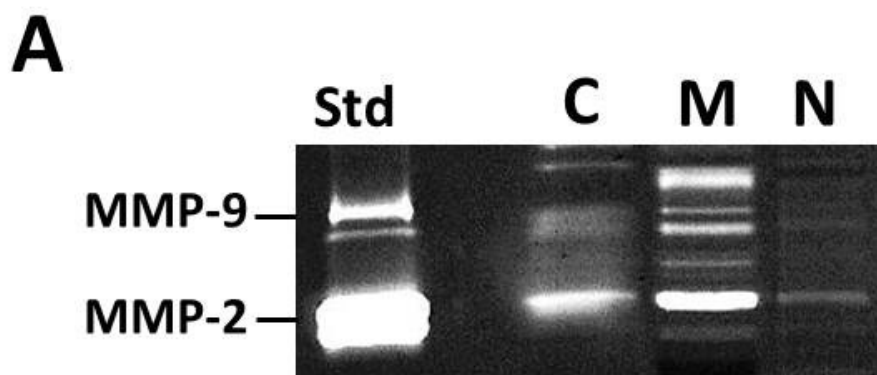


Figure 3.4: Nuclear localization of MMP-2 in HT1080 cells by confocal immunofluorescence microscopy.

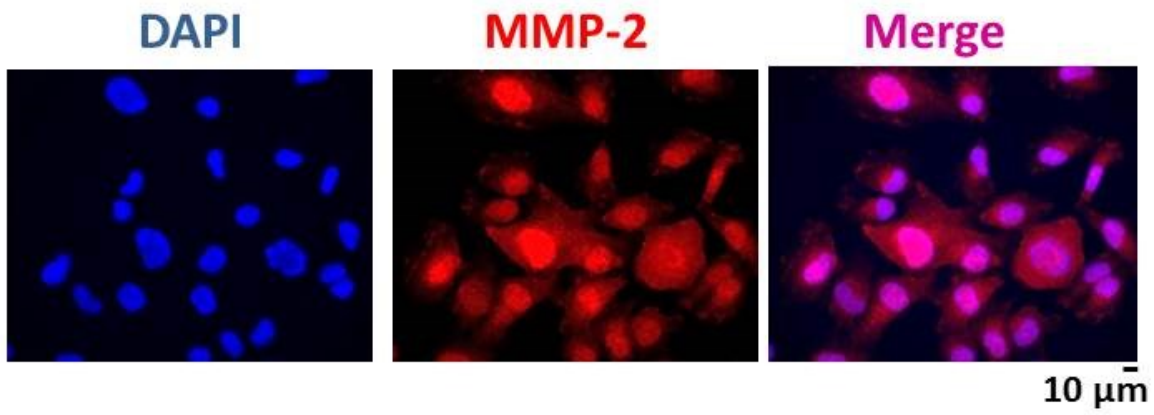
Fluorescence confocal microscopy was used to show that MMP-2 localizes to the nucleus in HT1080 cells. Nucleus was stained with DAPI (blue).

(A) The MMP-2 antibody Ab-19015 or the

(B) MMP-2 antibody against the S1' loop were used to stain for MMP-2 (red).

Fig 3.4

A



B

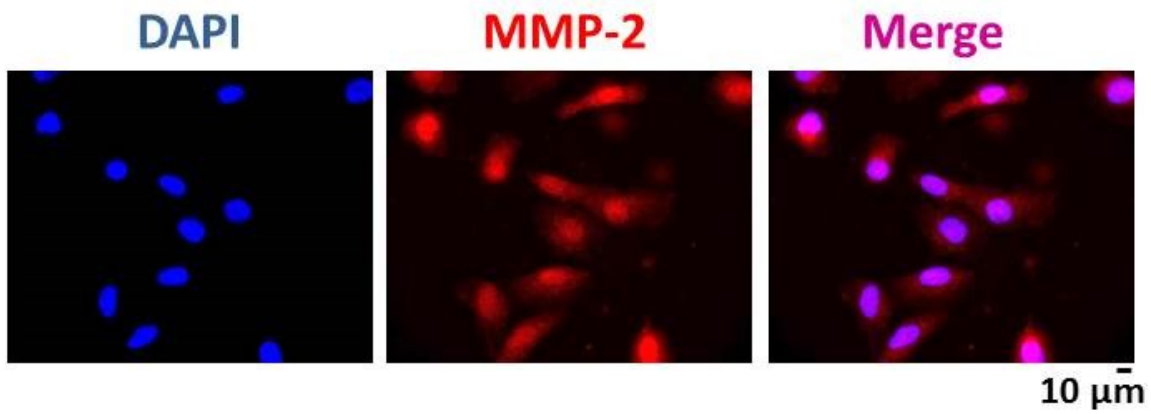


Figure 3.5: Nuclear localization of MMP-2 in HT1080 cells analyzed by imaging flow cytometry.

Imaging flow cytometry was used to show the percentage of HT1080 cells that have primarily nuclear or cytoplasmic localization of MMP-2. Nuclei were stained with DAPI (blue), MMP-2 antibody against the S1' loop was used to stain for MMP-2 (red).

(A) Representative images of cells that had primarily cytoplasmic MMP-2 localization.

(B) Representative images of cells that had primarily nuclear MMP-2 localization.

(C) Histogram of frequency of events showing cytosolic and nuclear localization of MMP-2.

Representative of n=3 individual experiments.

Fig 3.5

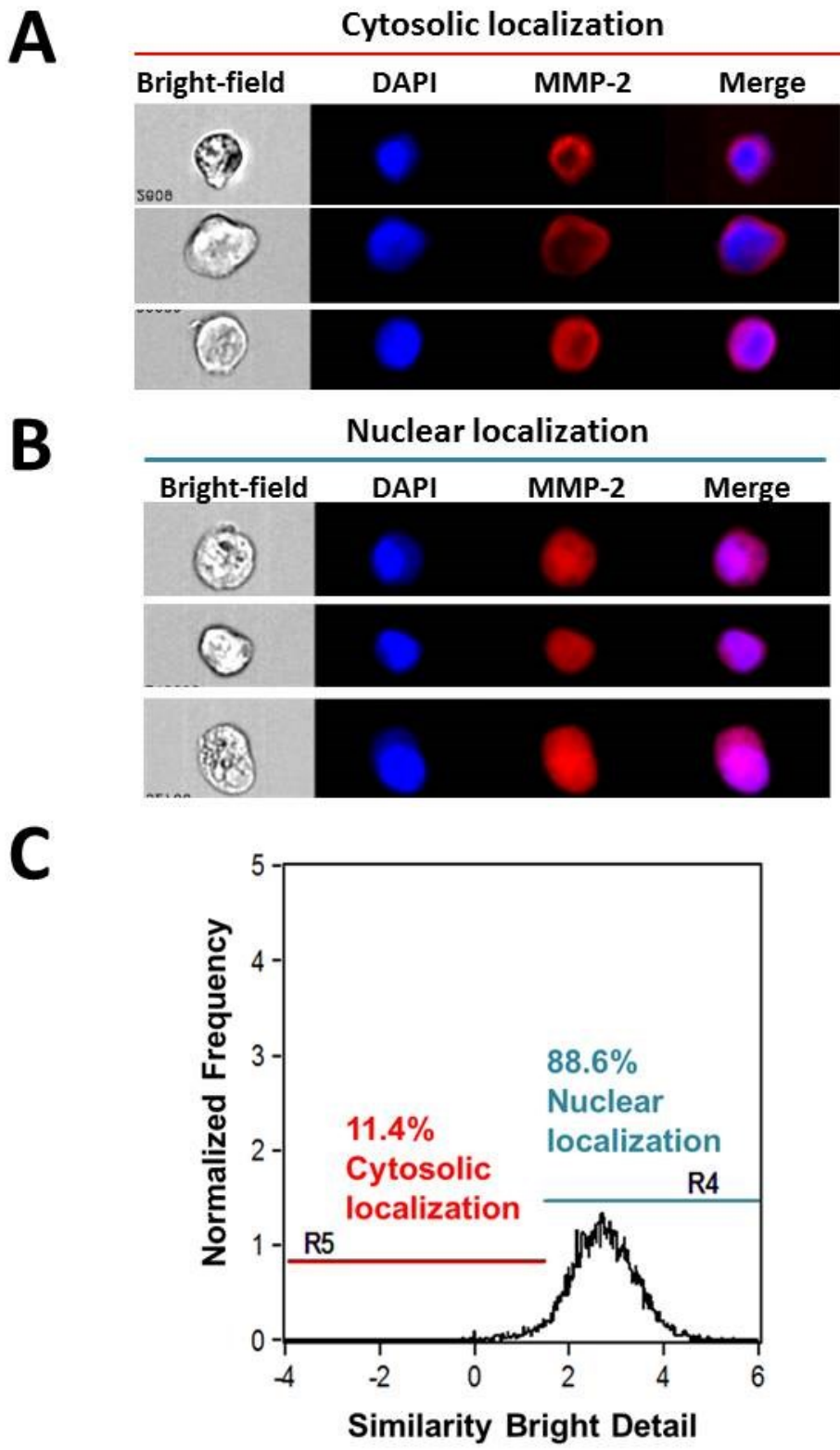
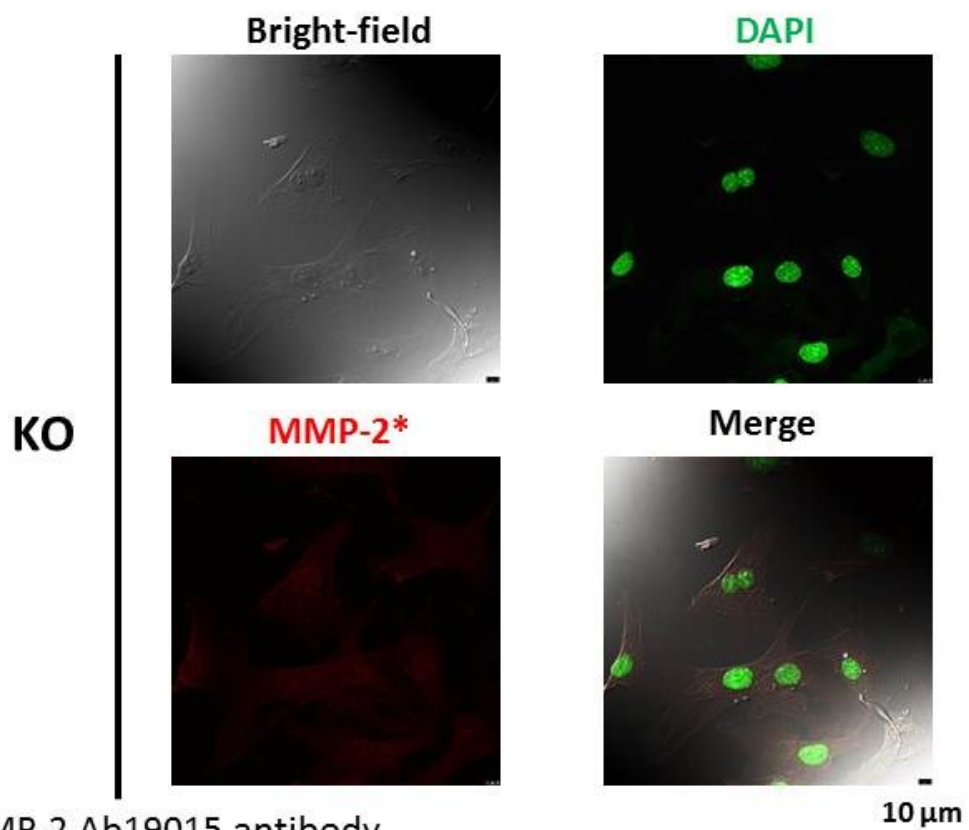
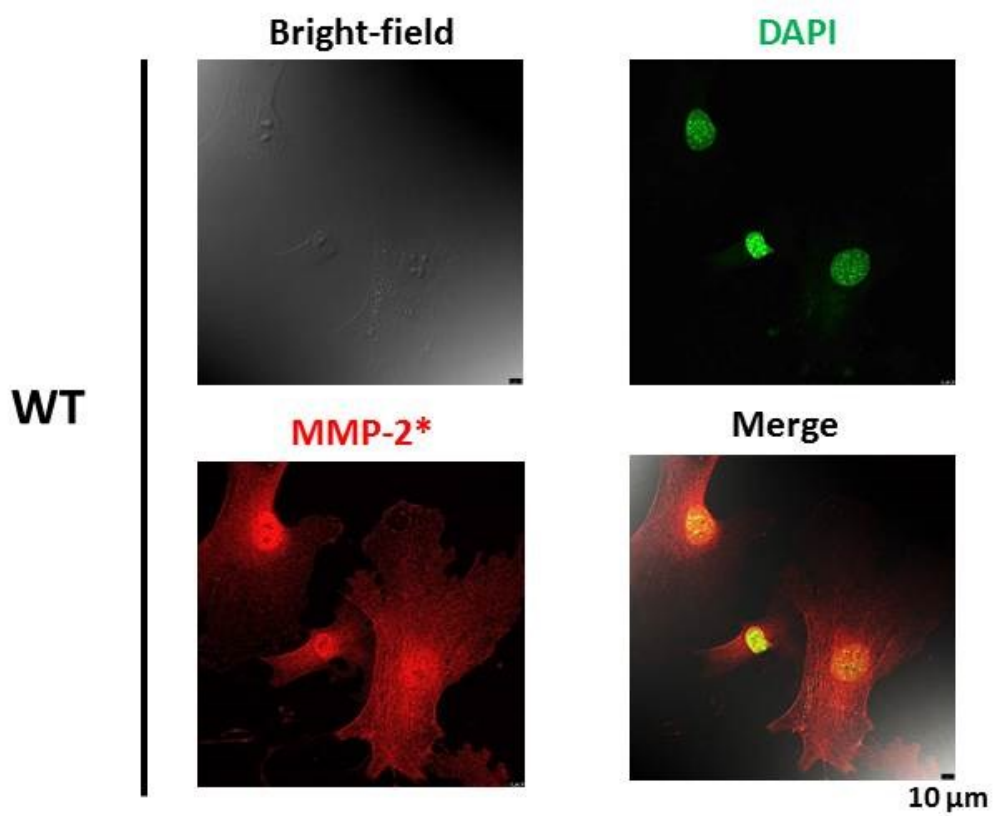


Figure 3.6: MMP-2 staining by Ab19015 MMP-2 antibody in wild type and MMP-2 knock out mouse neonatal fibroblasts visualized by confocal immunofluorescence microscopy.

Immunofluorescence confocal microscopy with MMP-2 antibody Ab19015 shows that MMP-2 is recognized in the nucleus of wild type (WT) mouse neonatal fibroblasts. Non-specific binding of MMP-2 antibody was not seen in neonatal fibroblasts from MMP-2 knock out (KO) mice. Nuclei were stained with DAPI (green) and the MMP-2 antibody Ab-19015 (red). Representative of one experiment.

Fig 3.6

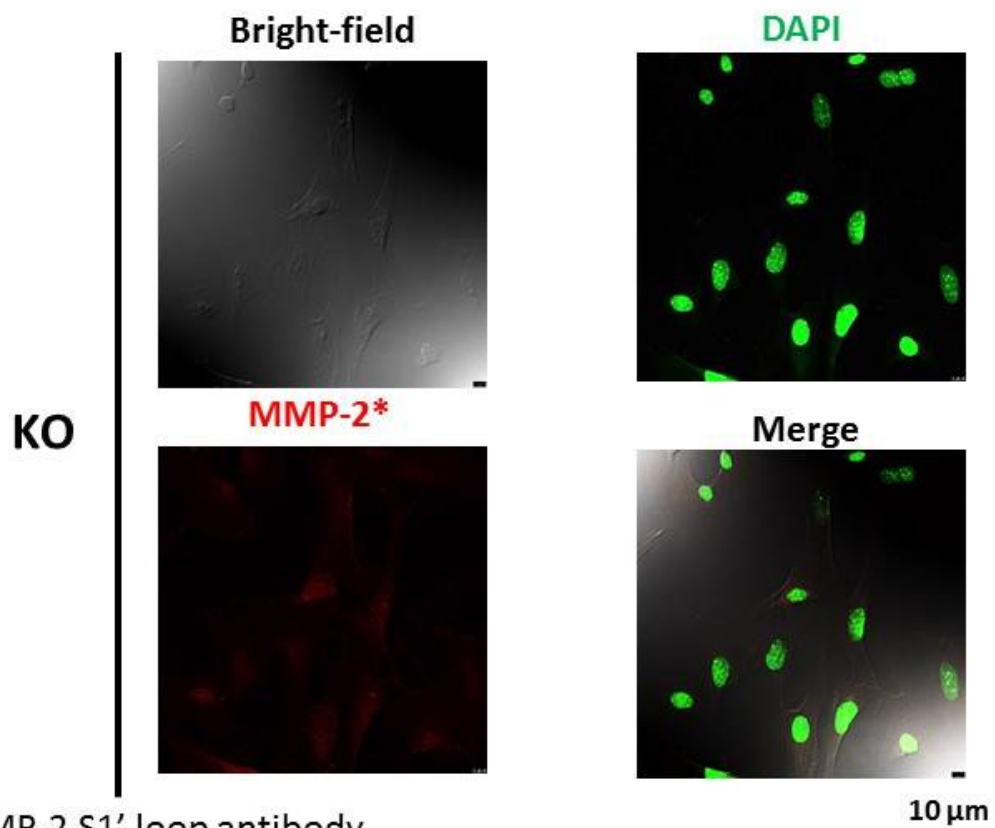
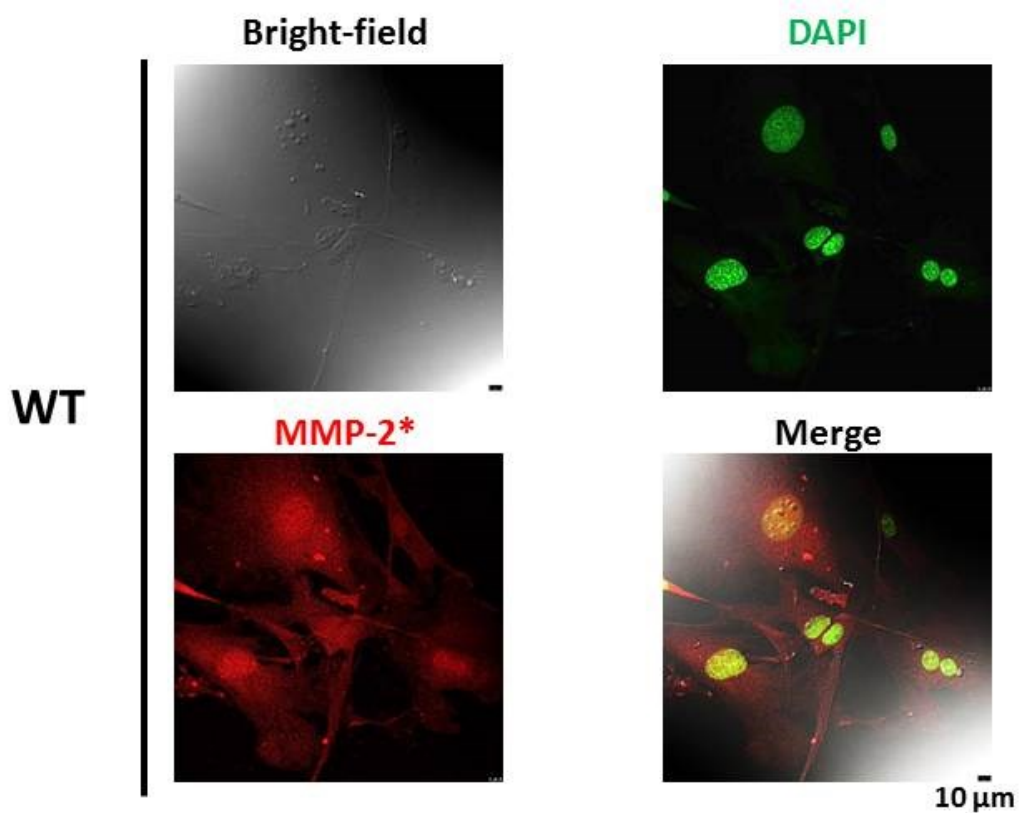


* MMP-2 Ab19015 antibody

Figure 3.7: MMP-2 staining with MMP-2 S1' loop antibody in wild type and MMP-2 knock out mouse neonatal fibroblasts visualized by confocal immunofluorescence microscopy.

Immunofluorescence confocal microscopy with MMP-2 S1' loop antibody shows that MMP-2 is recognized in the nucleus of wild type (WT) mouse neonatal fibroblasts. Non-specific binding of MMP-2 S1' loop antibody was not seen in neonatal fibroblasts from MMP-2 knock out (KO) mice. Nuclei were stained with DAPI (green) and the MMP-2 S1' loop antibody (red). Representative of one experiment.

Fig 3.7



* MMP-2 S1' loop antibody

Figure 3.8: Functional performance of isolated rat hearts subjected to ischemia-reperfusion (I/R) injury and the effect of the MMP inhibitor o-phenanthroline (O).

Isolated rat hearts were perfused either aerobically for 75 mins as control hearts (AE, black), or subjected to 20 mins of aerobic perfusion followed by 20 mins of global, no-flow ischemia and 35 mins of aerobic reperfusion with 100 μ M of o-phenanthroline (I/R+O, blue) or its vehicle (I/R, red). Note that vehicle (DMSO, 0.0625% v:v) was also infused in the control group. The light grey areas of the graph represent the length of time the vehicle or drug was infused, 10 mins before and after ischemia. Note that the control hearts received the vehicle for a total of 40 mins. The dark grey areas represent the global, no-flow ischemia that was performed only on I/R hearts. Physiological parameters measured include:

- (A)** Heart rate,
- (B)** coronary flow,
- (C)** left ventricular developed pressure and
- (D)** the product of heart rate and developed pressure.

n=7 hearts/group.

* $p < 0.05$ between I/R and I/R+O groups, two-way repeated measures ANOVA followed by Fisher's LSD test.

Heart perfusions were performed by Mathieu Poirier.

Fig 3.8

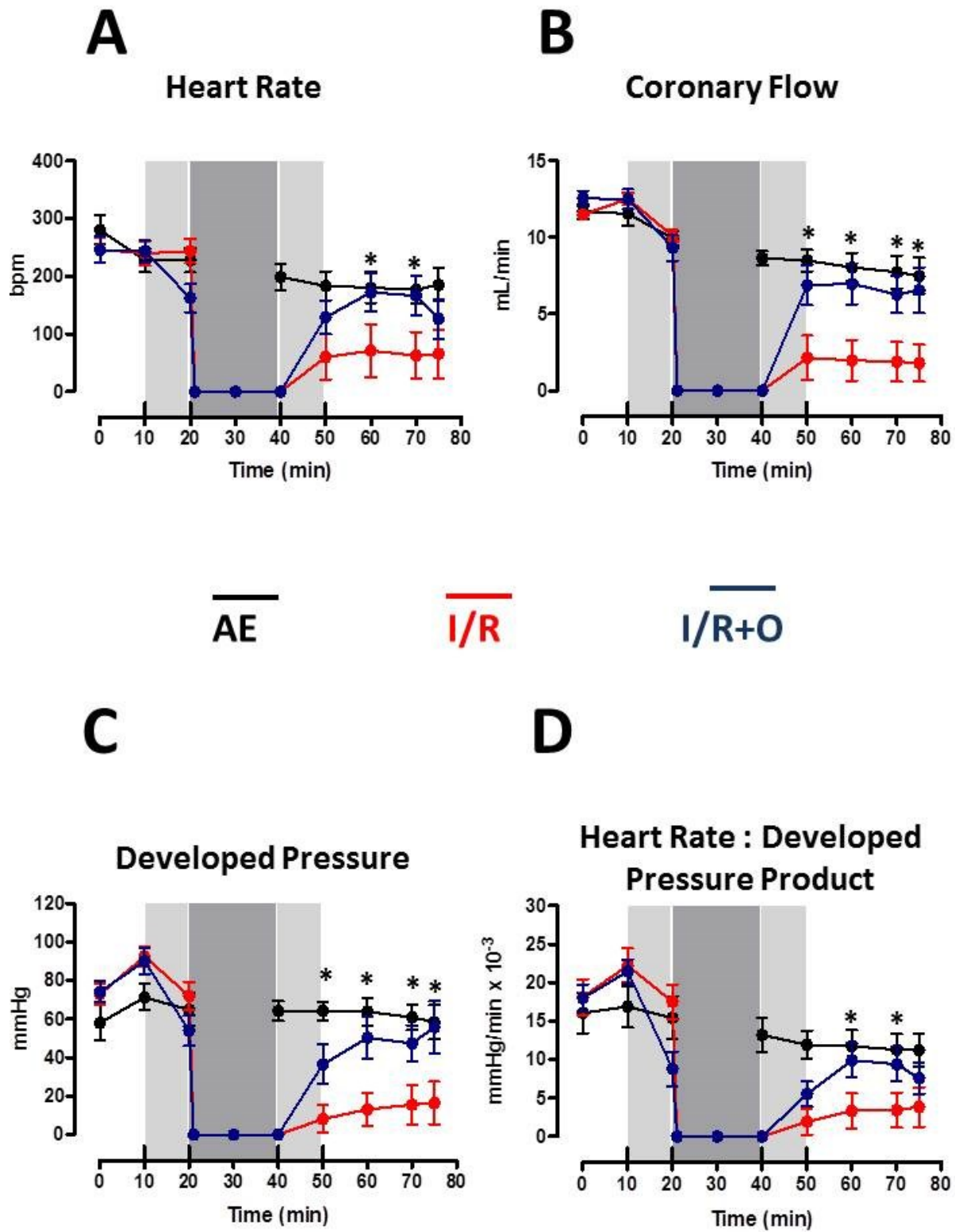


Figure 3.9: Purity of subcellular fractions prepared from normal rat heart ventricular tissue.

Western blots for specific cellular markers demonstrated that the nuclear fraction was free of cytosol and membrane contamination. Equal percent volume of each fraction collected was loaded for cytosol (15 μ L), membrane (15 μ L) and nuclear fractions (30 μ L). The cytosol, membrane bound organelle and nuclear fractions are denoted by C, M and N, respectively. Cytosol marker: GAPDH; Membrane bound organelle markers: SERCA2, VDAC; Nuclear marker: lamin A/C.

Representative of n=3 individual experiments.

Fig 3.9

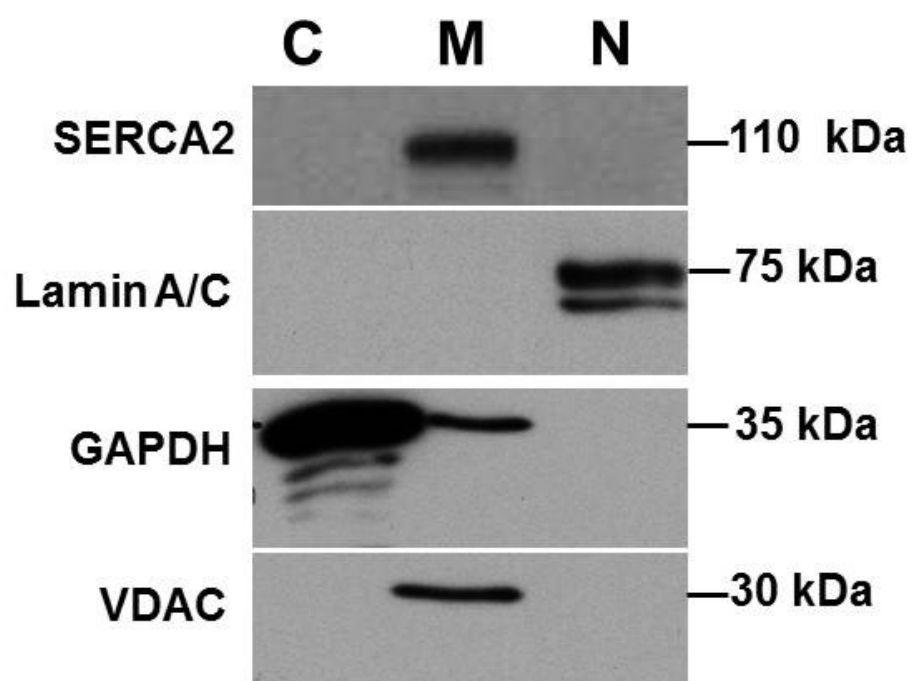


Figure 3.10: MMP-2 protein levels in subcellular fractions prepared from isolated rat hearts subjected to I/R injury.

The changes in protein levels of MMP-2 in cytosol (C), membrane (M) and nuclear (N) fractions in AE, I/R and I/R+O hearts were assessed by Western blot. A significant increase in MMP-2 protein levels was found in I/R+O hearts compared to AE hearts.

(A) Representative western blot showing MMP-2 protein levels in the subcellular fractions prepared from the hearts. The MMP standard (Std) used was purified human recombinant MMP-2.

(B) Quantitative analysis of the MMP-2 band in all subcellular fractions by densitometry.

The MMP-2 protein levels in the nuclear fraction from the three groups of hearts are shown separately in the enlarged graph.

n=7 hearts/group.

* $p < 0.05$, one-way ANOVA followed by Fisher's LSD test.

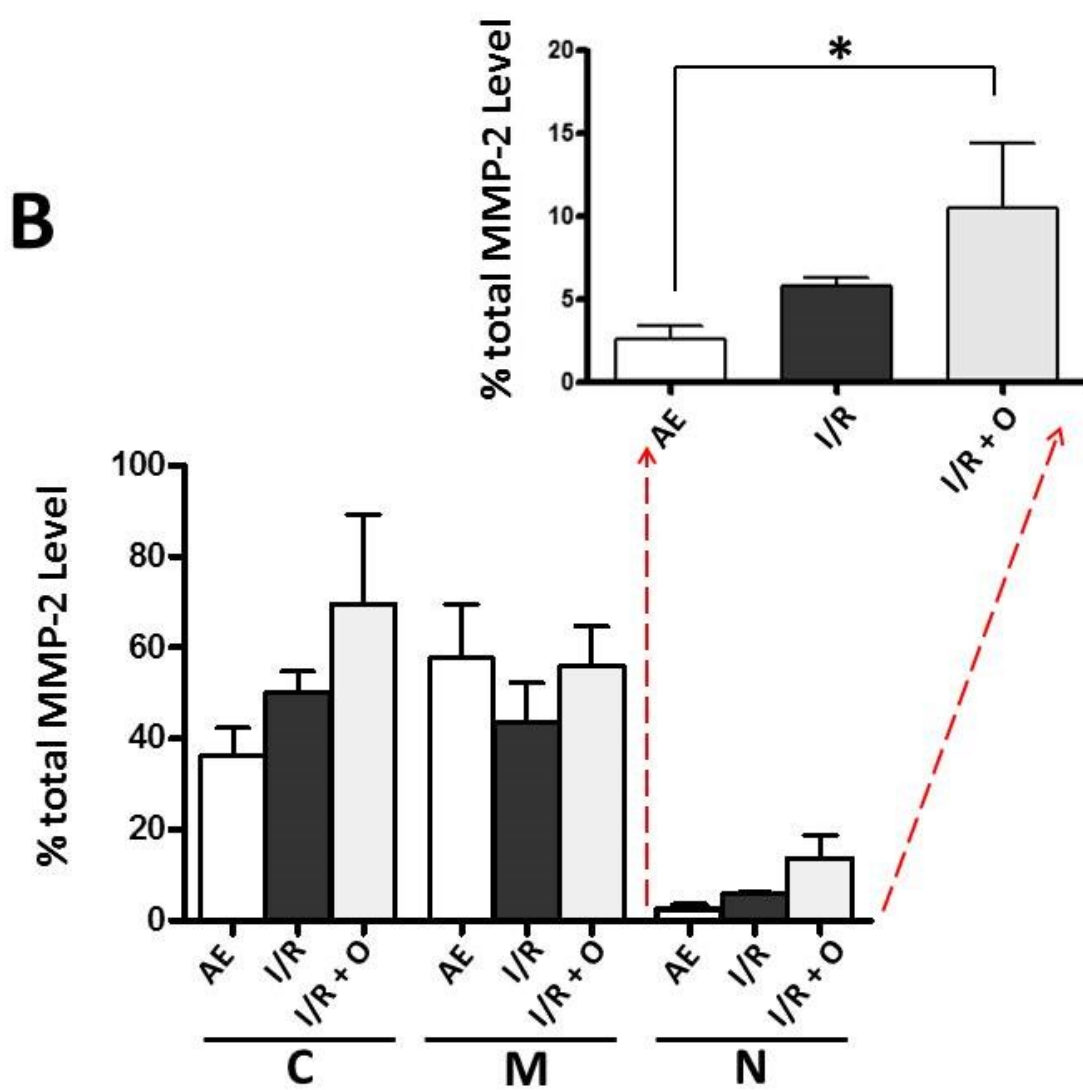
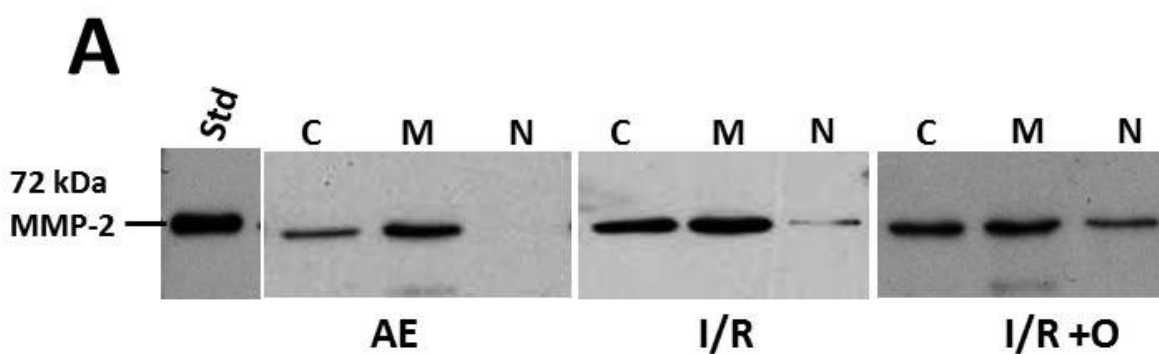


Figure 3.11: MMP-2 activity in subcellular fractions prepared from isolated rat hearts subjected to I/R injury.

The changes in MMP-2 activity in cytosol (C), membrane (M) and nuclear (N) fractions in AE, I/R and I/R+O hearts were assessed by gelatin zymography. A significant increase in MMP-2 activity was found in I/R hearts compared to the AE hearts.

(A) Representative gelatin zymogram showing the differences in activity of MMP-2 in the subcellular fractions prepared from the hearts. The MMP-2 standard (Std) used was conditioned media from HT1080 cells.

(B) Quantitative analysis of the MMP-2 band in all subcellular fractions by densitometry.

The change in MMP-2 activity in the nuclear fraction from the three groups of hearts are shown separately in the enlarged graph.

n=7 hearts/group.

* $p < 0.05$, one-way ANOVA followed by Fisher's LSD test.

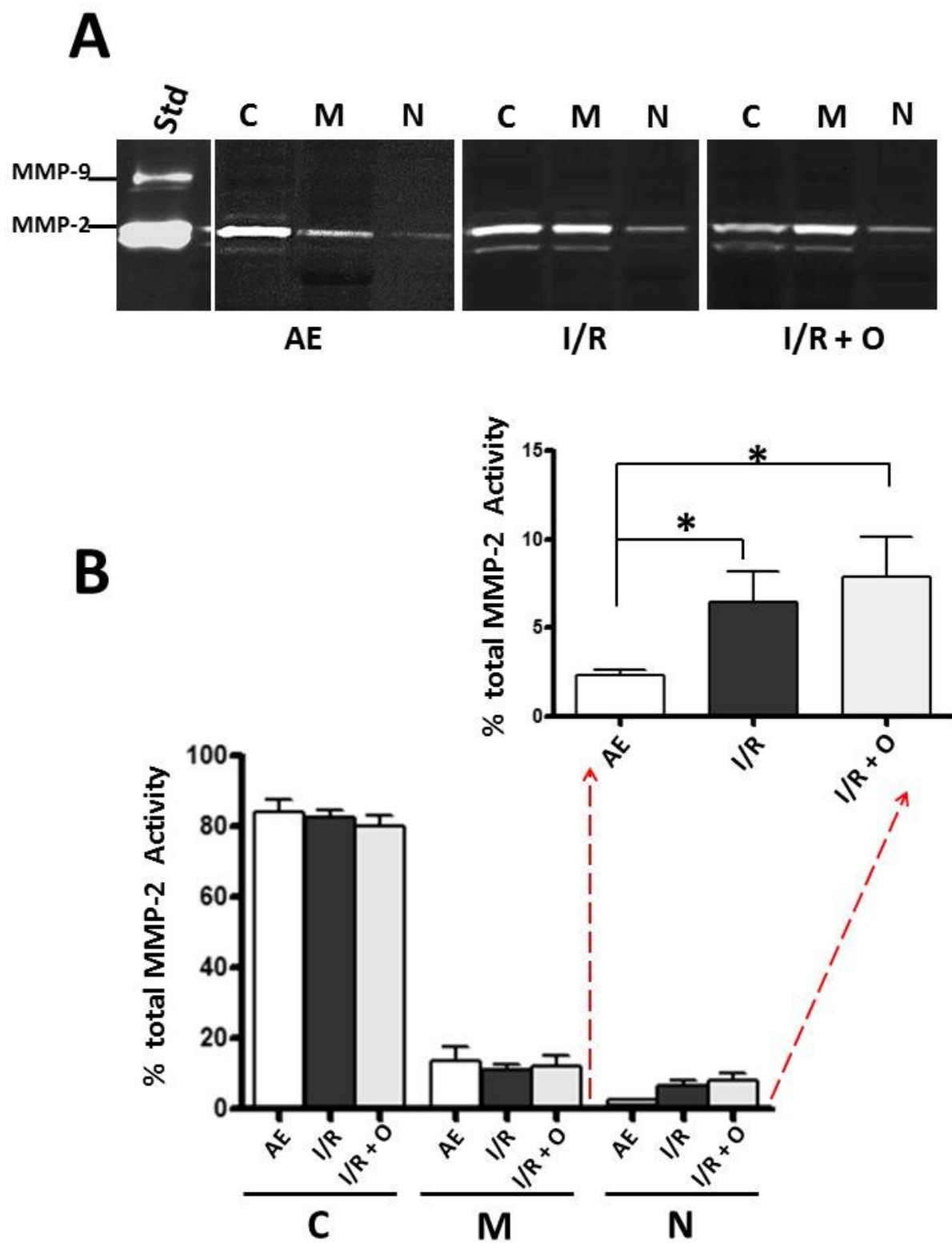


Figure 3.12: Nuclear protein lamin B is not proteolysed by MMP-2 in vitro.

Human recombinant MMP-2 was incubated with human recombinant lamin B (1 μg) for 2 hours at 37°C. MMP-2 did not proteolyse lamin B in vitro. This is revealed by the 68 kDa lamin B band intensity and 48 kDa band intensities remaining unchanged with increasing MMP-2 concentration. Troponin I (TnI) was used as a positive control for MMP-2 proteolysis activity. TnI was proteolysed at a MMP-2:TnI ratio of 1:125.

(A) Representative SDS PAGE gel of incubated samples stained with Comassie Blue.

(B) Quantitative analysis of Lamin B and 48 kDa band density.

Fig 3.12

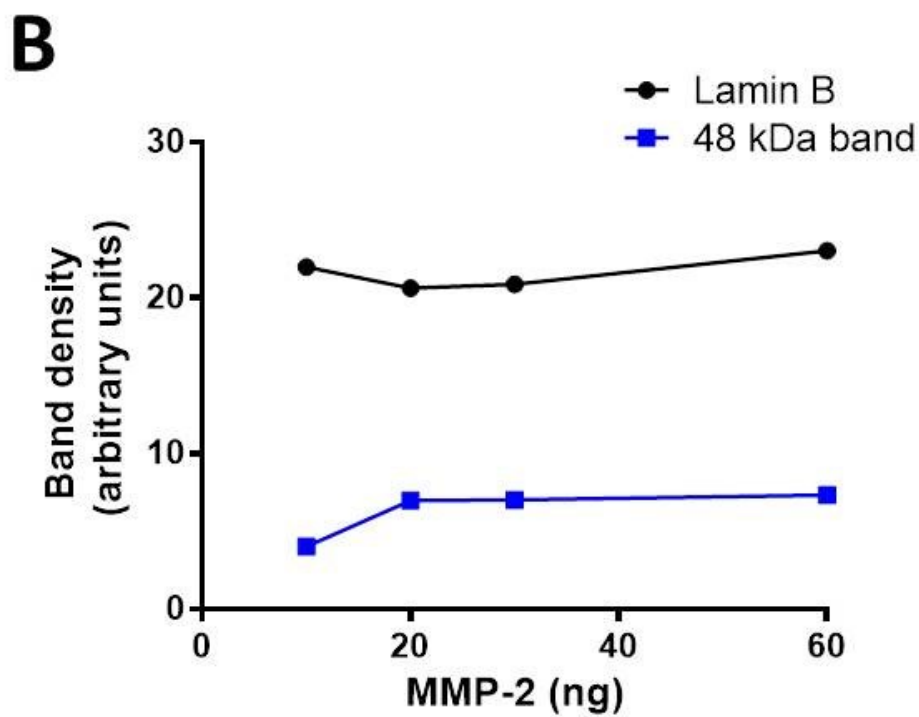
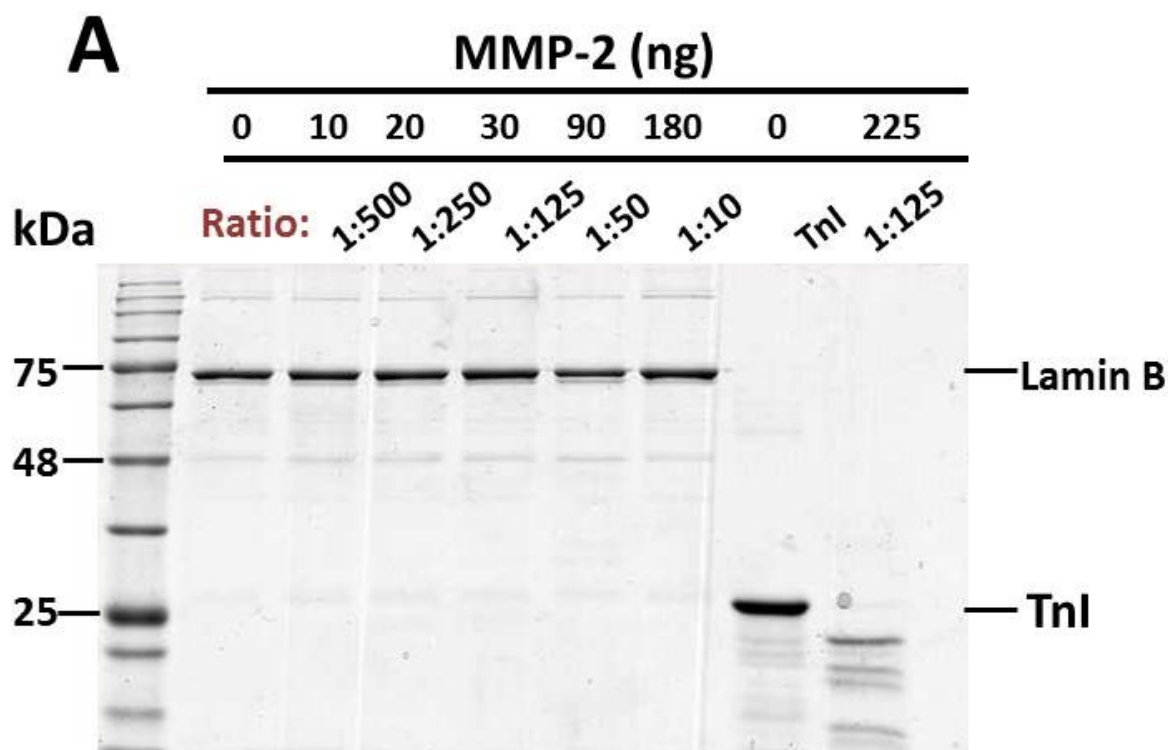


Figure 3.13: Nuclear protein lamin A is proteolysed by MMP-2 in vitro in a concentration dependent manner.

Human recombinant MMP-2 was incubated with human recombinant lamin A (0.5 μ g) for 30 mins at 37°C in the presence or absence of the MMP inhibitor, o-phenanthroline (o-phen, 100 μ M). MMP-2 proteolyzes lamin A in vitro in a concentration dependent manner with the indicated molar ratios of MMP-2:lamin A. This is revealed by the loss of 75kDa lamin A band intensity and the appearance of a 50 kDa putative lamin A fragment. Both were prevented by the addition of o-phenanthroline.

(A) Representative SDS PAGE gel of incubated samples stained with Comassie Blue.

(B) Quantitative analysis of lamin A and 50 kDa fragment band density.

This experiment was performed by Marcia Y. Kondo.

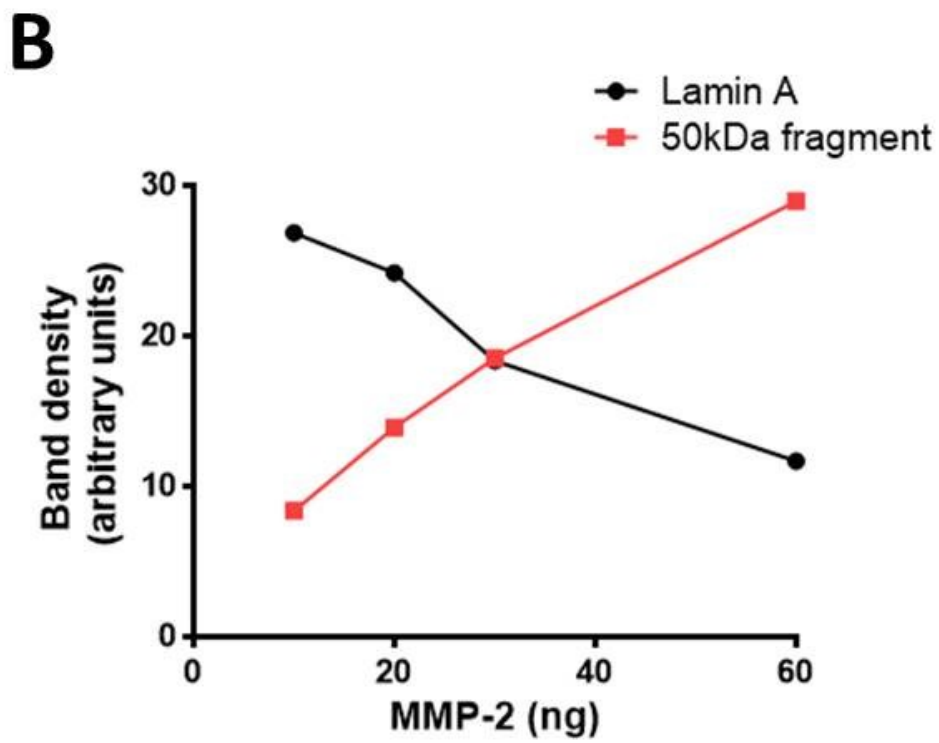
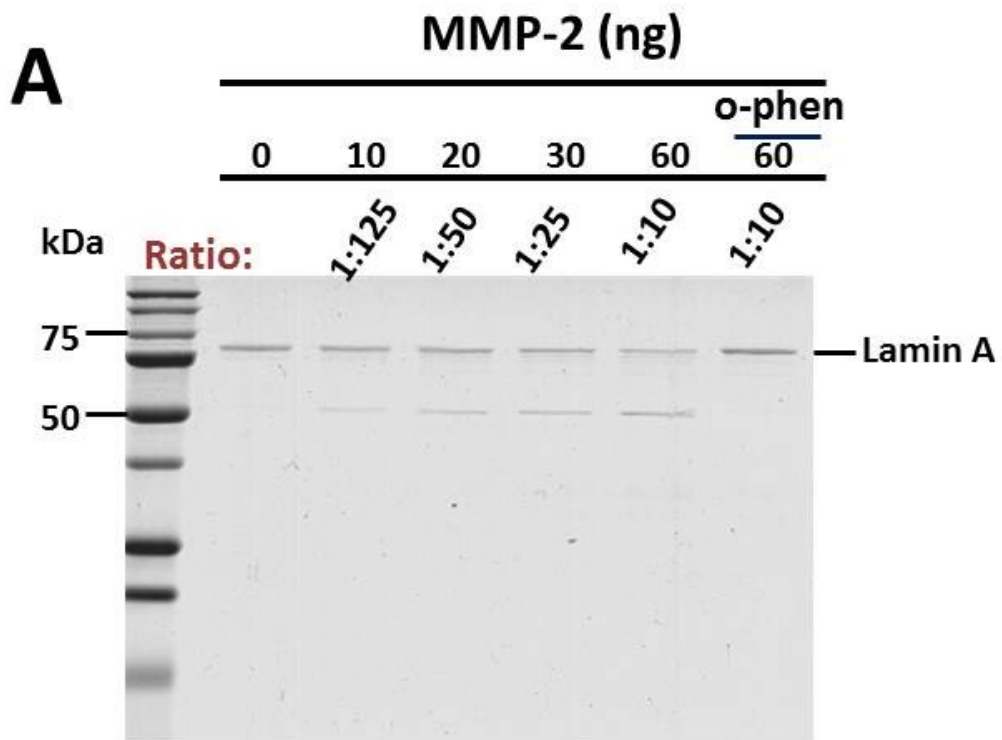


Figure 3.14: Troponin I protein levels in homogenates prepared from rat hearts subjected to ischemia-reperfusion injury.

Troponin I (TnI) protein levels in homogenates prepared from AE, I/R and I/R+O hearts as measured by Western blot.

(A) Representative Western blot of troponin I (20 µg total protein/lane) and Ponceau S stained area of the blot used to normalize data. The boxed area shown was averaged over each individual lane for the denominator. The standard (Std) used is purified human recombinant Troponin I.

(B) Quantitative analysis of the troponin I upper band.

(C) Quantitative analysis of the troponin I lower band.

n= 7 hearts/group.

* p<0.05, # p=0.091, one-way ANOVA followed by Fisher's LSD test.

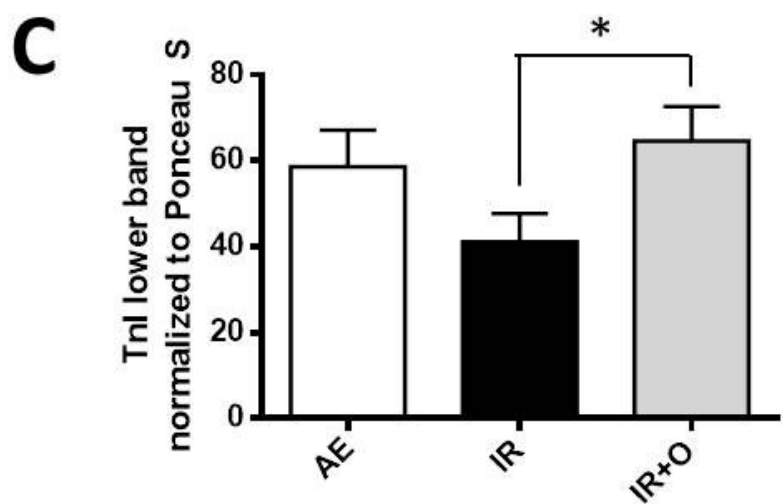
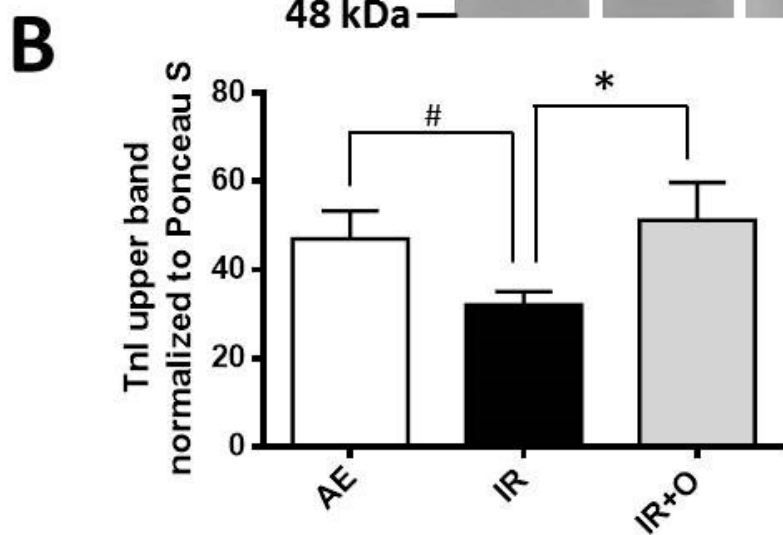
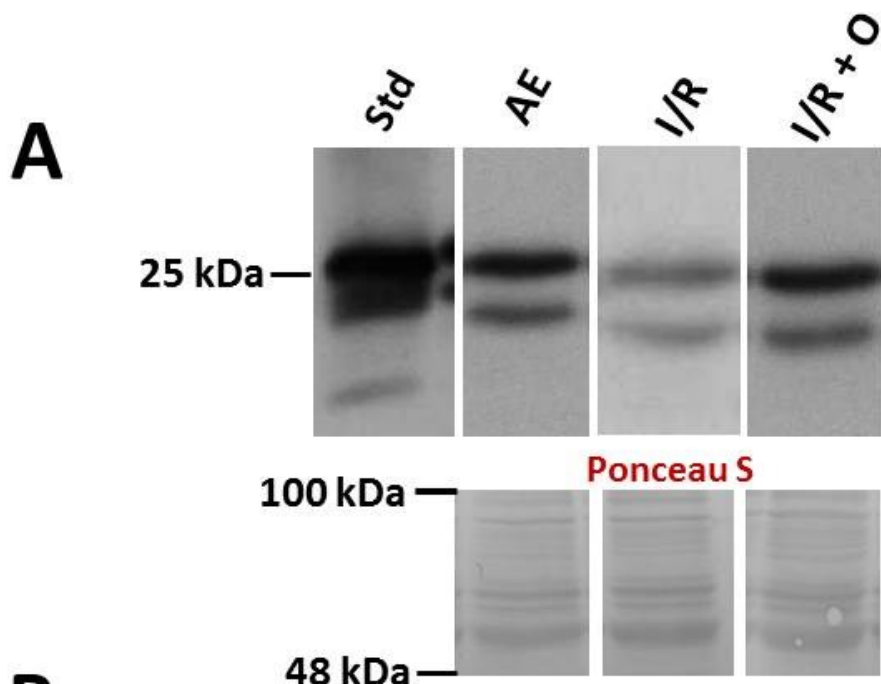


Figure 3.15: Correlational analysis between TnI protein levels and recovery of heart contractile function in isolated rat hearts subjected to ischemia-reperfusion (I/R) injury.

The relationship between the percentage recovery of heart contractile function and protein levels of TnI was explored using linear regression analysis. The percentage recovery of mechanical function was defined as the ratio of left ventricular developed pressure at the end of perfusion (75 min) over the same parameter at the start of perfusion (0 min during aerobic perfusion) – see Fig 3.9. There was no significant correlation between these parameters in I/R hearts.

(A) Scatterplot of TnI protein levels and % recovery of contractile function. AE hearts shown in black, I/R hearts shown in red, I/R+O shown in blue, combination of all data from hearts that underwent I/R shown in purple, combination of all data for all hearts shown in orange.

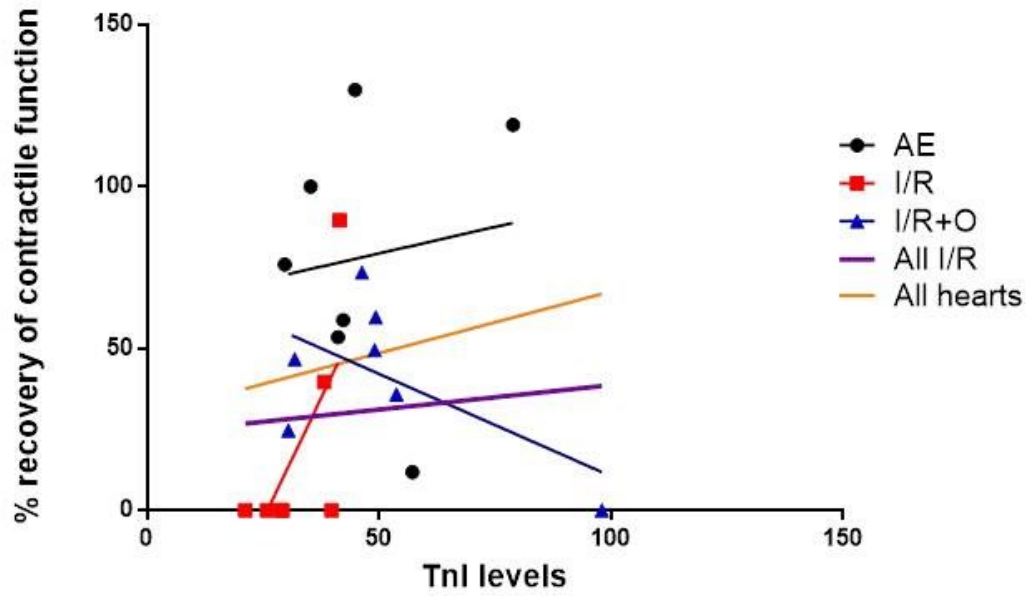
(B) The tabulated n-number, p-value and r^2 values of the scatterplot data.

n=6-7 hearts/group.

Spearman's rank-order correlation.

Fig 3.15

A



B

| | AE | I/R | I/R+O | All I/R | All hearts |
|----------------|-------|-------|-------|---------|------------|
| n | 7 | 7 | 7 | 14 | 21 |
| p-value | 0.839 | 0.142 | 0.661 | 0.076 | 0.112 |
| r ² | 0.011 | 0.435 | 0.045 | 0.241 | 0.126 |

Figure 3.16: 116 kDa PARP-1 protein levels in homogenates prepared from rat hearts subjected to ischemia-reperfusion injury.

116 kDa PARP-1 protein levels in AE, I/R and I/R+O hearts was measured by western blot. The level of 116 kDa PARP-1 was decreased in I/R+O hearts compared to I/R hearts. There were no significant changes in the 85 kDa PARP-1 fragment.

(A) Representative western blot of 116 kDa PARP-1 (30 µg total protein/lane) and Ponceau S stained area of the blot used to normalize data. The boxed area shown was averaged over each individual lane for the denominator.

(B) Quantitative analysis of the 116 kDa PARP-1 band by densitometry normalized to Ponceau S.

(C) Quantitative analysis of the 85 kDa PARP-1 fragment band by densitometry normalized to Ponceau S.

n= 5-7 hearts/group.

* p<0.05, one-way ANOVA followed by Fisher's LSD test.

Fig 3.16

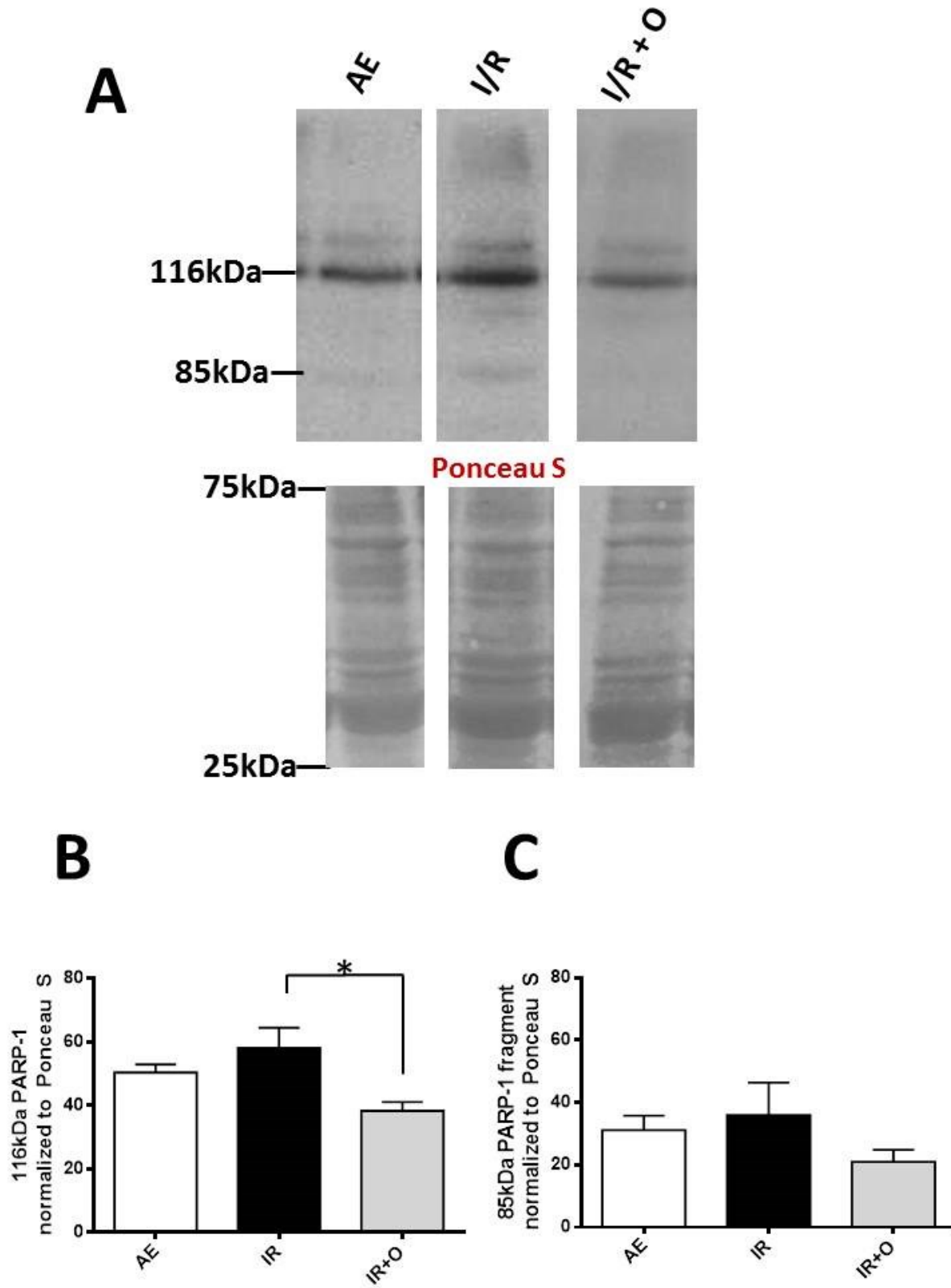


Figure 3.17: Correlational analysis between PARP-1 protein levels and recovery of heart contractile function in isolated rat hearts subjected to ischemia-reperfusion (I/R) injury.

The relationship between the percentage recovery of myocardial contractile function and protein levels of PARP-1 was explored using linear regression analysis. The percentage recovery of mechanical function was defined as the ratio of left ventricular developed pressure at the end of perfusion (75 min) over the same parameter at the start of perfusion (0 min during aerobic perfusion) – see Fig 3.9. There was a significant correlation between these parameters in I/R hearts.

(A) Scatterplot of PARP-1 protein levels and % recovery of contractile function. AE hearts shown in black, I/R hearts shown in red, I/R+O shown in blue, combination of all data from hearts that underwent I/R shown in purple, combination of all data for all hearts shown in orange.

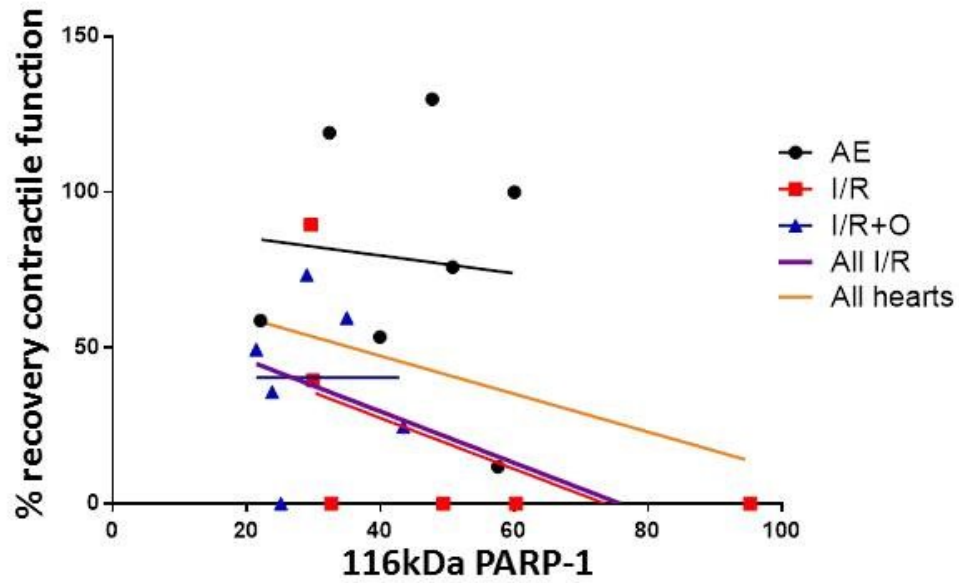
(B) The tabulated n-number, p-value and r^2 values of the scatterplot data.

n=6-7 hearts/group.

Spearman's rank-order correlation.

Fig 3.17

A



B

| | AE | I/R | I/R+O | All I/R | All hearts |
|----------------|-------|--------------|-------|--------------|------------|
| n | 7 | 7 | 6 | 13 | 20 |
| p-value | 0.906 | 0.034 | 1.000 | 0.046 | 0.2940 |
| r ² | 0.005 | 0.643 | 0.001 | 0.314 | 0.060 |

Figure 3.18: Lamin A and lamin C protein levels in the insoluble cellular fraction prepared from rat hearts subjected to ischemia-reperfusion injury.

Lamin A and lamin C protein levels in the insoluble cellular fraction prepared from AE, I/R and I/R+O hearts as measured by Western blot. No significant change in either lamin A or lamin C protein levels were found.

(A) Representative Western blot of lamin A or lamin C (30 μ L each) and Ponceau S stained area of the blot used to normalize protein concentration. The boxed area shown was averaged over each individual lane for the denominator. The standard (Std) used was commercially purchased human recombinant lamin A and C.

(B) Quantitative analysis of the lamin A and lamin C bands as well as the lamin A to C ratio.

n= 7 hearts/group.

One-way ANOVA followed by Fisher's LSD test, $p > 0.05$.

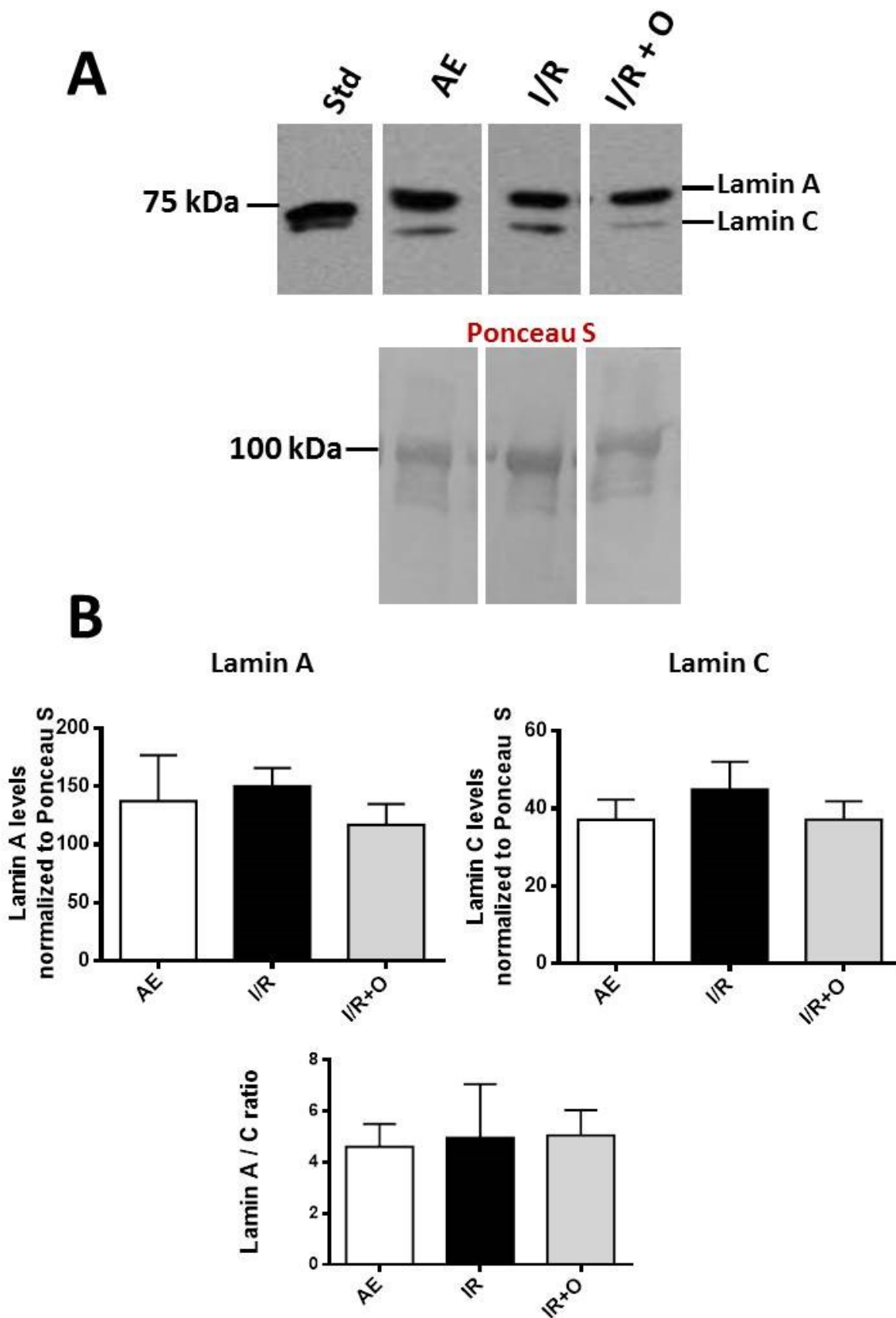


Figure 3.19: Lamin A and lamin C protein levels in homogenates prepared from rat hearts subjected to ischemia-reperfusion injury.

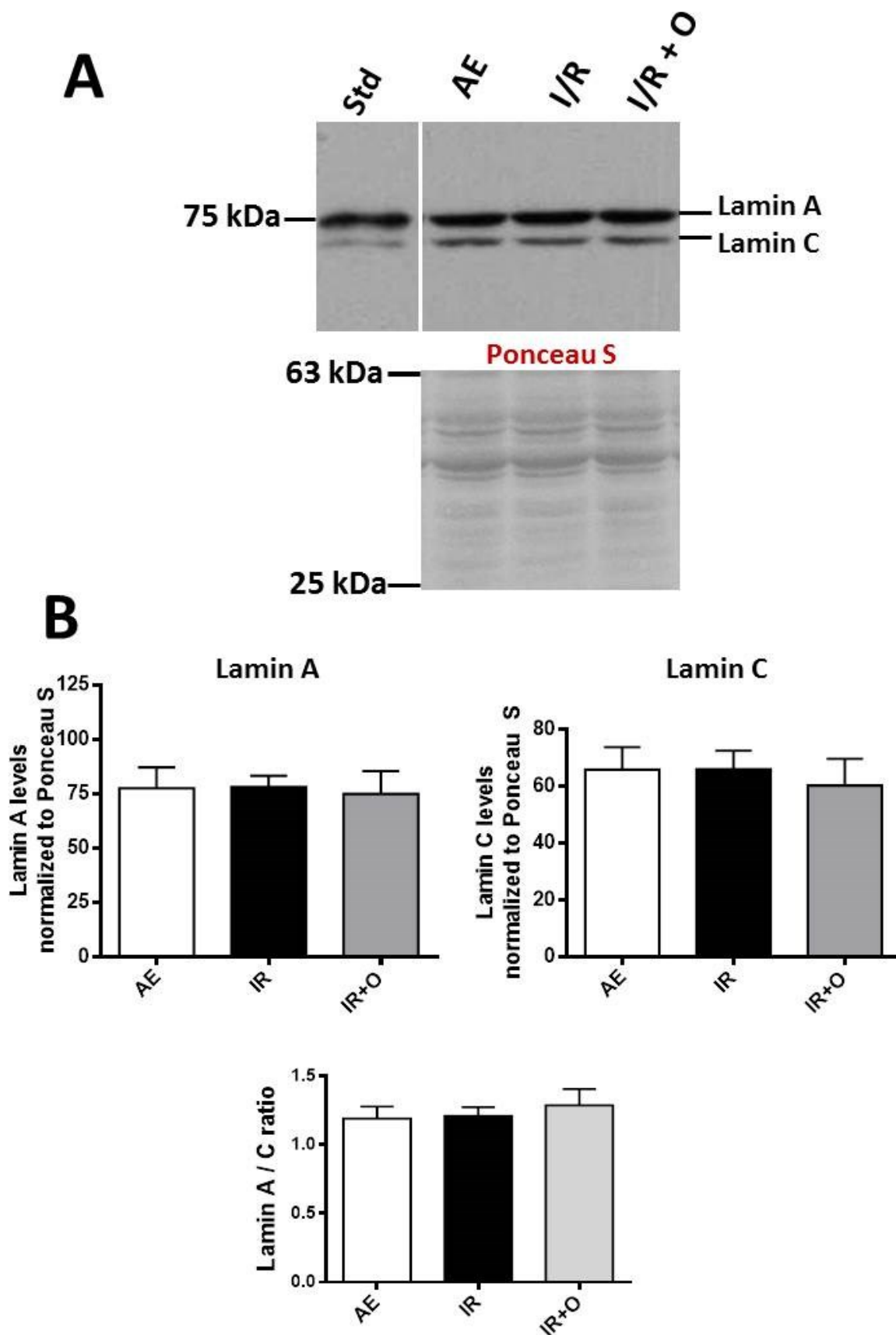
Lamin A and lamin C protein levels in homogenates prepared from AE, I/R and I/R+O hearts as measured by Western blot. No significant change in either lamin A or lamin C protein levels were found.

(A) Representative Western blots of lamin A or lamin C (50µg total protein/lane) and Ponceau S stained area of the blot used to normalize data. The boxed area shown was averaged over each individual lane for the denominator. The standard (Std) used was commercially purchased human recombinant lamin A.

(B) Quantitative analysis of the lamin A and lamin C bands as well as the lamin A to C ratio.

n= 7 hearts/group.

One-way ANOVA followed by Fisher's LSD test, $p > 0.05$.



CHAPTER 4 – DISCUSSION

4.1 Nuclear MMPs

The intracellular localization and activity of MMPs is now well recognized and well-studied. In cardiomyocytes MMP-2 has been localized to the sarcomere (Wang *et al.*, 2002), cytoskeleton (Sung *et al.*, 2007), caveolae (Chow *et al.*, 2007), mitochondria (Wang *et al.*, 2002), mitochondria-associated membrane (Hughes *et al.*, 2014) and nucleus (Kwan *et al.*, 2004). The first observation of nuclear MMP-2 sparked many other studies investigating nuclear functions of these proteases. MMPs have been shown to play a role in nuclear processes, where they proteolyse DNA repair proteins (Hill *et al.*, 2012; Kwan *et al.*, 2004; Yang *et al.*, 2010), act as transcription factors (Eguchi *et al.*, 2008; Zuo *et al.*, 2014) play a role in apoptosis (Pirici *et al.*, 2012), and participate in mitotic events leading up to cellular proliferation (Zimowska *et al.*, 2013). Even with all the knowledge that has been accumulated over the past decade since the discovery of the first nuclear MMP, there still remains a lot to be discovered. Improved understanding of the novel localization and functions of MMPs under conditions of both homeostasis and stress is important, as it will allow us to develop better, more specific MMP inhibitors via targeting them to specific cellular compartments.

In this study I found that MMP-2 is localized to the nucleus of unstimulated NRVMs and human fibrosarcoma HT 1080 cells by immunofluorescence confocal microscopy. Nuclear activity and protein levels were measured in highly pure nuclear fractions isolated from NRVMs. The protein levels and activity of nuclear MMP-2 were measured in isolated rat hearts subjected to I/R injury in the presence or ab-

sence of o-phenanthroline. MMP-2 activity, but not its protein level was significantly increased in I/R rat hearts. The ability of MMP-2 to proteolyse lamins in silico and in vitro was tested. Lamin A was proteolysed into an ~50 kDa fragment by MMP-2. Protein levels of known intracellular MMP-2 targets such as TnI and putative nuclear MMP-2 targets such as PARP-1, lamin A and C were measured in I/R hearts. TnI protein levels decreased in I/R hearts, and were rescued by o-phenanthroline as previously shown (Wang *et al.*, 2002). No changes in lamin A or C protein levels were observed in hearts subjected to I/R injury. PARP-1 protein levels were decreased in I/R+O hearts compared to I/R hearts, and PARP-1 protein levels correlated inversely with the recovery of myocardial contractile function.

4.2 Nuclear localization of MMP-2

Immunofluorescence confocal microscopy was used to visualize the distribution of MMP-2 in NRVMs (Figure 3.1) and HT 1080 (Figure 3.4) cells. In both the former and cancer cell line I saw a distribution of MMP-2 throughout the cytoplasm and in the nucleus of these cells. Nuclear localization of MMP-2 was seen in some but not all cells, which could be attributed to a natural nucleocytoplasmic flux of proteins prior to cells being fixed and stained. However, it has previously been reported that nuclear MMP-2 remains stable, with little export from the nucleus in human coronary artery endothelial cells (Sinha *et al.*, 2014). This would suggest that MMP-2 is recruited to the nucleus for a specific function, and a certain amount of MMP-2 continuously remains in the nucleus for normal physiological activity.

Imaging flow cytometry was used to identify the percentage of the population of HT 1080 cells that had nuclearly translocated MMP-2 (Figure 3.5). This tech-

nique combines regular flow cytometry with immunofluorescence microscopy. Thousands of cells can be imaged and analysed, making it easy to identify immunostained protein co-localization with the nuclear stain. The degree of correlation between the nuclear stain and the immunostained protein from each cell is calculated, which is defined as a similarity score (Barteneva *et al.*, 2012). In our experiment a similarity score of >1.5 was defined as nuclearly translocated MMP-2. ~10,000 cells were analyzed and it was determined that 11.4% of the cells had MMP-2 concentrated to the cytoplasm, while 88.6% of the cells had MMP-2 concentrated to the nucleus. This experiment confirmed that the majority of the HT 1080 cell population have MMP-2 localized to the nucleus.

Subcellular fractions were isolated from NRVMs and subcellular fraction purity was determined by western blot of specific cellular markers (Figure 3.2, A). The absence of the GAPDH band in the nuclear fraction confirmed the nuclear fraction purity from cytosolic contamination. MMP-2 protein levels (Figure 3.2) as well as activity (Figure 3.3) were measured in subcellular fractions by western blot and gelatin zymography, respectively. It was determined that 15% of the total cellular MMP-2 protein levels and 10% of total cellular MMP-2 activity was found in the nuclear fraction. The activity of MMP-2 measured by gelatin zymography is not representative of the actual activity one might expect to see *in vivo*. SDS in the gel denatures MMP-2 and -9; only after removal of SDS from the gel the partially renatured enzymes remain activated, since the active site is exposed. Potential gelatinolytic activity of MMP-2 and -9 is measured by this technique (Toth and Fridman, 2001). Gelatin zymography does not account for ways MMP-2 activity might be regulated in the cell, especially by TIMPs. TIMP-1 and TIMP-4 have been

found in the nucleus, which suggests that under homeostasis proteolysis of nuclear targets by MMPs is regulated (Ritter *et al.*, 1999; Si-Tayeb *et al.*, 2006; Zhao *et al.*, 1998). TIMP-1 has been reported to colocalize with MMP-2 in the nucleus by immunofluorescence (Sinha *et al.*, 2014). The activity of nuclear MMP-2 could be regulated by TIMP-1, which should be verified in future studies.

When comparing the overall protein levels in the nucleus as measured by Western blot and immunofluorescence microscopy it seemed that the protein density appeared greater by immunofluorescence. In order to identify if our observations were due to some type of immunologic artifact, such as non-specific binding, we tested the antibodies used in immunofluorescence experiment on fibroblasts isolated from neonatal wild type and MMP-2 knock out mice. There was little to no staining observed with Ab19015 antibody (Figure 3.6) or the antibody against S1' loop (Figure 3.7) in MMP-2 knock out fibroblasts, confirming that the antibodies indeed specifically recognize MMP-2. Therefore, it is likely that during the subcellular fractionation some of the MMP-2 leaked out of the nucleus, making it difficult to accurately measure the protein levels and activity of the enzyme. The cytosolic buffer used to lyse the cells had digitonin as the main component. Digitonin is a steroidal saponin that permeabilizes the plasma membrane by binding with cholesterol and other β -hydroxysterols, thereby leading to the formation of pores in the membrane and its subsequent disruption (Schulz, 1990). The plasma membrane does contain higher amounts of cholesterol compared to the nuclear membrane (Kleinig *et al.*, 1971). However, since the nuclear membrane contains some cholesterol digitonin could potentially bind it to cause the formation of pores and release of nuclear proteins. The protocol for subcellular fractionation was optimized to reduce the loss of

nuclear proteins by using very low concentrations of digitonin, however, it seems that the loss of nuclear proteins is not entirely unavoidable.

4.3 Nuclear MMP-2 in I/R hearts

One of the objectives of this study was to investigate nuclear MMP-2 activity and protein levels in hearts that underwent I/R injury. Isolated rat hearts were perfused for a total of 75 min by the Langendorff method in one of the following ways: 75 min of aerobic perfusion (AE, control), 20 min of aerobic perfusion followed by 20 min of global, no-flow ischemia and 35 min of aerobic reperfusion (I/R) without or with o-phenanthroline, an MMP inhibitor (I/R+O). The heart rate, coronary flow, developed pressure and heart rate pressure product were measured in all hearts (Figure 3.8). Control AE hearts that received the drug vehicle had no loss in contractile function, indicating that the vehicle on its own was not having an effect on the hearts. I/R hearts had significantly reduced recovery in contractile function after global, no-flow ischemia compared to I/R hearts that received o-phenanthroline. O-phenanthroline improved the contractile function of hearts after I/R injury, indicating that inhibiting the activity of MMPs functionally protects rat hearts that undergo I/R injury. The protective effect of o-phenanthroline and doxycycline were previously shown on hearts that underwent I/R injury (Wang *et al.*, 2002). Oxidative stress in the first few min of reperfusion following ischemia results in the activation of 72 kDa MMP-2 by S-glutathiolation, leading to proteolysis of sarcomeric and cytoskeletal proteins (Ali *et al.*, 2011).

The cytosol, membrane and nuclear fractions were isolated from rat hearts. The purity of the fractions was assessed by western blot against specific markers

(Figure 3.9). GAPDH was used as the major cytosolic marker (Tristan *et al.*, 2011), SERCA2 and VDAC were used as membrane markers since they are associated with the sarco/endoplasmic reticulum and mitochondria, respectively (Raturi and Simmen, 2013), and lamin A/C was used as a nuclear marker. The bulk of GAPDH was found in the cytosolic fraction, with a lower amount in the membrane fraction. GAPDH can be found in the mitochondria and small vesicular structures of the cell when exposed to stressors which cause a dynamic subcellular redistribution of GAPDH (Tristan *et al.*, 2011). Both SERCA2 and VDAC were present in the membrane fraction and absent from the cytosolic and nuclear fractions. Lamin A/C was found exclusively in the nuclear fraction isolated from hearts. This confirmed that the subcellular fractions and especially the nuclear fraction were pure and free of contamination.

MMP-2 protein levels (Figure 3.10) and activity (Figure 3.11) were measured in all fractions. The percent total nuclear MMP-2 protein levels (Figure 3.10, B) and percent total MMP-2 activity (Figure 3.11, B) were significantly increased in I/R+O compared to AE control hearts. There was no increase in percent total nuclear MMP-2 protein levels in I/R hearts, in contrast percent total nuclear MMP-2 activity increased in I/R hearts. The increase in nuclear MMP-2 activity was not accompanied by an increase in protein levels, suggesting that post-translational modifications such as S-glutathiolation of the Cys¹⁰² residue as a result of increased RONS is the cause. The addition of o-phenanthroline to I/R hearts functionally protected the hearts although this was not accompanied by reduction of protein levels or activity of nuclear MMP-2. This is due to the fact that o-phenanthroline does not interfere with the increased expression or activation of MMP-2 by RONS. It was previously

shown that MMP-2 activity is increased in the nucleus due to RONS activating MMP-2, by S-glutathiolation, in pulmonary artery endothelial cells that were subjected to cigarette smoke (Ruta *et al.*, 2009). Increased nuclear MMP-2 activity was also observed in rat brains subjected to 90 min of middle cerebral artery occlusion followed by reperfusion, which resulted in reduced protein levels of PARP-1 and XRCC1 in ischemic rat brains. BB1101, an MMP inhibitor, attenuated PARP-1 and XRCC1 proteolysis, and reduced the early oxidative DNA damage in ischemic rat brains (Yang *et al.*, 2010).

4.4 Proteolysis targets of MMP-2 in cytoplasm and nucleus

The nucleus has a protein skeleton for support and organization, known as the nuclear matrix, that is interconnected with the cytoskeleton and the extracellular matrix through complex structures (Albrethsen *et al.*, 2009). Scientists are still in the process of discovering the nuclear matrix proteins, but so far some of the major components include: the nuclear mitotic apparatus protein, heterogeneous nuclear ribonucleoprotein, matrisins, actins and lamins (Nickerson, 2001; Razin *et al.*, 2014). The filamentous network of lamins acts as a structural support of the nuclear membrane. The lamins are subdivided into A-type lamins (lamin A & C) and B-type lamins (lamin B1 & B2) (Aebi *et al.*, 1986). In ischemia-reperfusion injury MMP-2 has been shown to proteolyse structural proteins of the sarcomere and cytoskeleton (Ali *et al.*, 2011). Lamins are major structural support proteins of the nucleus, thus they were investigated further as possible nuclear MMP-2 targets.

In silico proteolysis by MMP-2 of lamin A and B protein sequence (Table 3.1) showed that MMP-2 could potentially proteolyse A or B at two distinct sites. The

ability of MMP-2 to proteolyse lamins was tested further by an in vitro proteolysis assay, where MMP-2 was incubated with lamin A (Figure 3.12) or B (Figure 3.13). TnI was used as positive control of MMP-2 proteolysis (Figure 3.13). Lamin B was not proteolysed by MMP-2 in vitro, consequently the assay allowed us to eliminate lamin B as a possible MMP-2 target. Alternatively, lamin A was proteolyzed by MMP-2 in vitro, in a concentration dependent manner. The proteolysis yielded a fragment that was observed at 50 kDa molecular weight marker, and approximately matched a fragment (43 kDa) predicted by the in silico analysis. This fragment contains the C-terminal globular domain, the Ig-like structure and nuclear localization signal. The N-terminal fragment predicted by in silico analysis at 36 kDa, would then contain the globular domain, the central α -helical rod-like domains that are believed to mediate the dimerization of lamin A/C and hence formation of the complex structure that supports the inner nuclear membrane (Liu and Zhou, 2008). Thus, the proteolysis of lamin A/C by MMP-2 could potentially result in deformed or weak nuclei.

The protein levels of lamin A or C were measured in homogenates (Figure 3.14) and in the insoluble cellular fraction (Figure 3.15) from isolated perfused rat hearts subjected to I/R injury. There was no significant change in protein levels of lamin A or C or the lamin A to C ratio between the three heart groups. Lamin A or C protein levels were not affected by I/R injury or by o-phenanthroline treatment in our experimental model. MMP-2 is able to proteolyse lamin A in vitro, however the increase of nuclear MMP-2 activity did not result in reduction of lamin A or C in I/R injury.

Loss of lamin has been previously shown by immunohistochemistry in heart tissue that underwent 90 min irreversible ischemia with 6 hours of reperfusion that resulted in apoptosis. In contrast, in reversible I/R injury apoptosis was not triggered and no changes in lamin protein levels were detected. Lamin breakdown is required for release of nuclear contents during apoptosis (Freude *et al.*, 2000). In our experimental model I/R injury is reversible, therefore, no changes in lamin protein levels were observed. Oxidative stress during the reperfusion phase of reversible I/R injury can result in changes in lamin structure without proteolysis. Oxidation of the conserved C-terminal cysteine residues in the tail domain of lamin A has been shown to cause dysmorphic nuclei, cellular senescence and lead to further susceptibility to RONS-induced damage (Pekovic *et al.*, 2011; Sieprath *et al.*, 2012). Therefore, lamin A might still be playing a role in cardiac I/R injury, even if its overall protein levels are not altered.

The enhanced biosynthesis of RONS in I/R injury is known to result in DNA oxidation that can lead to single strand DNA breaks and further damage in the cell (Sieprath *et al.*, 2012). Single strand DNA breaks activate nuclear PARP-1 which repairs the damage (Pacher and Szabo, 2007). PARP-1 plays an important role in cell survival and was previously reported to be proteolysed by MMP-2 in vitro (Kwan *et al.*, 2004; Yang *et al.*, 2010). PARP-1 protein levels were measured in heart homogenates from AE, I/R and I/R+O hearts by western blot (Figure 3.17). The protein levels of 116 kDa full length PARP-1 were significantly decreased in I/R+O hearts compared to I/R hearts. No significant changes were measured in the 85 kDa PARP-1 fragment, a caspase-3 generated fragment during apoptosis (Freude *et al.*, 2000).

Further analysis was performed on the relationship between the heart contractile function and the nuclear protein levels of 116 kDa PARP-1 (Figure 3.18). PARP-1 was increased in hearts that had a lower percent recovery of contractile function. Increased PARP-1 during I/R injury was previously shown in many in vitro and in vivo studies (Szabados *et al.*, 1999; Virag and Szabo, 2002). Overactivation of PARP-1 was shown to reduce contractile function of hearts, by depleting the energy stores (Virag and Szabo, 2002). Pharmacological inhibition of PARP-1 (Pacher and Szabo, 2007) or knock out of PARP-1 have been shown to have cardioprotective effects (Zingarelli *et al.*, 2004).

In order to validate the activity of intracellular MMP-2 in I/R injury, troponin I, a known sarcomeric target, was measured by western blot (Figure 3.16). Troponin I protein levels were reduced in I/R hearts this was attenuated by o-phenanthroline. These results confirmed that MMP-2 was proteolyzing known sarcomeric targets intracellularly (Wang *et al.*, 2002), however intra-nuclearly we were not able to discover the target(s) of the proteolytic activity of MMP-2.

4.5 Limitations

Many limitations of the scientific methods used in this study have been already addressed throughout this chapter. In this section a more detailed discussion of some of the major limitations are presented. The assay used to assess MMP-2 and -9 activities was gelatin zymography, which uses a normal acrylamide separating gel of SDS-PAGE that is embedded with gelatin (Vandooren *et al.*, 2013). The non-reducing conditions help to maintain activity of the enzyme; however SDS in the gel causes the proteins to denature. SDS is removed from the gel with a non-

ionic detergent, allowing the enzymes to partially refold before testing the activity (Toth and Fridman, 2001). Once partially refolded previously inactive enzymes in the sample become activated, as well as any MMP-TIMP complexes are disrupted. Therefore, activity measured by gelatin zymography is not biologically representative, but a measure of potential gelatinolytic activity (Vandooren *et al.*, 2013). In addition to that while gelatin is a good indicator of extracellular MMP-2 activity, it is likely not the ideal substrate for measuring intracellular and intranuclear proteolytic activity of MMP-2.

In this study the isolated heart perfusion were performed by the Langendorff method at constant pressure. This method is very useful as it allows studying the contractile function of hearts at physiological and pathological conditions, with or without pharmacological manipulations. After perfusion biochemical analyses can be performed with fresh or frozen heart tissue homogenates, to investigate biological changes of proteins. While a lot can be learned by using this technique it comes with its own set of limitations worth mentioning. First, the heart is studied in isolation from the animal without hormonal and neuronal regulations present *in vivo* (Skrzypiec-Spring *et al.*, 2007). Second, the perfusions are performed with Krebs Henseleit solution which is supposed to mimic the ionic composition of the blood as well as provide fuel to support myocardial contraction; however it lacks many vital components of blood. Perfusion with Krebs Henseleit solution has been reported to result in accumulation of water in tissue (oedema), especially in I/R hearts. Third, the temperature has to be maintained at physiological 37°C, however heat loss during ischemia is unavoidable, and low coronary flow-rate set ups are even more prone to heat loss (Bell *et al.*, 2011). These limitations should be kept in mind when

interpreting the results. The findings with ex vivo experiments have to be followed up with in vivo animal models, to make these findings more translational and clinically relevant (Bell *et al.*, 2011).

O-phenanthroline, an MMP inhibitor, is a zinc chelating agent that was used in the experimental model of isolated rat heart perfusions, and in the in vitro proteolysis assay to inhibit MMP-2. O-phenanthroline inhibits a broad range of MMPs, but it has been reported to have other possible effects such as the scavenging of RONS (Peterson, 2004). The in vitro proteolysis assay o-phenanthroline is quite useful, as it can only inhibit MMP-2 activity within the experiment. In isolated rat hearts, o-phenanthroline being a zinc chelating agent, it can inhibit other MMPs, and metalloproteinases of different families (Peterson, 2004). Therefore, the results should take into account the effects that o-phenanthroline can have beyond inhibiting MMPs.

4.6 Future directions

This study examined nuclear localization of MMP-2 and the increase of MMP-2 activity during I/R injury. Novel and known targets were tested for proteolysis by MMP-2 in silico, in vitro and in heart tissue after I/R injury. This study built on the existing knowledge of nuclear MMPs, but more questions remain to be answered. Lamin A or C protein levels did not change in I/R injured hearts, leaving the nuclear targets and functions of MMP-2 in I/R hearts to be determined. Future studies should examine in more detail what happens to nuclear MMP-2 after longer I/R injury, and the effect this would have on the putative targets. Nuclear actin and fi-

bronectin have been suggested as possible targets of nuclear MMP-2, and should be investigated in future studies.

Little is still known when, how, or why MMP-2 enters the nucleus. The stimuli that cause MMP-2 to translocate to the nucleus should be further explored, and whether or not translocation of MMP-2 requires any post-translational modifications, such as phosphorylation. More careful investigation into the exact nuclear localization, and co-localization with nuclear bodies would provide more clues as to the nuclear function of MMP-2. In this study we determined that the majority of unstimulated HT 1080 cell population has nuclear MMP-2. It seems that nuclear MMP-2 is there under normal physiological conditions; however the role it plays is still undetermined. Having more nuclearly translocated MMP-2 might relate to different stages of the cell cycle. It is possible that more nuclear MMP-2 is found in cells undergoing replication, or in cells that are preparing for cell division. Nuclear matrix remodeling is required to prepare the cell for division, and the role of nuclear MMP-2 in cell cycle, therefore, has to be carefully examined.

TIMPs (-1 and -4) the endogenous inhibitors of MMPs are present in the nucleus as well. Nuclear MMP-2 can be regulated by TIMPs to prevent proteolysis of targets during homeostasis, but the relationship between nuclear TIMPs and MMPs has yet to be determined. MMP-14, a major activator of MMP-2, has been found to co-localize with MMP-2 in ischemic nuclei and in nuclear extracts. MMP-2 endogenous inhibitors are present in the nucleus, and the mechanisms of nuclear MMP-2 regulation under homeostasis and stress remain to be explored.

Although MMPs are commonly thought of in terms of their proteolytic abilities, proteolysis of nuclear proteins is not the only possible function of nuclear

MMPs. For example, MMP-3 (Eguchi *et al.*, 2008) and MMP-12 (Marchant *et al.*, 2014) have been shown to act as transcription factors. MMP-3 regulates the expression of the connective tissue growth factor gene, binding the enhancer sequences of the connective tissue growth factor promoter and activating gene transcription (Eguchi *et al.*, 2008). The transcriptional role of MMP-12 was identified in virus infected cells, binding the promoter of the nuclear factor of kappa light polypeptide gene (Marchant *et al.*, 2014). Thus, nuclear MMP-2 may play a yet undiscovered role in the activation of genes in myocardial stunning injury.

References:

- Aebi, U., J. Cohn, L. Buhle and L. Gerace. 1986. The nuclear lamina is a meshwork of intermediate-type filaments. *Nature* **323**(6088): 560-564.
- Albrethsen, J., J. C. Knol and C. R. Jimenez. 2009. Unravelling the nuclear matrix proteome. *J Proteomics* **72**(1): 71-81.
- Ali, M. A., W. J. Cho, B. Hudson, Z. Kassiri, H. Granzier and R. Schulz. 2010. Titin is a target of matrix metalloproteinase-2: implications in myocardial ischemia/reperfusion injury. *Circulation* **122**(20): 2039-2047.
- Ali, M. A., A. K. Chow, A. D. Kandasamy, X. Fan, L. J. West, B. D. Crawford, T. Simmen and R. Schulz. 2012. Mechanisms of cytosolic targeting of matrix metalloproteinase-2. *J Cell Physiol* **227**(10): 3397-3404.
- Ali, M. A., X. Fan and R. Schulz. 2011. Cardiac sarcomeric proteins: novel intracellular targets of matrix metalloproteinase-2 in heart disease. *Trends Cardiovasc Med* **21**(4): 112-118.
- Baker, A. H., D. R. Edwards and G. Murphy. 2002. Metalloproteinase inhibitors: biological actions and therapeutic opportunities. *J Cell Sci* **115**(Pt 19): 3719-3727.
- Barteneva, N. S., E. Fasler-Kan and I. A. Vorobjev. 2012. Imaging flow cytometry: coping with heterogeneity in biological systems. *J Histochem Cytochem* **60**(10): 723-733.
- Bell, R. M., M. M. Mocanu and D. M. Yellon. 2011. Retrograde heart perfusion: the Langendorff technique of isolated heart perfusion. *J Mol Cell Cardiol* **50**(6): 940-950.
- Bergman, M. R., S. Cheng, N. Honbo, L. Piacentini, J. S. Karliner and D. H. Lovett. 2003. A functional activating protein 1 (AP-1) site regulates matrix metalloproteinase 2 (MMP-2) transcription by cardiac cells through interactions with JunB-Fra1 and JunB-FosB heterodimers. *Biochem J* **369**(Pt 3): 485-496.
- Boisvert, F. M., S. van Koningsbruggen, J. Navascues and A. I. Lamond. 2007. The multifunctional nucleolus. *Nat Rev Mol Cell Biol* **8**(7): 574-585.
- Carmosino, M., S. Torretta, G. Procino, A. Gerbino, C. Forleo, S. Favale and M. Svelto. 2014. Role of nuclear Lamin A/C in cardiomyocyte functions. *Biol Cell* **106**(10): 346-358.
- Cauwe, B. and G. Opdenakker. 2010. Intracellular substrate cleavage: a novel dimension in the biochemistry, biology and pathology of matrix metalloproteinases. *Crit Rev Biochem Mol Biol* **45**(5): 351-423.
- Cheung, P. Y., G. Sawicki, M. Wozniak, W. Wang, M. W. Radomski and R. Schulz. 2000. Matrix metalloproteinase-2 contributes to ischemia-reperfusion injury in the heart. *Circulation* **101**(15): 1833-1839.
- Cho, W. J., A. K. Chow, R. Schulz and E. E. Daniel. 2007. Matrix metalloproteinase-2, caveolins, focal adhesion kinase and c-Kit in cells of the mouse myocardium. *J Cell Mol Med* **11**(5): 1069-1086.

- Chow, A. K., J. Cena, A. F. El-Yazbi, B. D. Crawford, A. Holt, W. J. Cho, E. E. Daniel and R. Schulz. 2007. Caveolin-1 inhibits matrix metalloproteinase-2 activity in the heart. *J Mol Cell Cardiol* **42**(4): 896-901.
- Chow, A. K., J. Cena and R. Schulz. 2007. Acute actions and novel targets of matrix metalloproteinases in the heart and vasculature. *Br J Pharmacol* **152**(2): 189-205.
- Cremer, T. and C. Cremer. 2001. Chromosome territories, nuclear architecture and gene regulation in mammalian cells. *Nat Rev Genet* **2**(4): 292-301.
- Cuadrado, E., A. Rosell, M. Borrell-Pages, L. Garcia-Bonilla, M. Hernandez-Guillamon, A. Ortega-Aznar and J. Montaner. 2009. Matrix metalloproteinase-13 is activated and is found in the nucleus of neural cells after cerebral ischemia. *J Cereb Blood Flow Metab* **29**(2): 398-410.
- Dahl, K. N., A. J. Ribeiro and J. Lammerding. 2008. Nuclear shape, mechanics, and mechanotransduction. *Circ Res* **102**(11): 1307-1318.
- DeCoux, A., M. L. Lindsey, F. Villarreal, R. A. Garcia and R. Schulz. 2014. Myocardial matrix metalloproteinase-2: inside out and upside down. *J Mol Cell Cardiol* **77**: 64-72.
- Eguchi, T., S. Kubota, K. Kawata, Y. Mukudai, J. Uehara, T. Ohgawara, S. Ibaragi, A. Sasaki, T. Kuboki and M. Takigawa. 2008. Novel transcription-factor-like function of human matrix metalloproteinase 3 regulating the CTGF/CCN2 gene. *Mol Cell Biol* **28**(7): 2391-2413.
- Ferrai, C., I. J. de Castro, L. Lavitas, M. Chotalia and A. Pombo. 2010. Gene positioning. *Cold Spring Harb Perspect Biol* **2**(6): a000588.
- Filipiak, K., K. Kubinski, U. Hellman, A. Ramos and B. de Pascual-Teresa. 2014. Human protein kinase CK2 phosphorylates matrix metalloproteinase 2 and inhibits its activity. *Chembiochem* **15**(13): 1873-1876.
- Fong, L. G., J. K. Ng, J. Lammerding, T. A. Vickers, M. Meta, N. Cote, B. Gavino, X. Qiao, S. Y. Chang, S. R. Young, S. H. Yang, C. L. Stewart, R. T. Lee, C. F. Bennett, M. O. Bergo and S. G. Young. 2006. Prelamin A and lamin A appear to be dispensable in the nuclear lamina. *J Clin Invest* **116**(3): 743-752.
- Freude, B., T. N. Masters, F. Robicsek, A. Fokin, S. Kostin, R. Zimmermann, C. Ullmann, S. Lorenz-Meyer and J. Schaper. 2000. Apoptosis is initiated by myocardial ischemia and executed during reperfusion. *J Mol Cell Cardiol* **32**(2): 197-208.
- Gall, J. G. 2003. The centennial of the Cajal body. *Nat Rev Mol Cell Biol* **4**(12): 975-980.
- Golub, L. M., H. M. Lee, M. E. Ryan, W. V. Giannobile, J. Payne and T. Sorsa. 1998. Tetracyclines inhibit connective tissue breakdown by multiple non-antimicrobial mechanisms. *Adv Dent Res* **12**(2): 12-26.
- Gu, Z., M. Kaul, B. Yan, S. J. Kridel, J. Cui, A. Strongin, J. W. Smith, R. C. Liddington and S. A. Lipton. 2002. S-nitrosylation of matrix metalloproteinases: signaling pathway to neuronal cell death. *Science* **297**(5584): 1186-1190.

- Hill, J. W., R. Poddar, J. F. Thompson, G. A. Rosenberg and Y. Yang. 2012. Intranuclear matrix metalloproteinases promote DNA damage and apoptosis induced by oxygen-glucose deprivation in neurons. *Neuroscience* **220**(0): 277-290.
- Holden, P. and W. A. Horton. 2009. Crude subcellular fractionation of cultured mammalian cell lines. *BMC Res Notes* **2**: 243.
- Hughes, B. G., X. Fan, W. J. Cho and R. Schulz. 2014. MMP-2 is localized to the mitochondria-associated membrane of the heart. *Am J Physiol Heart Circ Physiol* **306**(5): H764-770.
- Hutchison, C. J. 2011. The role of DNA damage in laminopathy progeroid syndromes. *Biochem Soc Trans* **39**(6): 1715-1718.
- Ip, Y. C., S. T. Cheung and S. T. Fan. 2007. Atypical localization of membrane type 1-matrix metalloproteinase in the nucleus is associated with aggressive features of hepatocellular carcinoma. *Mol Carcinog* **46**(3): 225-230.
- Itoh, Y., S. Binner and H. Nagase. 1995. Steps involved in activation of the complex of pro-matrix metalloproteinase 2 (progelatinase A) and tissue inhibitor of metalloproteinases (TIMP)-2 by 4-aminophenylmercuric acetate. *Biochem J* **308** (Pt 2): 645-651.
- Jacob-Ferreira, A. L., M. Y. Kondo, P. K. Baral, M. N. James, A. Holt, X. Fan and R. Schulz. 2013. Phosphorylation status of 72 kDa MMP-2 determines its structure and activity in response to peroxynitrite. *PLoS One* **8**(8): e71794.
- Kalogeris, T., C. P. Baines, M. Krenz and R. J. Korthuis. 2012. Cell biology of ischemia/reperfusion injury. *Int Rev Cell Mol Biol* **298**: 229-317.
- Kandasamy, A. D., A. K. Chow, M. A. Ali and R. Schulz. 2010. Matrix metalloproteinase-2 and myocardial oxidative stress injury: beyond the matrix. *Cardiovasc Res* **85**(3): 413-423.
- Karnabi, E., Y. X. Qu, S. Mancarella, Y. K. Yue, R. Wadgaonkar and M. Boutjdir. 2009. Silencing of Cav1.2 gene in neonatal cardiomyocytes by lentiviral delivered shRNA. *Biochem Biophys Res Commun* **384**(4): 409-414.
- Kleinig, H., H. Zentgraf, P. Comes and J. Stadler. 1971. Nuclear membranes and plasma membranes from hen erythrocytes. II. Lipid composition. *J Biol Chem* **246**(9): 2996-3000.
- Kohrmann, A., U. Kammerer, M. Kapp, J. Dietl and J. Anacker. 2009. Expression of matrix metalloproteinases (MMPs) in primary human breast cancer and breast cancer cell lines: New findings and review of the literature. *BMC Cancer* **9**: 188.
- Kwan, J. A., C. J. Schulze, W. Wang, H. Leon, M. Sariahmetoglu, M. Sung, J. Sawicka, D. E. Sims, G. Sawicki and R. Schulz. 2004. Matrix metalloproteinase-2 (MMP-2) is present in the nucleus of cardiac myocytes and is capable of cleaving poly (ADP-ribose) polymerase (PARP) in vitro. *Faseb J* **18**(6): 690-692.

- Lalu, M. M., E. Pasini, C. J. Schulze, M. Ferrari-Vivaldi, G. Ferrari-Vivaldi, T. Bachetti and R. Schulz. 2005. Ischaemia-reperfusion injury activates matrix metalloproteinases in the human heart. *Eur Heart J* **26**(1): 27-35.
- Limb, G. A., K. Matter, G. Murphy, A. D. Cambrey, P. N. Bishop, G. E. Morris and P. T. Khaw. 2005. Matrix Metalloproteinase-1 Associates with Intracellular Organelles and Confers Resistance to Lamin A/C Degradation during Apoptosis. *The American Journal of Pathology* **166**(5): 1555-1563.
- Linask, K. K., M. Han, D. H. Cai, P. R. Brauer and S. M. Maisastry. 2005. Cardiac morphogenesis: matrix metalloproteinase coordination of cellular mechanisms underlying heart tube formation and directionality of looping. *Dev Dyn* **233**(3): 739-753.
- Linnemann, A. K. and S. A. Krawetz. 2009. Maintenance of a functional higher order chromatin structure: The role of the nuclear matrix in normal and disease states. *Gene Ther Mol Biol* **13**(1): 231-243.
- Liu, B. and Z. Zhou. 2008. Lamin A/C, laminopathies and premature ageing. *Histol Histopathol* **23**(6): 747-763.
- Liu, J., T. Rolef Ben-Shahar, D. Riemer, M. Treinin, P. Spann, K. Weber, A. Fire and Y. Gruenbaum. 2000. Essential roles for *Caenorhabditis elegans* lamin gene in nuclear organization, cell cycle progression, and spatial organization of nuclear pore complexes. *Mol Biol Cell* **11**(11): 3937-3947.
- Lopez-Soler, R. I., R. D. Moir, T. P. Spann, R. Stick and R. D. Goldman. 2001. A role for nuclear lamins in nuclear envelope assembly. *J Cell Biol* **154**(1): 61-70.
- Mannello, F. and V. Medda. 2012. Nuclear localization of matrix metalloproteinases. *Prog Histochem Cytochem* **47**(1): 27-58.
- Marchant, D. J., C. L. Bellac, T. J. Moraes, S. J. Wadsworth, A. Dufour, G. S. Butler, L. M. Bilawchuk, R. G. Hendry, A. G. Robertson, C. T. Cheung, J. Ng, L. Ang, Z. S. Luo, K. Heilbron, M. J. Norris, W. M. Duan, T. Bucyk, A. Karpov, L. Devel, D. Georgiadis, R. G. Hegele, H. L. Luo, D. J. Granville, V. Dive, B. M. McManus and C. M. Overall. 2014. A new transcriptional role for matrix metalloproteinase-12 in antiviral immunity. *Nat Med* **20**(5): 497-506.
- McLane, L. M. and A. H. Corbett. 2009. Nuclear localization signals and human disease. *IUBMB Life* **61**(7): 697-706.
- Morgunova, E., A. Tuuttila, U. Bergmann, M. Isupov, Y. Lindqvist, G. Schneider and K. Tryggvason. 1999. Structure of Human Pro-Matrix Metalloproteinase-2: Activation Mechanism Revealed. *Science* **284**(5420): 1667-1670.
- Nickerson, J. 2001. Experimental observations of a nuclear matrix. *J Cell Sci* **114**(Pt 3): 463-474.
- Novak, M. J., L. P. Johns, R. C. Miller and M. H. Bradshaw. 2002. Adjunctive benefits of subantimicrobial dose doxycycline in the management of severe, generalized, chronic periodontitis. *J Periodontol* **73**(7): 762-769.

- Okamoto, T., T. Akaike, T. Sawa, Y. Miyamoto, A. van der Vliet and H. Maeda. 2001. Activation of matrix metalloproteinases by peroxynitrite-induced protein S-glutathiolation via disulfide S-oxide formation. *J Biol Chem* **276**(31): 29596-29602.
- Osorio, D. S. and E. R. Gomes. 2013. The contemporary nucleus: a trip down memory lane. *Biol Cell* **105**(9): 430-441.
- Pacher, P. and C. Szabo. 2007. Role of poly(ADP-ribose) polymerase 1 (PARP-1) in cardiovascular diseases: the therapeutic potential of PARP inhibitors. *Cardiovasc Drug Rev* **25**(3): 235-260.
- Pekovic, V., I. Gibbs-Seymour, E. Markiewicz, F. Alzoghaibi, A. M. Benham, R. Edwards, M. Wenhert, T. von Zglinicki and C. J. Hutchison. 2011. Conserved cysteine residues in the mammalian lamin A tail are essential for cellular responses to ROS generation. *Aging Cell* **10**(6): 1067-1079.
- Peterson, J. T. 2004. Matrix metalloproteinase inhibitor development and the remodeling of drug discovery. *Heart Fail Rev* **9**(1): 63-79.
- Pirici, D., I. Pirici, L. Mogoanta, O. Margaritescu, V. Tudorica, C. Margaritescu, D. A. Ion, C. Simionescu and M. Coconu. 2012. Matrix metalloproteinase-9 expression in the nuclear compartment of neurons and glial cells in aging and stroke. *Neuropathology* **32**(5): 492-504.
- Raturi, A. and T. Simmen. 2013. Where the endoplasmic reticulum and the mitochondrion tie the knot: the mitochondria-associated membrane (MAM). *Biochim Biophys Acta* **1833**(1): 213-224.
- Razin, S. V., V. V. Borunova, O. V. Iarovaia and Y. S. Vassetzky. 2014. Nuclear matrix and structural and functional compartmentalization of the eucaryotic cell nucleus. *Biochemistry (Mosc)* **79**(7): 608-618.
- Ritter, L. M., S. H. Garfield and U. P. Thorgeirsson. 1999. Tissue inhibitor of metalloproteinases-1 (TIMP-1) binds to the cell surface and translocates to the nucleus of human MCF-7 breast carcinoma cells. *Biochem Biophys Res Commun* **257**(2): 494-499.
- Ruta, A., B. Mark, B. Edward, P. Jawaharlal and Z. Jianliang. 2009. Nuclear Localization of Active Matrix Metalloproteinase-2 in Cigarette Smoke-Exposed Apoptotic Endothelial Cells. *Exp Lung Res* **35**(1): 59-75.
- Sariahmetoglu, M., B. D. Crawford, H. Leon, J. Sawicka, L. Li, B. J. Ballermann, C. Holmes, L. G. Berthiaume, A. Holt, G. Sawicki and R. Schulz. 2007. Regulation of matrix metalloproteinase-2 (MMP-2) activity by phosphorylation. *Faseb J* **21**(10): 2486-2495.
- Sawicki, G., H. Leon, J. Sawicka, M. Sariahmetoglu, C. J. Schulze, P. G. Scott, D. Szczesna-Cordary and R. Schulz. 2005. Degradation of myosin light chain in isolated rat hearts subjected to ischemia-reperfusion injury: a new intracellular target for matrix metalloproteinase-2. *Circulation* **112**(4): 544-552.

- Schirmer, E. C., L. Florens, T. Guan, J. R. Yates, 3rd and L. Gerace. 2003. Nuclear membrane proteins with potential disease links found by subtractive proteomics. *Science* **301**(5638): 1380-1382.
- Schreiber, K. H. and B. K. Kennedy. 2013. When lamins go bad: nuclear structure and disease. *Cell* **152**(6): 1365-1375.
- Schulz, I. 1990. Permeabilizing cells: some methods and applications for the study of intracellular processes. *Methods Enzymol* **192**: 280-300.
- Schulze, C. J., W. Wang, W. L. Suarez-Pinzon, J. Sawicka, G. Sawicki and R. Schulz. 2003. Imbalance between tissue inhibitor of metalloproteinase-4 and matrix metalloproteinases during acute myocardial [correction of myoectardial] ischemia-reperfusion injury. *Circulation* **107**(19): 2487-2492.
- Shimizu-Hirota, R., W. Xiong, B. T. Baxter, S. L. Kunkel, I. Maillard, X. W. Chen, F. Sabeh, R. Liu, X. Y. Li and S. J. Weiss. 2012. MT1-MMP regulates the PI3Kdelta.Mi-2/NuRD-dependent control of macrophage immune function. *Genes Dev* **26**(4): 395-413.
- Si-Tayeb, K., A. Monvoisin, C. Mazzocco, S. Lepreux, M. Decossas, G. Cubel, D. Taras, J.-F. Blanc, D. R. Robinson and J. Rosenbaum. 2006. Matrix Metalloproteinase 3 Is Present in the Cell Nucleus and Is Involved in Apoptosis. *The American Journal of Pathology* **169**(4): 1390-1401.
- Si-Tayeb, K., A. Monvoisin, C. Mazzocco, S. Lepreux, M. Decossas, G. Cubel, D. Taras, J. F. Blanc, D. R. Robinson and J. Rosenbaum. 2006. Matrix metalloproteinase 3 is present in the cell nucleus and is involved in apoptosis. *The American Journal of Pathology* **169**(4): 1390-1401.
- Sieprath, T., R. Darwiche and W. H. De Vos. 2012. Lamins as mediators of oxidative stress. *Biochem Biophys Res Commun* **421**(4): 635-639.
- Sinha, S. K., K. Asotra, H. Uzui, S. Nagwani, V. Mishra and T. B. Rajavashisth. 2014. Nuclear localization of catalytically active MMP-2 in endothelial cells and neurons. *Am J Transl Res* **6**(2): 155-162.
- Skrzypiec-Spring, M., B. Grotthus, A. Szelag and R. Schulz. 2007. Isolated heart perfusion according to Langendorff---still viable in the new millennium. *J Pharmacol Toxicol Methods* **55**(2): 113-126.
- Smith, G. N., Jr., E. A. Mickler, K. A. Hasty and K. D. Brandt. 1999. Specificity of inhibition of matrix metalloproteinase activity by doxycycline: relationship to structure of the enzyme. *Arthritis Rheum* **42**(6): 1140-1146.
- Solli, A. I., B. Fadnes, J. O. Winberg, L. Uhlin-Hansen and E. Hadler-Olsen. 2013. Tissue- and cell-specific co-localization of intracellular gelatinolytic activity and matrix metalloproteinase 2. *J Histochem Cytochem* **61**(6): 444-461.
- Spann, T. P., A. E. Goldman, C. Wang, S. Huang and R. D. Goldman. 2002. Alteration of nuclear lamin organization inhibits RNA polymerase II-dependent transcription. *J Cell Biol* **156**(4): 603-608.

- Starr, D. A. and H. N. Fridolfsson. 2010. Interactions between nuclei and the cytoskeleton are mediated by SUN-KASH nuclear-envelope bridges. *Annu Rev Cell Dev Biol* **26**: 421-444.
- Strongin, A. Y., I. Collier, G. Bannikov, B. L. Marmer, G. A. Grant and G. I. Goldberg. 1995. Mechanism of cell surface activation of 72-kDa type IV collagenase. Isolation of the activated form of the membrane metalloprotease. *J Biol Chem* **270**(10): 5331-5338.
- Stuurman, N., S. Heins and U. Aebi. 1998. Nuclear lamins: their structure, assembly, and interactions. *J Struct Biol* **122**(1-2): 42-66.
- Sung, M. M., C. G. Schulz, W. Wang, G. Sawicki, N. L. Bautista-Lopez and R. Schulz. 2007. Matrix metalloproteinase-2 degrades the cytoskeletal protein alpha-actinin in peroxynitrite mediated myocardial injury. *J Mol Cell Cardiol* **43**(4): 429-436.
- Szabados, E., G. M. Fischer, F. Gallyas, Jr., G. Kispal and B. Sumegi. 1999. Enhanced ADP-ribosylation and its diminution by lipoamide after ischemia-reperfusion in perfused rat heart. *Free Radic Biol Med* **27**(9-10): 1103-1113.
- Toth, M. and R. Fridman. 2001. Assessment of Gelatinases (MMP-2 and MMP-9) by Gelatin Zymography. *Methods Mol Med* **57**: 163-174.
- Tristan, C., N. Shahani, T. W. Sedlak and A. Sawa. 2011. The diverse functions of GAPDH: views from different subcellular compartments. *Cell Signal* **23**(2): 317-323.
- van Leeuwenhoek, A. 1700. Part of a Letter from Mr Anthony van Leeuwenhoek, F. R. S. to the Publisher, concerning Several Microscopical Observations. *Philosophical Transactions* **22**(260-276): 903-907.
- Vandooren, J., N. Geurts, E. Martens, P. E. Van den Steen and G. Opdenakker. 2013. Zymography methods for visualizing hydrolytic enzymes. *Nat Methods* **10**(3): 211-220.
- Vergnes, L., M. Peterfy, M. O. Bergo, S. G. Young and K. Reue. 2004. Lamin B1 is required for mouse development and nuclear integrity. *Proc Natl Acad Sci U S A* **101**(28): 10428-10433.
- Viappiani, S., A. C. Nicolescu, A. Holt, G. Sawicki, B. D. Crawford, H. Leon, T. van Mulligen and R. Schulz. 2009. Activation and modulation of 72kDa matrix metalloproteinase-2 by peroxynitrite and glutathione. *Biochem Pharmacol* **77**(5): 826-834.
- Virag, L. and C. Szabo. 2002. The therapeutic potential of poly(ADP-ribose) polymerase inhibitors. *Pharmacol Rev* **54**(3): 375-429.
- Wang, W., G. Sawicki and R. Schulz. 2002. Peroxynitrite-induced myocardial injury is mediated through matrix metalloproteinase-2. *Cardiovasc Res* **53**(1): 165-174.
- Wang, W., C. J. Schulze, W. L. Suarez-Pinzon, J. R. Dyck, G. Sawicki and R. Schulz. 2002. Intracellular action of matrix metalloproteinase-2 accounts for acute myocardial ischemia and reperfusion injury. *Circulation* **106**(12): 1543-1549.

- Yamada, A., A. Uegaki, T. Nakamura and K. Ogawa. 2000. ONO-4817, an orally active matrix metalloproteinase inhibitor, prevents lipopolysaccharide-induced proteoglycan release from the joint cartilage in guinea pigs. *Inflamm Res* **49**(4): 144-146.
- Yang, Y., E. Candelario-Jalil, J. F. Thompson, E. Cuadrado, E. Y. Estrada, A. Rosell, J. Montaner and G. A. Rosenberg. 2010. Increased intranuclear matrix metalloproteinase activity in neurons interferes with oxidative DNA repair in focal cerebral ischemia. *J Neurochem* **112**(1): 134-149.
- Yasmin, W., K. D. Strynadka and R. Schulz. 1997. Generation of peroxynitrite contributes to ischemia-reperfusion injury in isolated rat hearts. *Cardiovasc Res* **33**(2): 422-432.
- Youssef, N. and R. Schulz. 2011. Intracellular MMP-2: Role in Normal and Diseased Hearts. 17-28.
- Zhao, W. Q., H. Li, K. Yamashita, X. K. Guo, T. Hoshino, S. Yoshida, T. Shinya and T. Hayakawa. 1998. Cell cycle-associated accumulation of tissue inhibitor of metalloproteinases-1 (TIMP-1) in the nuclei of human gingival fibroblasts. *J Cell Sci* **111** (Pt 9): 1147-1153.
- Zimowska, M., M. Swierczynska and M. A. Ciemerych. 2013. Nuclear MMP-9 role in the regulation of rat skeletal myoblasts proliferation. *Biol Cell* **105**(8): 334-344.
- Zingarelli, B., P. W. Hake, M. O'Connor, A. Denenberg, H. R. Wong, S. Kong and B. J. Aronow. 2004. Differential regulation of activator protein-1 and heat shock factor-1 in myocardial ischemia and reperfusion injury: role of poly(ADP-ribose) polymerase-1. *Am J Physiol Heart Circ Physiol* **286**(4): H1408-1415.
- Zuo, X., W. Pan, T. Feng, X. Shi and J. Dai. 2014. Matrix metalloproteinase 3 promotes cellular anti-dengue virus response via interaction with transcription factor NFkappaB in cell nucleus. *PLoS One* **9**(1): e84748.

Appendix A - Buffers and Gel Protocols

2.3 Isolated rat heart perfusions

Krebs-Henseleit solution: 118 mM NaCl, 25 mM NaHCO₃, 4.7 mM KCl, 1.2 mM MgSO₄, 1.2 mM KH₂PO₄, 11 mM glucose and 3 mM CaCl₂

2.4 Preparation of subcellular fractions from tissue and cells

Cytosolic buffer: 150 mM NaCl, 50 mM HEPES, 25 ug/mL digitonin, 1 M Hexylene Glycol, pH 7.4

Membrane buffer: 150 mM NaCl, 50 mM HEPES, 1% (v/v) Igepal, 1 M Hexylene Glycol, pH 7.4

Nuclear buffer: 150 mM NaCl, 50 mM HEPES, 0.5% (w/v) Sodium Deoxycholate, 0.1% (w/v) SDS, 1 M Hexylene Glycol, pH 7.4

2.5 Preparation of frozen tissue homogenates

RIPA buffer: 150 mM NaCl, 1.0% (v/v) Igepal, 0.5% (w/v) sodium deoxycholate, 0.1% (w/v) SDS, and 50 mM Tris, pH 8.0

2.7 Western blotting

6x SDS PAGE Loading buffer: 7 ml 0.5 M Tris-HCl, pH 6.8, 0.4% (w/v) SDS, 30% (v/v) glycerol, 10% (w/v) SDS, 0.6 M DTT, 0.012% (v/v) bromophenol blue

Towbin buffer: 20% (v/v) methanol, 25 mM Tris, 192 mM glycine, 0.05% (w/v) SDS

TTBS buffer: 0.01 M Tris pH 7.6, 0.1% (v/v) Tween, 0.1 M NaCl

2.8 Gelatin zymography

Zymo loading buffer: 0.5 M Tris-HCl, pH 6.8, 30% (v/v) glycerol, 0.4% (w/v) SDS, 0.012% (v/v) bromophenol blue

Zymography incubation buffer: 50 mM Tris-HCl pH 7.6, 150 mM NaCl, 5 mM CaCl₂, 0.05% (w/v) NaN₃

Coomassie zymography staining solution: 0.05% (w/v) Coomassie Brilliant Blue G-250, 25% (v/v) methanol, 10% (v/v) acetic acid

2.13 In vitro proteolysis assay

Activation Buffer: 100 mM Tris-HCl, 10 mM CaCl₂, pH 7.6

Incubation buffer: 50 mM Tris-HCl, 5 mM CaCl₂, 150 mM NaCl, pH 7.6

SDS PAGE 8% separating gel

This recipe makes two 1.5 mm gels.

The solutions that make up the gel are:

40% (w/v) acrylamide / 3.3% (w/v) bis-acrylamide (Bio-Rad, Mississauga, ON)

0.5 M Tris-Cl/ 0.4% (w/v) SDS made in H₂O

10% (w/v) Ammonium Persulfate made in H₂O

TEMED (Millipore, Oakville, ON)

| Solution | Volume (mL) |
|---|--------------------|
| 40% (w/v) acrylamide / 3.3% (w/v) bis-acrylamide 29:1 | 3.000 |
| 0.5 M Tris-Cl/ 0.4% (w/v) SDS, pH 6.8 | 3.750 |
| H ₂ O | 8.250 |
| 10% (w/v) Ammonium Persulfate | 0.050 |
| TEMED | 0.010 |

SDS PAGE 10% separating gel

This recipe makes two 1.5 mm gels.

| Solution | Volume (mL) |
|---|--------------------|
| 40% (w/v) acrylamide / 3.3% (w/v) bis-acrylamide 29:1 | 3.750 |
| 0.5 M Tris-Cl/ 0.4% (w/v) SDS, pH 6.8 | 3.750 |
| H ₂ O | 7.500 |
| 10% (w/v) Ammonium Persulfate | 0.050 |
| TEMED | 0.010 |

Gelatin zymography 8% separating gel

This recipe makes four 0.75 mm gels.

| Solution | Volume (mL) |
|---|--------------------|
| 40% (w/v) acrylamide / 3.3% (w/v) bis-acrylamide 29:1 | 3.000 |
| 0.5 M Tris-Cl/ 0.4% (w/v) SDS, pH 6.8 | 3.750 |
| Gelatin (20 mg/mL) | 1.500 |
| H ₂ O | 6.750 |
| 10% (w/v) Ammonium Persulfate | 0.050 |
| TEMED | 0.010 |

SDS PAGE and Gelatin zymography stacking gel

This recipe makes four 0.75 mm gels or two 1.5 mm gels.

| Solution | Volume (mL) |
|---|--------------------|
| 40% (w/v) acrylamide / 3.3% (w/v) bis-acrylamide 29:1 | 0.975 |
| 0.5 M Tris-Cl/ 0.4% (w/v) SDS, pH 6.8 | 2.500 |
| H ₂ O | 6.525 |
| 10% (w/v) Ammonium Persulfate | 0.050 |
| TEMED | 0.010 |

Publications arising from this thesis

Peer reviewed journals:

Baghirova, S., B.G. Hughes, M.J. Hendzel and R. Schulz. Sequential fractionation and isolation of subcellular proteins from tissue or cultured cells. *MethodsX* in press. doi:10.1016/j.mex.2015.11.001.

On-line commentaries:

Hughes, B.G., S. Baghirova, M.J. Hendzel and R. Schulz. 2015. Commentary on Marchant D.J. et al: A new transcriptional role for matrix metalloproteinase-12 in antiviral immunity. *Nature Medicine*, 2014, 20: 493-502. *PubMed Commons*. <http://1.usa.gov/1IwWIPq>

Abstracts:

Baghirova, S., M.Y. Kondo, B.G. Hughes and R. Schulz. 2015. Nuclear localization and biological function of matrix metalloproteinase-2. *FASEB Journal*. Experimental Biology, Boston, Massachusetts, 2015-04-01

Baghirova, S., M.Y. Kondo, F. Fan, B.G. Hughes and R. Schulz. 2014. Determining the nuclear localization and targets of nuclear matrix metalloproteinase-2. *WCHRI Abstract Book*. Women and Children's Health Research Institute (WCHRI) Research Day, Edmonton, 2014-11-12

Baghirova, S., M.Y. Kondo, F. Fan, B.G. Hughes and R. Schulz. 2014. Determining the nuclear localization and targets of nuclear matrix metalloproteinase-2. Cancer Research Institute of Northern Alberta (CRINA) Inaugural Research Day, Edmonton, 2014-11-15

Baghirova, S., M.Y. Kondo, F. Fan, B.G. Hughes and R. Schulz. 2014. Nuclear localization of matrix metalloproteinase-2 and identification of possible nuclear targets. Pharmacology Research Day, Edmonton, 2014-06-04

Baghirova, S., M.Y. Kondo, F. Fan, B.G. Hughes and R. Schulz. 2014. Nuclear localization and activity of matrix metalloproteinase-2 in cardiac myocytes. Cardiac Sciences Day, Edmonton, 2014-06-06

Baghirova, S., M.Y. Kondo, F. Fan, B.G. Hughes and R. Schulz. 2014. Nuclear localization and activity of matrix metalloproteinase-2 in cardiac myocytes. CIHR Young Investigators Forum, Edmonton, 2014-05-26